Aalborg Universitet

AALBORG UNIVERSITY
DENMARK

Customized modeling and simulations for control of motor neuroprostheses for walking

Dosen, Strahinja

Publication date:
2008

Document Version
Publisher's PDF, also known as Version of record

Customized Modeling and Simulations
for Control of Motor Neuroprostheses for Walking

– PhD THESIS –

STRAHINJA DOŠEN

Center for Sensory-Motor Interaction, Aalborg University

Aalborg, September 2008

List of abbreviations

ANN	artificial neural networks
CAS	constant-amplitude segment
CCC	cross-correlation coefficient
CMS	customized modeling and simulations
CNS	central nervous system
COP	center of pressure
CPG	central pattern generator
CVA	cerebro-vascular accident
DO	dynamic optimization
DoF	degrees of freedom
EMG	electromyography
FES	functional electrical stimulation
FSR	force sensing resistor
GRF	ground reaction force
MAX_{TE}	maximal value of absolute tracking error
MEAN_{TE}	mean value of absolute tracking error
MEMS	microelectromechanical systems
MNP	motor neuroprosthesis
MWDO	moving-window dynamic optimization
NLP	nonlinear programming
NMAXTE_{T}	normalized maximum tracking error from target trajectory
NRMSE	normalized root mean square error
NRMSTE_{E}	normalized root mean square tracking error from estimated trajectory
NRMSTE_{T}	normalized root mean square tracking error from target trajectory
PWC	piecewise constant
RBC	rule-based control
RMSE	root mean square error
SCI	spinal cord injury
SDJA	standard deviation of joint angles
SMM	sensorimotor model
SO	static optimization
STD_{TE}	standard deviation of absolute tracking error

The thesis is based on the following articles:

1. S. Došen, D. B. Popović, C. Azevedo-Coste, "Optiwalk: Un nouvel outil pour la conception et la simulation de lois de commande pour le contrôle de la marche de patients atteints de déficits moteurs," *Journal Européen des Systèmes Automatises*, JESA, vol. 41, pp. 239-259, 2007. (DOI: 10.3166/jesa.41.239-259)

2. S. Došen, and D. B. Popović, "Moving-Window Dynamic Optimization: Design of Stimulation Profiles for Walking," *IEEE Transactions on Biomedical Engineering*, (in press).

3. S. Došen and D. B. Popović, "Accelerometers and force sensing resistors for optimal control of walking of a hemiplegic," *IEEE Transactions on Biomedical Engineering*, vol. 55, no. 8, pp. 1973-1984, 2008. (DOI: 10.1109/TBME.2008.919715)

4. S. Došen, D. B. Popović, and M. B. Popović, "Design of Optimal Profiles of Electrical Stimulation for Restoring of the Walking," *Medical Engineering & Physics*, (submitted).

The research work has been carried out at the Center for Sensory-Motor Interaction, Aalborg University, Denmark.

Acknowledgements

Table of contents

Motivation for this research

Motor neuroprosthesis (MNP) is a system that uses electrical stimulation to restore a motor function (e.g., standing, walking, reaching, or grasping) that is lost or diminished due to the injury or disease of the nervous system [1]. First successful application of an MNP for assisting of the walking was reported by Liberson *et al.* [2] in 1961, that is, more than forty years ago. During that long period, many systems have been designed and tested, and all components of MNPs (i.e., stimulator, electrodes, and sensors) reached maturity. However, the MNPs are still not widely used for restoration of the walking. The most likely reason is that the control is not effective enough to make an MNP operate at the level that improves the quality of life of a disabled person. Better control and thereby improved performance that would meet the needs of disabled individuals, would lead to a wider usage of MNPs.

We suggest that operation of MNP should be based on life-like control. The artificial controller should mimic the operation of sensory-motor systems characteristic for healthy individuals. This is necessary because the controller must be integrated into those components of biological (volitional) control that are still preserved and functional after the injury or disease of the central nervous system (CNS). However, the problem that one immediately faces when trying to design a life-like controller is the fact that the biological mechanisms for the control of walking are still not completely known and understood. The seminal paper by Prochazka *et al.* [3] illustrates the controversy that still surrounds even the most basic concepts of motor control.

Different mechanisms have been suggested to operate to control walking [1], [3]–[6]. Most authors would agree that the CNS uses a combination of feedforward and feedback control. Predefined motor programs and central pattern generator (CPG) act as feedforward commands and afferent inputs (reflexes) provide feedback. The reflexes operate in the manner of finite-state control as discrete triggers that activate motor programs or initiate state transitions (e.g., swing, stance) within the CPG. Alternatively, they could provide continuous displacement, velocity, acceleration or force feedback that constantly modulates the feedforward signals. However, these mechanisms are understood at a fairly general level. The details of how they actually operate and combine to generate and control walking are still largely unknown. Unfortunately, that is exactly the type of knowledge that is necessary for designing the life-like controller.

The lack of this knowledge was primary motivation for our research. The topic of this thesis was to improve the methods for life-like control of multichannel MNPs for assisting of the walking. We started from the so called sensorimotor hypothesis [3]. In essence, the hypothesis states that the entire function of the CNS is to convert sensory inputs coming from internal and external environments into appropriate motor outputs. Therefore, although the knowledge about the operation of the biological controller is unavailable in an explicit form, it is certainly coded implicitly within the set of sensory-motor patterns that characterize the movement of interest. Consequently, it is likely that the life-like rules and strategies could be reconstructed if the sensory inputs and motor outputs of the controller (i.e., sensorimotor model) are provided.

Importantly, the sensorimotor model of the controller can be generated by using biomechanical gait simulations [7]. When the goal is to control gait in persons with disability, the simulations have to deal with an additional level of complexity; they have to take into account the facts that the neuromuscular system is impaired and that it is actuated artificially by electrical stimulation [8]. If the sensorimotor model is available, the control rules can be handcrafted or computer-generated by using machine learning [9]. Now we can define the specific goal of this thesis. Specifically, the goal was to develop novel, flexible and efficient simulation methods and tools that can be used to generate the knowledge (i.e., sensorimotor models) that is necessary for designing the life-like control of MNPs for gait restoration.

REFERENCES

[1] D. Popović, and T. Sinkjaer, *Control of Movement for the Physically Disabled*, 1 ed. London: Springer, 2000.

[2] W. Liberson, H. Holmquest, and M. Scott, "Functional electrotherapy: Stimulation of the common peroneal nerve synchronized with the swing phase of gait of hemiplegic subjects," *Arch. Phys. Med. Rehabil.*, vol. 42 pp. 202-205, 1961.

[3] A. Prochazka, F. Clarac, G. E. Loeb, J. C. Rothwell, and J. R. Wolpaw, "What do reflex and voluntary mean? Modern views on an ancient debate," *Exp. Brain Res.*, vol. 130, no. 4, pp. 417-432, 2000.

[4] "The organization of movement," in Kandel, E. R., Schwartz, J. H., and Jessell, T. M. (eds.) *Principles of neural science* 4 ed. McGraw-Hill, 2000, pp. 653-673.

[5] Latash, M. L., *Neurophysiological Basis of Movement*, Urbana, IL: Human Kinetics, 1998.

[6] A. Prochazka, "Comparison of natural and artificial control of movement," *IEEE Trans. Rehabil. Eng.*, vol. 1, no. 1, pp. 7-17, 1993.

[7] M. G. Pandy, "Computer modeling and simulation of human movement," *Annu. Rev. Biomed. Eng.*, vol. 3 pp. 245-273, 2001.

[8] D. Popović, R. B. Stein, M. N. Oguztoreli, M. Lebiedowska, and S. Jonić, "Optimal control of walking with functional electrical stimulation: A computer simulation study," *IEEE Trans. Rehabil. Eng.*, vol. 7, no. 1, pp. 69-79, 1999.

[9] Tomović, R., Popović, D., and Stein, R. B., *Nonanalytical Methods for Motor Control*, Singapore: World Scientific Publishing Co Pte. Ltd., 1995.

CHAPTER 1
Introduction

Summary–In this chapter, we provide background information, explain terms and definitions used throughout the thesis, set goals and scope of the thesis, identify open problems, and formulate research questions that are to be answered by the thesis. Overall goal of this research was to improve the control of motor neuroprostheses (MNPs) based on functional electrical stimulation (FES) for restoration of the walking. Contemporary clinically-used MNPs implement very simple control. Typically, handcrafted stimulation sequences are triggered by using a hand switch or a gait sensor and delivered in an open-loop manner. As a result, generated gait is slow, jerky and with high energy demands. Improving the control of FES is essential for increasing the performances of MNPs to a level that would satisfy the needs of disabled individuals. Several closed-loop error-driven control methods have been presented in literature. However, in these studies, the system was typically reduced to a muscle or at most a joint. Therefore, this approach is not yet practical enough to be used for gait restoration. We suggest that an MNP should use life-like control. The artificial controller should mimic biological mechanisms for the control of movement. Therefore, we use artificial reflex control which is a form of rule-based control that is inspired by the biology. We believe that this method could lead to a practical and effective system for gait restoration by means of FES. Control algorithm in this framework is a set of rules (artificial reflexes) that map system states to appropriate motor responses. The biggest difficulty in designing the artificial reflex control is the lack of an expert knowledge that can be used to construct the rules. Namely, biological mechanisms for the control of walking are still not fully known and understood. In the cases like this, when an explicit knowledge is unavailable, machine learning could be used to induce the rules from a set of examples. The critical task then becomes to generate the examples (knowledge base) to be used for implementation of the learning. Our goal is to restore normal gait in disabled individuals. Therefore, the knowledge base for machine learning is a sensorimotor (SMM) model of gait comprising two components: 1) sensory component, that is, sensor data acquired by recording normal gait of able-bodied subjects, and 2) motor component, that is, muscle activation profiles that produce muscle forces adequate to generate normal gait in a disabled individual. The SMM can be generated by using biomechanical gait simulations. The sensory and motor components of the SMM are used as inputs and target outputs for machine learning, respectively. Therefore, the sensory data are incorporated into the inputs (feedback) while the muscle activations become the outputs (feedforward commands) of the generated rule-based controller. Now, the specific goal of this thesis can be stated. Specifically, the goal was to develop novel methods and tools for biomechanical modeling and simulations that can be used to generate the knowledge (i.e., sensorimotor models) that is necessary for designing life-like control of multichannel MNPs for assisting of the walking. Importantly, the task of the simulations was to provide the sensorimotor data in the form that leads to a rule-based control which is effective, robust and convenient for implementation within a practical assistive system. That is to say that the simulations should allow feedforward and feedback component of the rule-based controller to be shaped iteratively thorough offline experiments, and then, when the results are satisfactory, the control could be implemented online in just one step (by applying machine learning). Machine learning was not the topic of this thesis; however, the problem was treated extensively elsewhere.

1. MOTOR NEUROPROSTHESES

Cerebrovascular accidents (CVA) and spinal cord injuries (SCI) are the most common causes of paralysis with reported prevalence of 12000/million and 800/milion, respectively [1]. Disabilities that follow CVA (hemiplegia) or SCI (paraplegia, tetraplegia) severely impair motor functions (e.g., standing, walking, reaching and grasping) and thereby prevent the affected individuals from healthy-like participation in daily activities. Tetraplegia refers to loss of motor and/or sensory function in the cervical segments of the spinal cord. It results in impairment of function in the arms, trunk, legs and pelvic organs. Paraplegia refers to loss of motor and/or sensory function in thoracic, lumbar or sacral segments. Consequently, the arm functioning is spared, but the trunk, legs and pelvic organs can be affected. Hemiplegia is paralysis of the side of the body contralateral to the CVA. In many cases it comprises weakness of the leg on the affected side, where the drop-foot syndrome often prevents the walking [2].

Motor neuroprosthesis (MNP) has been suggested as an effective assistance for restoration of motor functions in individuals with paralysis [2]. MNP is a man-made system that uses functional electrical stimulation (FES). FES activates paralyzed muscles by means of electrical stimulation of motor or sensory nerves aiming to generate functional movement. The basic principle of operation of an MNP is shown in Fig 1.1.

MNP [3], [4] delivers electrical charge in form of bursts of pulses; therefore, it integrates pulse generator, control unit, and electrodes as the interface to the sensory-motor systems (see Fig. 1.2). The electrodes can be at the surface of the body or implanted [2], [3], [4]. The control unit generates command signals to the pulse generator that provides proper amount of electrical charge for producing muscle forces adequate to generate desired movement. The control unit needs feedback (sensory information) for optimal performance of MNP.
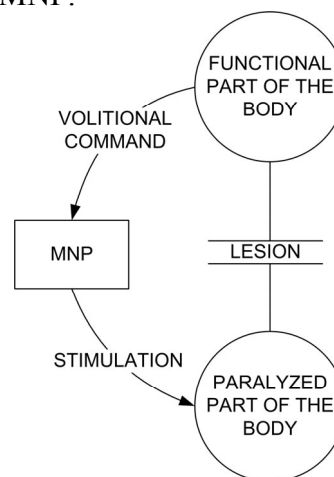
Fig. 1.1. MNP as a bypass of damaged sensory-motor systems. User volitionally triggers delivery of electrical stimulation by using functional part of the body (above lesion). Electrical pulses stimulate motor and/or sensory nerves, thereby generating movement by activating paralyzed muscles.
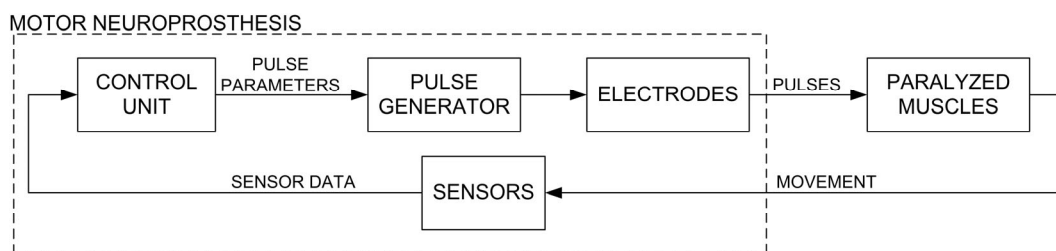
Fig. 1.2. Components of an MNP. Movement generated by means of FES is monitored by a set of sensors. Based on the sensory information, a control unit calculates appropriate stimulation parameters (frequency, pulse width and pulse amplitude). Pulse generator produces the pulses which are delivered to paralyzed muscles via a set of electrodes.

2. MOTOR NEUROPROSTHESES FOR WALKING

The first successful application of a portable MNP was presented by Liberson *et al.* (1961) for correction of drop-foot in individuals with hemiplegia [5]. They timely stimulated *Common Peroneal n.* using surface electrodes in order to elicit ankle dorsiflexion during swing phase of gait. Since then, many devices, based on the same principle and named drop-foot or peroneal stimulators, were developed. Some achieved broad clinical application. First drop-foot systems with surface electrodes were manufactured and evaluated in stroke patients in 60's in Ljubljana, Slovenia (e.g., Ljubljana functional electronic peroneal brace FEPB [6]). ODFS [7], WalkAid [8], and NESS L300 [9] are examples of similar present-day FDA-approved devices. In early 70's, first implanted peroneal nerve stimulators were developed by Medtronic Inc., USA [10], [11] and University of Ljubljana, Slovenia [12]. ActiGait [13] and Finetech Dropped Foot System [14]　are two examples of contemporary implantable systems. ActiGait was developed at the Center for Sensory-Motor Interaction, Aalborg University, Denmark and Neurodan A/S, Aalborg, Denmark. The system uses multi-polar multi-channel cuff electrode to activate different fascicles in the peroneal nerve resulting in activation of different muscles in the lower leg. Therefore, balanced dorsiflexion movement (without excessive eversion/inversion) can be achieved. Furthermore, it was demonstrated that an eletroneurographic signal recorded from the sensory nerve [15] can be used to trigger the stimulation [16]. Finetech Dropped Foot System was developed at the University of Twente, Netherlands and at the Roessingh Research and Development, Enschede, Netherlands. It uses two intra-neural electrodes to achieve balanced dorsiflexion. One electrode is placed under the epineurium of *Superficial Peroneal n.* (controls eversion) and one under the epineurium of *Deep Peroneal n.* (controls dorsiflexion and inversion).

Pioneering work in multichannel FES with surface electrodes was done by a research group from Ljubljana, Slovenia [17]. First, they developed a three-channel system for assisting the swing phase in individuals with hemiplegia. Later, three more channels were added [18] with the aim to stimulate all three joints of paretic leg during both stance and swing [19]. In order to restore paraplegic walking at least four stimulation channels are needed (i.e., two channels per leg). *Quadriceps* muscles are stimulated bilaterally in order to lock the knees and allow standing. During walking, *Quadriceps* muscles are activated in stance phase, while flexion withdrawal reflex (stimulation of *Common Peroneal n.*) is elicited to generate movement that can be considered as the swing. Systems for restoration of paraplegic gait developed in Ljubljana [20] were successfully tested in a number of SCI patients [21], [22]. This research led to development of ParastepTM (Sigmedics, USA), the only commercially available and FDA-approved system for therapy in paraplegic population [23]. Vienna FES system [24], Compex Motion [25] and UNA FET [26] are examples of similar multichannel transcutaneous systems that can be used for gait restoration in individuals with hemiplegia or paraplegia.

In order to overcome deficiencies of the surface systems (e.g., donning and doffing, proper electrode placement, poor stimulation selectivity), a number of percutaneous and implanted systems were suggested. Kobetič and Marsolais [27], [28] developed a percutaneous system for restoration of paraplegic gait that could activate up to 48 muscles. The system was later adapted to be used as a therapeutic device for gait training in stroke patients [29]. Praxis FES24 [30], SUAW [31], and CWRU/VA [32] are examples of implanted systems with 22, 16 and 16 electrodes, respectively. Recently, an implanted stimulator was presented [33] that used surface electromyography recorded from partially paralyzed muscles to detect user's intent and trigger the stimulation.

The aforementioned MNPs differ in many aspects when compared to each other: they have different number and types of electrodes (e.g., from 1 to as many as 64 electrodes), use different inputs to trigger stimulation (e.g., from mechanical switches to natural sensors), and implement different functions (e.g., from swing-through gait to walking backwards). Although being technologically very different, the systems use the same control strategy, that is, simple open-loop control. In most cases, stimulation is triggered by a hand switch. Few systems are somewhat automated and use a gait sensor to provide the trigger signals. However, the sensor typically detects only the most basic gait events (e.g., heel strike, heel off). Stimulation sequences are handcrafted, and therefore simple and crude. Figs. 1.3 and 1.4 show the principle of operation and the stimulation sequences for a 4 channel surface and a 16 channel percutaneous stimulator, respectively. The figures demonstrate that the operation of these technologically

very different systems is, in fact, quite similar and simple. Most of the contemporary clinically-used FES systems use very similar control.

Human body is a highly complex musculoskeletal system. However, the example control shown in Figs. 1.3 and 1.4, which is supposed to drive the system, is very simple and uses the control signals that are rather coarse. Therefore, it is not surprising that gait patterns generated by using contemporary MNPs are still far from the performances typical for normal gait of able-bodied individuals. The movements are rather robotic and jerky. Walking is frequently accompanied with significant energy expenditure and high heart rates [2]. Paraplegic patients using ParastepTM walk very slowly (0.1–0.2 m/s), with energy requirements up to eight times that of people without disability walking at the same pace [32]. All in all, contemporary clinically-used MNPs can be regarded more as tools for a healthy exercise than as practical orthotic devices.
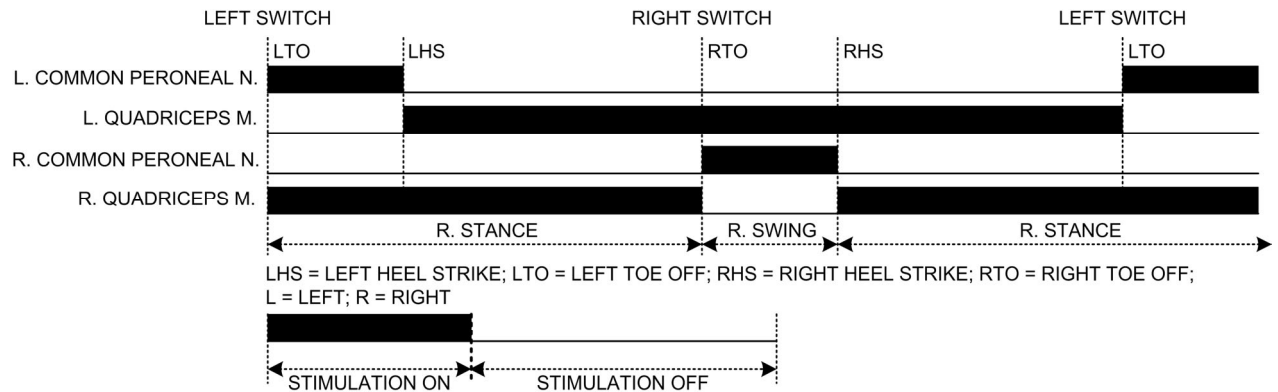
Fig. 1.3. The control of a transcutaneous stimulator with 4 channels. *Quadriceps* muscles are stimulated during the stance phase. Swing phase is generated by switching off *Quadriceps* stimulation and stimulating *Common Peroneal n.*, thereby evoking flexion withdrawal reflex. Hand or heel switches can be used for control. Adapted from Popović [34].
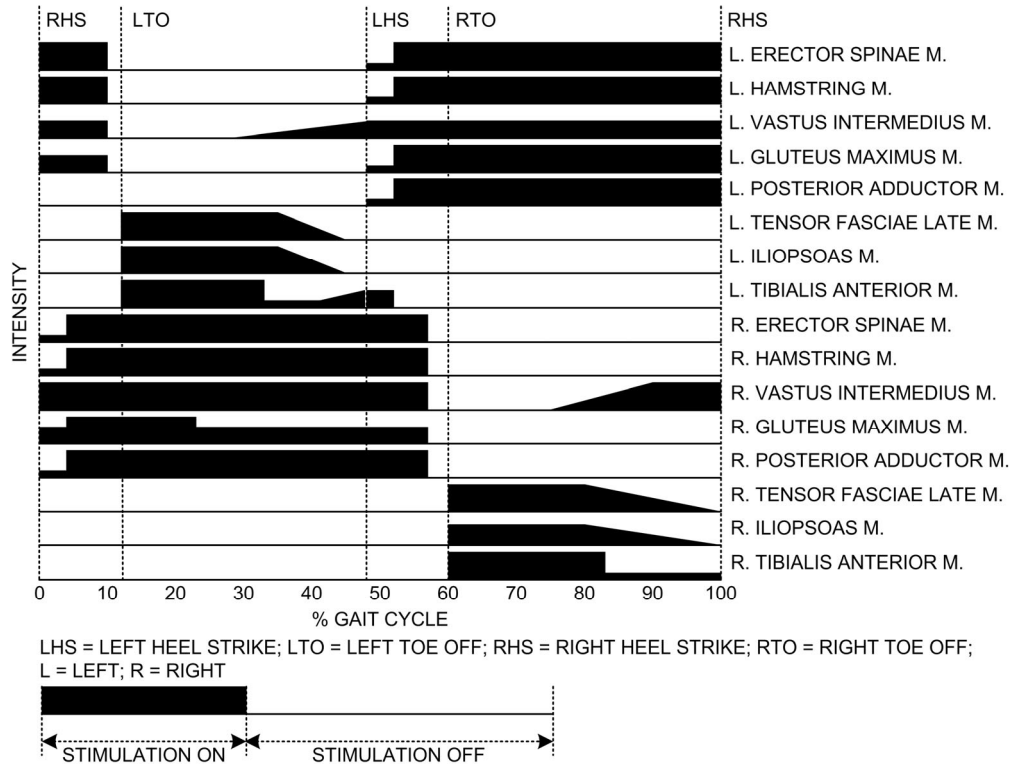
Fig. 1.4. The control of a percutaneous stimulator with 16 channels. Eight muscles on each side of the body are stimulated. The stimulation sequences can be triggered by using hand or heel switches. Adapted from Kobetič *et al.* [27] © IEEE.

3. AUTOMATIC CONTROL OF MOTOR NEUROPROSTHESES FOR WALKING

Improving the control of FES is essential for generating better gait by means of MNP. In turn, this could lead to a wider usage of FES for both therapeutic and orthotic applications. Instead of the open-loop approach, more sophisticated closed-loop error-driven control could be used. In this method, controller uses tracking error, that is, a deviation of the system from desired trajectory, to calculate stimulation parameters that will reduce the error. However, musculoskeletal system of lower extremities is highly complex, nonlinear, time variant, mechanically unstable (multi-segment inverted pendulum) and redundant system. Furthermore, there is a delay between the onsets of stimulation and actual force production in the muscles. States of the system (joint angles and velocities) and interactions with the environment (ground reaction forces) are hard or even impossible to measure by using practical sensors. Finally, mathematical model of the musculoskeletal system is far too complex for real-time implementation within a programmable electronic stimulator. Nevertheless, various advanced closed-loop error-driven control techniques such as local model networks [35], model based control [36], H_∞ robust control [37], gain scheduling [38], virtual reference feedback tuning [39], sliding mode control [40], [41], and model predictive control [42] have been investigated. In some studies the methods were tested only in simulations. If tested experimentally, the methods were applied to a simplified system reduced to a single muscle or at most a joint. Therefore, these control approaches are still far from being applicable to restoration of gait. Facing the constraints of the open-loop and error-driven closed-loop methods, we adopted an alternative framework termed rule-based control (RBC). We believe that RBC could lead to a practical and effective system for automatic (sensor-driven) control of FES for gait restoration.

RBC was used by several research groups for the control of above knee prosthesis, MNPs, and hybrid systems [43]–[45]. Examples of MNPs based on RBC for mobility restoration in paraplegics are given in [46] and [47]. We suggest that MNP should use life-like control. The artificial controller should mimic biological mechanisms for the control of movement. Therefore, we use a form of RBC termed artificial reflex control which is (as the name implies) inspired by the biology [34]. Studies done in a number of different animals (from insects to vertebrae) suggest that central nervous system uses both feedforward commands (central pattern generator and motor programs) and feedback (reflexes) for control [44], [48]. Importantly, it seems that both of these control strategies can be described in the form of IF–THEN rules. The "IF part" of a rule specifies a particular state of the musculoskeletal system and the "THEN part" gives an appropriate motor responses [44]. Analogously, the control algorithm in artificial reflex control is a set of rules (i.e., a rule base). The system states are detected by using a set of gait sensors. The corresponding motor responses are specified as muscle activation profiles that produce muscle forces adequate to generate desired movement. Therefore, similarly to biological control, sensory information is used to trigger predefined motor programs. RBC is very robust approach; the rules can be changed, deleted and/or added to the rule base without affecting overall integrity of the controller. Typically, the rule base comprises regular and hazard rules. The regular rules are active as long as the system progresses through the normal (expected) sequence of gait phases and events. The hazard rules (e.g., corrective stumbling reaction) are triggered in case of unexpected events (e.g., hitting an obstacle) that tend to disrupt the desired state flow (see Fig. 1.5).

The rules for rule-based control can be handcrafted [28]. However, handcrafting requires both considerable expertise and substantial time. In addition, the mechanisms for the control of walking are still not fully understood (certainly not at the level that is required for the design of a practical system). Consequently, expert knowledge that is necessary for deriving the rules is not yet available. In order to circumvent the lack of an explicit knowledge, the rules can be computer-generated [49]. In this case, the rules are automatically extracted (inferred) from a set of examples (knowledge base) by using machine learning. The task of machine learning is to identify and represent, in the form of rules, important sensory-to-motor mappings that characterize desired system behavior. The most difficult and critical step in this approach is to generate an appropriate knowledge that can be used for deriving the rules.

ARTIFICIAL REFLEX CONTROLLER
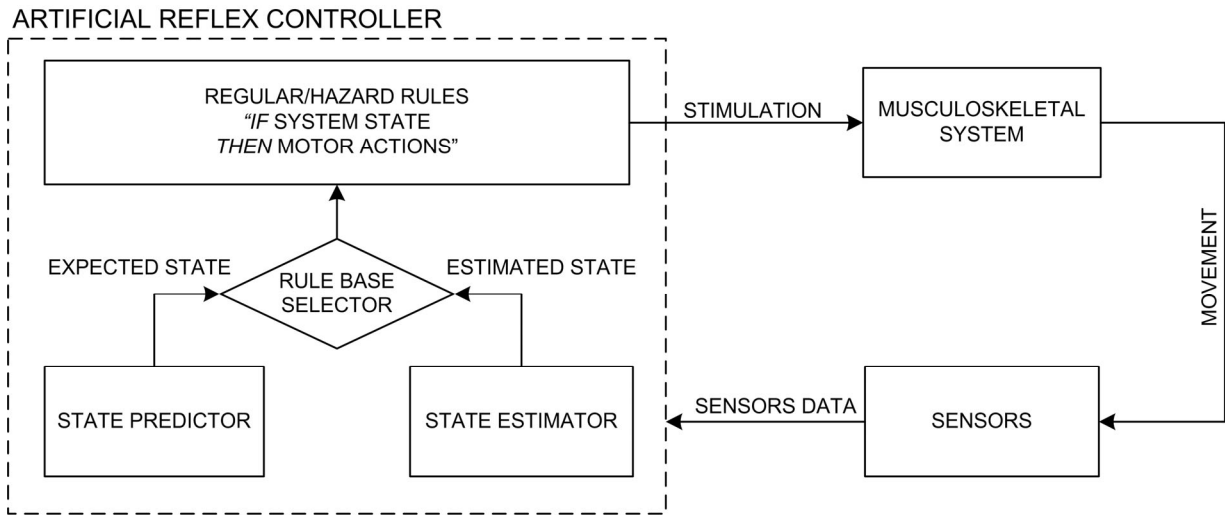
Fig. 1.5. Artificial reflex control for gait restoration. Current system state is estimated from sensor data (state estimator). If expected system state (state predictor) matches the estimated system state (state estimator) then the system progresses through the normal sequence of gait phases and events. Therefore, rules from regular rule base are used. Otherwise, hazard rule base is activated. The rules are IF-THEN statements that, based on the system state ("IF" part), determine the appropriate motor action ("THEN" part).
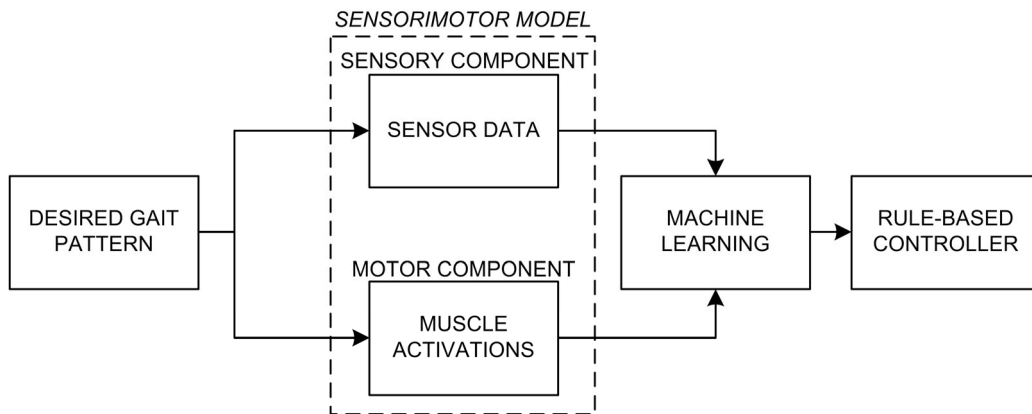
Fig. 1.6. Generation of rules for RBC of gait. SMM is used as a knowledge base for machine learning. SMM comprises sensory and motor components. Machine learning generates the rules that map the sensor data to muscle activations.

4. SENSORIMOTOR MODEL FOR RULE-BASED CONTROL OF WALKING

In RBC for gait restoration, the goal is to generate normal looking gait in a disabled individual. Therefore, a knowledge base for machine learning is a sensorimotor model (SMM) of gait comprising two components: 1) sensory component, that is, sensor data recorded by using a set of gait sensors during walking of able-bodied individuals, and 2) motor component, that is, muscle activations that produce muscle forces that are adequate to generate normal gait in disabled individual. Fig. 1.6 depicts the design of rules by applying machine learning to an SMM of gait.

Creating an SMM of gait is the most important step in designing the rule-based controller. The type and form of sensorimotor data in the SMM determines the structure, complexity and number of the rules that are generated by machine learning. The sensor data from the SMM are used as inputs and the muscle activation profiles as target outputs for machine learning. As a result, a real-time controller (i.e., a set of rules) will be obtained and its inputs (feedback) and outputs (feedforward commands) created from the sensory and motor components of the SMM, respectively. Basically, gait sensors used for acquiring the sensor data will provide sensory feedback for the controller. Based on the sensory information, the controller will reproduce (in real time) the muscle activation profiles from the SMM. Taking these into account, we can define certain properties that an SMM should have in order to lead to a practical and effective system for gait restoration.

The set of sensors used for building the sensory part of the SMM has to be practical and convenient for daily application. The sensors should be robust, physically small, low power, and easy to don and doff.

This is important because, as already noted, the same set of sensors will provide real-time inputs for rule-based controller. Furthermore, using practical sensors will allow creating a comprehensive SMM (many gait strides, different gait speeds, and different subjects). This will provide a large knowledge base for machine learning and the end result will be a robust controller. After the proper sensors have been selected, the sensory part of the SMM is created by recording normal gait of able-bodied subjects. Gait kinematics and kinetics is traditionally recorded by using sophisticated laboratory-fixed gait analysis systems, such as, camera based motion capture and force plates. These sensors represent a "golden" standard for measuring human movement. However, they can not be part of a practical assistive system. Possible sensors that are convenient for real-time control are piezoresistive force sensing resistors and accelerometers made in microelectromechanical technology [50]. The sensors are practical and give reproducible measurements [51]. Microelectromechanical sensors are often used in contemporary gait analysis systems [52], [53].

The motor part of the SMM comprises desired muscle activations. In principle, it could be created by using two different approaches: 1) electromyography (EMG) recorded from muscles of able-bodied subjects could be used as a template for determining the muscle activations, or alternatively 2) muscle activations could be directly computed by using biomechanical gait simulations.

The first method (SMM from EMG) was used in several studies [54]–[56]. However, as discussed in detail in Chapter 5, there are certain concerns regarding this approach. Namely, an SMM based on the normal EMG profiles would lead to a controller (rules) that would drive the limbs of a disabled individual by using the control signals taken from a healthy subject; yet, the two neuromusculoskeletal systems, one impaired and the other healthy, are completely different. After the CNS injury, there are a number of pathological changes: weaker muscles, spasticity, hyperactive reflexes, abnormal central control, altered joint elasticity and viscosity etc. Therefore, the control signals appropriate for the healthy system would likely generate completely different (unsatisfactory) response when applied to the system altered by the injury.

Alternative approach is to use musculoskeletal modeling and simulations to calculate muscle activations. There are a number of very sophisticated musculoskeletal models described in literature [57], [58]. Simulations based on these models are very important for gaining insights into general principles and mechanisms governing human gait. However, as explained in Chapter 2, these approaches can not be directly used for real-time control. The models are very detailed and too complex. Moreover, they have a number of parameters which are very hard or even impossible to identify. Therefore, the models can not be customized for a specific subject. Because of the aforementioned changes of biomechanical parameters after the CNS injury, the ability to customize the model is very important for effective control. Namely, the simulation should use inertial and muscle parameters that reflect the impairment caused by the lesion. In addition, the simulation has to consider the constraints arising from the fact that FES is used to activate muscles and generate movement (e.g., low selectivity in targeting individual muscles with surface FES).

Popović et al. [59] developed a biomechanical model of gait specifically designed for application in FES. They introduced a number of deliberate simplifications to develop a reduced model with parameters that can be experimentally identified [60]. Therefore, the model can be customized for a disabled subject. Using the model, they developed a simulation of optimal control based on dynamic programming. Inputs for the simulation were the model of a disabled subject and a desired gait pattern recorded from an able-bodied person. Outputs from the simulation were muscle activations necessary to generate the pattern. The activations were determined by minimizing tracking errors from the desired gait pattern while penalizing total muscle efforts. Since the simulation implements a customized model, the generated muscle activations are subject-specific. They are obtained by taking into account the current status of the subject's neuromuscular system. The method was validated in a clinical study on individuals with paraplegia [61]. We will refer to simulations that follow the aforementioned principles as customized modeling and simulations (CMS). Fig. 1.7 depicts the CMS approach.

As for the sensory component, since the goal is to design a practical system, the motor component of the SMM (a set of muscle activations) has to be in the form that is convenient for implementation within a programmable electronic stimulator.
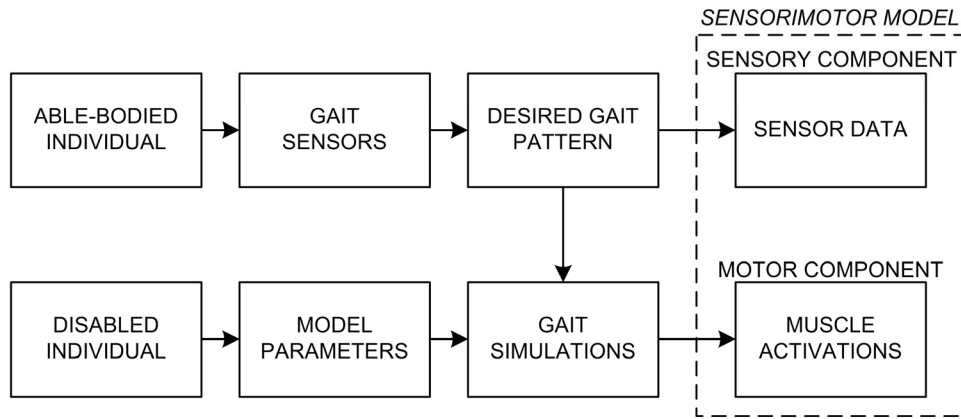
Fig. 1.7. CMS approach. Desired gait pattern is recorded from an able-bodied individual. Model parameters are experimentally identified from a disabled subject. Using a model customized to the subject, biomechanical gait simulations determine muscle activations that are adequate to generate the desired gait. The output from the CMS is an SMM. The SMM is then used as a knowledge base for machine learning. Machine learning generates customized rule-based controller (see Fig. 1.6).

5. PHD PROJECT GOALS

The topic of this research was to improve the methods for the synthesis of life-like control for multichannel MNP for assisting of the walking. The methods that we propose are based on some promising applications of rule-based control in the form of artificial reflex control [34], [61]–[65]. As explained in the previous sections, a serious obstacle for designing the rules for life-like control of walking is the lack of an explicit knowledge. Most researches would agree that the central nervous system uses a combination of feedforward and feedback control. However, the details of how these mechanisms operate individually or work together to generate and control walking are still largely unknown. The problem is even more complex when one considers the control of walking in individuals with disability. In this case, the plant to be controlled (neuromusculoskeletal system) is changed due to the injury and the muscles are activated artificially by using electrical stimulation.

The goal of this thesis was therefore to develop a set of methods and tools for generating the knowledge that is necessary for designing the life-like control of walking. Analogously to biological control, the controller in artificial reflex control comprises predefined motor programs (feedforward command) that are triggered by sensory information (feedback). The knowledge necessary for creating the controller is a sensorimotor model (SMM) that describes its desired operation. Namely, the SMM comprises sensory inputs (sensor data) and desired motor responses (muscle activations). The controller is computer generated from the SMM by using machine learning. The sensory data are used as inputs and the muscle activations as target outputs for the learning. Therefore, the feedback and the motor programs for the controller are created from the sensory data and muscle activations that are provided by the SMM, respectively.

This is depicted in Fig. 1.8. The figure shows the concept of customized modeling and simulations for generation of the SMMs (upper part) and its relationship to the components of a rule-based controller (lower part). With reference to Fig. 1.8, we can define the specific goal of this research. Specifically, the goal was to develop novel methods and tools for customized modeling and simulations that can be used to generate SMMs of gait. Importantly, the methods that we develop should be efficient and flexible, so that the simulations can be run with different inputs and parameters. This allows experimenting offline and generating SMMs until the sensorimotor data are obtained in the form that leads to a rule-based control which is effective, robust and convenient for implementation within a practical assistive system. That is to say that both feedforward and feedback component of the controller could be shaped iteratively thorough offline simulations, and then, when the results are satisfactory, implemented online in just one step (i.e., implementation of machine learning). Machine learning was not the topic of this thesis; however, the problem was treated extensively in literature [49], [64], [65].

We tested the simulation methods developed in the thesis by designing the control for an MNP that could be used to assist gait in individuals with hemiplegia. This significantly simplified the modeling
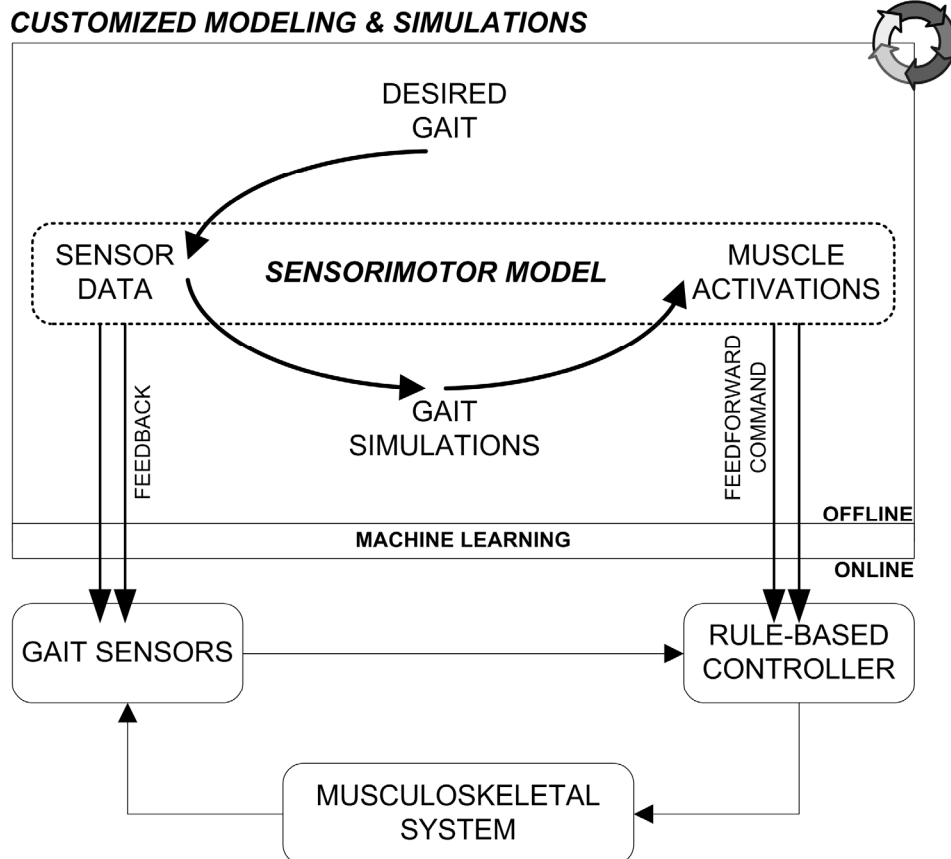
Fig. 1.8. Customized modeling and simulations for artificial reflex control of walking. The goal of the thesis was to develop novel, flexible and efficient simulation methods that can be used to generate sensorimotor (SMM) models of gait. The muscle activations and sensor data from the SMM provide, through implementation of machine learning, the feedforward commands and the feedback for the rule-based controller, respectively. Therefore, both components of the real-time control can be shaped thorough iterative simulations off-line (circular arrows, upper right corner) and then, when the results are satisfactory, implemented online in one step (i.e., machine learning).

part. The simulations that would aim to generate the control for restoration of paraplegic walking would have to use more complex models that take into account the control of balance in the frontal plane and use of hands and/or crutches for support (i.e., quadrupedal walking). However, it is important to acknowledge that the simulation methods that we developed are general and do not depend on the specific model used. Therefore, they are by no means restricted to the control of hemiplegic gait only.

By analyzing the previous results in the field of customized modeling and simulations for rule-based control [49], [59], [63]–[65], we identified following open problems, and formulated corresponding research questions:

PROBLEM 1: *Flexible methods for optimal control simulations are required.* In order to implement the concept of Fig. 1.8 (upper part), novel simulation methods are required that are flexible enough to allow manipulating the simulation inputs and outputs until the sensory and motor component of the SMM are generated in the desired form. Previous studies [59], [63] used optimal control based on dynamic programming for calculating the muscle activations. The inputs for the simulation were subject-specific model parameters and a desired gait pattern. The optimization minimized the tracking errors from the desired trajectories while penalizing muscle efforts. The method was very efficient since it gave a closed form (analytical) solution. In cases when the subject's muscles were strong enough, the method guaranteed good tracking of desired trajectories. However, the simulation used unconstrained optimization and a cost function in a specific (quadratic) form. This considerably limited the flexibility of the simulation, since the cost functions and the constraints are the basic instruments for manipulating the simulation inputs (sensor data) and outputs (muscle activations).

<u>RESEARCH QUESTIONS (RQ1):</u> What are the appropriate optimization methods that are flexible enough with respect to the form of cost functions and constraints? Is it possible to develop simulations based on these methods? What specific improvements in the simulations could be made by using novel

optimization methods?

DISCUSSION: There are a number of numerical optimization methods (e.g., linear, quadratic, and nonlinear programming) for finding the optimum of different classes of multivariable functions subject to different types of constraints. These methods could implement both static and dynamic optimizations [66]. Importantly, the flexibility in defining the cost functions and constraints, characteristic for these methods, could be used to realize some specific goals (see RQ2 and RQ3) that were not possible to achieve by using previous simulation algorithms based on dynamic programming [59], [63]. The constraints imposed by the musculoskeletal physiology could be taken into account. Static optimization can deal with algebraic constraints (e.g., range of motion in the joints) while more powerful dynamic optimization can accommodate the constraints in the form of differential equations (e.g., muscle activation dynamics).

RESEARCH QUESTIONS (RQ2): What is the shape of muscle activation profiles that is convenient for implementation within an electronic stimulator? Is it possible to develop simulation method that will generate the profiles in the selected form and which optimization method (static, dynamic) should be used? How will the fact that the control signals are constrained to have a prescribed (simple) shape affect the quality of tracking of desired trajectories?

DISCUSSION: Motor component of the SMM (muscle activations) determined by the simulation is used as a feedforward command within the rule-based controller (see Fig. 1.8). Therefore, the activation profiles should be convenient for implementation within an electronic stimulator. The profiles in the form of piecewise constant signals could be a possible choice. Such profiles are convenient for machine learning. They have uniform and simple structure that will likely result with the rules that are relatively simple. Since imposing the shape of controls is a complex constraint, it is likely that the simulation would have to be based on dynamic optimization. Importantly, the control in the form of piecewise constant signals, being relatively coarse and crude, could show to be unable to provide good tracking of desired trajectories. This must be tested by using experimental data.

RESEARCH QUESTIONS (RQ3): Is it possible to include in the simulation the control of stiffness at the joint level? How will an increase/decrease in joint stiffness affect the quality of tracking of desired trajectories?

DISCUSSION: This question, like the previous one, addresses the techniques for generating the motor component of the SMM in the form that leads to an effective rule-based controller. The previous question raises the issue of implementation, and this one deals with robustness of the generated control signals (muscle activation profiles). The original method based on dynamic programming minimized the overlap of agonist and antagonist activity (i.e., cocontractions). It was pointed out in [59] that, although this decreases net muscle activity and thereby reduces muscle fatigue, the absence of cocontractions may not be completely beneficial. In biological control (central nervous system), coactivation of agonist and antagonistic muscles is used to regulate joint stiffness and thereby resistance to perturbations [67]. Analogously, the simulation could generate the profiles that have minimal level of cocontractions prescribed and thereby achieve the control of joint stiffness. However, this should not compromise the quality of tracking.

PROBLEM 2: *Providing the inputs for the simulations by using practical set of gait sensors*. The sensory component of the SMM (sensor data) determines the real-time feedback for the rule-based controller (see Fig. 1.8). Therefore, being able to use a practical set of gait sensors to create the sensory part of the SMM is very important. The problem of selecting the sensors is equivalent to finding a proper set of sensory signals to represent a desired gait pattern (see Fig. 1.6). In the previous studies [59], [63]–[65] the desired gait was described by recording joint angles (goniometry, camera based motion capture systems) and ground reaction forces (force plates). However, the sensors used to measure these signals can not be part of a practical assistive system. Therefore, although the methods presented in these studies successfully demonstrated the concept of customized modeling and simulation for rule-based control, they were not directly applicable for real-time control of FES.

RESEARCH QUESTIONS (RQ4): Is it feasible to track desired gait patterns by using angular velocities or angular accelerations as the desired trajectories (instead of angles)? Will this lead to the simulation that converges?

DISCUSSION: One of the goals of the thesis is to develop novel optimization methods that are intended to be flexible (Problem 1). This flexibility could be exploited to define new cost functions that use tracking errors expressed in terms of angular velocities or angular accelerations. This would then allow using data recorded by practical gait sensors (gyroscopes, accelerometers) as the inputs for the simulations. However, using the data from these sensors directly in the simulation can lead to divergence [68]. The alternative is to develop methods for transforming the data into a form that leads to the simulation that converges. This is addressed by the next research question.

RESEARCH QUESTIONS (RQ5): What are the appropriate methods for data processing that can be used to estimate gait trajectories required for the simulation from the data recorded by practical sensors? What is the set of practical sensors (number, type, and placement) that provides robust and sufficiently redundant information that leads to satisfactory estimation? Is it possible to track with satisfactory precision desired gait patterns recorded by using the selected sensors?

DISCUSSION: The research question suggests the following three-step procedure for customized modeling and simulations: 1) recording the desired gait pattern by using practical sensors (instead of using laboratory fixed motion capture system), 2) estimating gait kinetics and kinematics that are required for the simulation from the data recorded by the sensors, and 3) generating muscle activations by tracking the estimated trajectories (instead of the original gait pattern). There are two potential sources of errors in the aforementioned procedure: 1) the estimation errors and 2) the tracking errors. Therefore, the feasibility of tracking the recorded gait patterns has to be tested by using experimentally collected data.

PROBLEM 3: *Comparing the simulation-generated control (muscle activation profiles) with the control used by the biology (EMG profiles).* As stated earlier, our goal was to develop methods that can be used to design life-like control of walking. That is to say that the control should mimic the operation of sensory-motor systems characteristic for healthy individuals. Therefore, it was of interest to compare the simulation-determined muscle activation profiles with the profiles of recorded EMG, since the latter reflects the control signals generated by the biological controller residing within the central nervous system (i.e., reference controller for life-like control). However, in addition to being life-like, the control that we develop should consider the fact that the muscles are activated artificially by electrical stimulation and that the plant to be controlled can be altered by the injury. This should be taken into account when comparing the profiles and analyzing the similarities and differences.

RESEARCH QUESTIONS (RQ6): Is the simulation-determined muscle activity in agreement with the activity recorded by the EMG? What are the trajectories generated when the EMG or simulation-determined activations are used as the controls? What are the conclusions with respect to designing the control for motor neuroprostheses?

DISCUSSION: This research question reflects the fact that the control for motor neuroprostheses could be designed by using two methods: 1) desired muscle activations (feedforward commands) can be derived from the EMG recorded in healthy individuals and 2) desired muscle activations (feedforward commands) can be calculated by using the customized modeling and simulations (the approach we advocate). Therefore, it is of interest to compare these two methods by using the same input data, that is, EMG recorded in parallel with gait kinetics and kinematics (simulation inputs) in an able-bodied subject.

6. ORGANIZATION OF PHD THESIS

The thesis is organized into chapters. Chapter 1 gives a scope and focus of the research presented in this thesis. It begins with an overview of clinically tested and commercially available MNPs. The special attention is given to the control methods which are implemented in these systems. Approaches for automatic control of MNPs are described and a rule-based control in the form of artificial reflex control was highlighted as the framework that we will use. Sensorimotor model of gait, which is crucial for implementation of artificial reflex control, is defined and different methods for designing its sensory and motor components are given and discussed. The overall goal of the PhD project is stated, that is, development of novel methods for customized modeling and simulations that will improve life-like control of MNPs for gait restoration. Finally, by analyzing the previous research in the field of customized modeling and simulations, we defined open problems and formulated research questions.

Chapters 2-5 illustrate the methods that were developed in order to answer the research questions

(RQ1-RQ6). The chapters are based on the following articles:

Chapter 2: S. Došen, D. B. Popović, C. Azevedo-Coste, "Optiwalk: Un nouvel outil pour la conception et la simulation de lois de commande pour le contrôle de la marche de patients atteints de déficits moteurs," *Journal Européen des Systèmes Automatises*, JESA, vol. 41, pp. 239-259, 2007.

Chapter 3: S. Došen, and D. B. Popović, "Moving-Window Dynamic Optimization: Design of Stimulation Profiles for Walking," *IEEE Transactions on Biomedical Engineering*, (in press).

Chapter 4: S. Došen and D. B. Popović, "Accelerometers and force sensing resistors for optimal control of walking of a hemiplegic," *IEEE Transactions on Biomedical Engineering*, vol. 55, no. 8, pp. 1973-1984, 2008.

Chapter 5: S. Došen, D. B. Popović, and M. B. Popović, "Design of Optimal Profiles of Electrical Stimulation for Restoring of the Walking," *Medical Engineering & Physics*, (submitted).

Chapter 2 describes in detail our customized modeling and simulation approach and its implementation in the form of a user friendly software tool for biomechanical gait simulations (OptiWalk). First, an extensive overview of existing musculoskeletal modeling and simulation methods is given. The reasons why complex models are not suitable for the control of walking by means of FES are stated. Our reduced model of gait and its inertial and muscle parameters are then described in detail. Our novel simulation algorithm, based on static optimization (see RQ1), for the tracking of desired trajectories in different phase spaces (i.e., angles, angular velocities, and angular accelerations) is explained (see RQ4). The OptiWalk software architecture and organization are outlined. A typical use case scenario is described and an example is given.

Chapter 3 describes our novel moving-window dynamic optimization (MWDO) method for generation of piecewise constant muscle excitations (see RQ1 and RQ2). The algorithm, based on dynamic optimization, is described in detail. The results of testing the MWDO simulation by using experimental data recorded from an able-bodied subject walking at a range of gait speeds are presented. It is shown how the coarseness of the MWDO-generated profiles can be controlled by using optimization parameters and how this in turn affects the tracking error. Flexibility of MWDO is discussed from the viewpoint of robustness, practical application, implementation and generation of rules for rule-based control.

Chapter 4 describes the methods that were developed in order to integrate a set of practical sensors (see RQ5) within the customized modeling and simulation methods described in Chapters 2 and 3. An optimal controller that uses data from accelerometers and force sensing resistors as inputs and generates muscle activations as outputs is presented. The methods for data recording, estimation of gait kinematics/kinetics from the recorded sensor data and simulations that use the estimated trajectories as inputs are described. The results of testing the optimal controller on experimental data collected from several subjects walking at a range of gait speeds are given. Finally, the estimation and simulation results are evaluated and discussed.

Chapter 5 represents a comparative study in which biologically selected activation profiles (EMG) are compared to activation profiles generated by using customized modeling and simulations (see RQ6). First, a brief overview of the studies that used either simulation outputs or EMG for designing the stimulation profiles for FES is given. Then, the methods used in this study for collecting experimental data and conducting the simulations are described. Optimization constraints that allow prescribing a desired level of coactivation for pairs of antagonistic muscles are formulated (see RQ3). The results compare (see RQ6): 1) the EMG patterns and muscle activities determined through simulation, and 2) trajectories achieved when EMG or simulated activities were used as controls to drive the joints of the biomechanical model. This is followed by a comprehensive discussion of both approaches outlining differences and similarities between the simulation and EMG. Results obtained by using different simulation algorithms (developed in Chapters 2 and 3) are also compared and discussed. Special focus is given to discussing the role of cocontractions in biological control (EMG) and in the simulations (see

RQ3).

Chapter 6 concludes the thesis. It summarizes how the methods developed in the thesis answer the research questions RQ1-6 defined in Chapter 1. Furthermore, it shows how these methods complement the results of previous studies to give a comprehensive framework for the design of life-like control for multichannel MNPs for assisting of the walking.

REFERENCES

[1] G. M. Lyons, T. Sinkjaer, J. H. Burridge, and D. J. Wilcox, "A review of portable FES-based neural orthoses for the correction of drop foot," *IEEE Trans. Neural Syst. Rehabil. Eng.*, vol. 10, no. 4, pp. 260-279, 2002.

[2] D. Popović and T. Sinkjaer, "Neuroprosthesis," in *Control of Movement for the Physically Disabled*, 1 ed., London: Springer, 2000, pp. 209-294.

[3] P. H. Peckham and J. S. Knutson, "Functional electrical stimulation for neuromuscular applications," *Annu. Rev. Biomed. Eng.*, vol. 7 pp. 327-360, 2005.

[4] L. R. Sheffler and J. Chae, "Neuromuscular electrical stimulation in neurorehabilitation," *Muscle Nerve*, vol. 35, no. 5, pp. 562-590, 2007.

[5] W. Liberson, H. Holmquest, and M. Scott, "Functional electrotherapy: Stimulation of the common peroneal nerve synchronized with the swing phase of gait of hemiplegic subjects," *Arch. Phys. Med. Rehabil.*, vol. 42 pp. 202-205, 1961.

[6] F. Gračanin, T. Prevec, and J. Trontelj, "Evaluation of use of functional electronic peroneal brace in hemiparetic patients," in *Proc. Advances in External Control of Human Extremities* (CD), Dubrovnik, 1967.

[7] J. H. Burridge, P. N. Taylor, S. A. Hagan, D. E. Wood, and I. D. Swain, "The effects of common peroneal stimulation on the effort and speed of walking: A randomized controlled trial with chronic hemiplegic patients," *Clin. Rehabil.*, vol. 11, no. 3, pp. 201-210, 1997.

[8] M. Wieler, R. B. Stein, M. Ladouceur, M. Whittaker, A. W. Smith, S. Naaman, H. Barbeau, J. Bugaresti, and E. Aimone, "Multicenter evaluation of electrical stimulation systems for walking," *Arch. Phys. Med. Rehabil.*, vol. 80, no. 5, pp. 495-500, 1999.

[9] J. M. Hausdorff and H. Ring, "Effects of a new radio frequency-controlled neuroprosthesis on gait symmetry and rhythmicity in patients with chronic hemiparesis," *Am. J. Phys. Med. Rehabil.*, vol. 87, no. 1, pp. 4-13, 2008.

[10] W. G. Yergler, W. Wilemon, and D. McNeal, "An implantable peroneal nerve stimulator to correct equinovarus during walking," *J. Bone & Joint Surg.*, vol. 53 pp. 1660, 1971.

[11] R. L. Waters, D. McNeal, and J. Perry, "Experimental correction of footdrop by electrical stimulation of the peroneal nerve," *J. Bone & Joint Surg.*, vol. 57, no. 8, pp. 1047-1054, 1975.

[12] A. Jeglić, E. Vavken, and M. Benedik, "Implantable muscle/nerve stimulator as a part of an electronic brace," in *Proc. Advances in External Control of Human Extremities* (CD), Dubrovnik, 1970.

[13] J. Burridge, M. Haugland, B. Larsen, R. M. Pickering, N. Svaneborg, H. K. Iversen, P. B. Christensen, J. Haase, J. Brennum, and T. Sinkjaer, "Phase II trial to evaluate the ActiGait implanted drop-foot stimulator in established hemiplegia," *J. Rehabil. Med.*, vol. 39, no. 3, pp. 212-218, 2007.

[14] L. Kenney, G. Bultstra, R. Buschman, P. Taylor, G. Mann, H. Hermens, J. Holsheimer, A. Nene, M. Tenniglo, H. Van Der Aa, and J. Hobby, "An implantable two channel drop foot stimulator: Initial clinical results," *Artif. Organs*, vol. 26, no. 3, pp. 267-270, 2002.

[15] M. K. Haugland, A. Hoffer, and T. Sinkjaer, "Skin contact force information in sensory nerve signals recorded by implanted cuff electrodes," *IEEE Trans. Rehabil. Eng.*, vol. 2, no. 1, pp. 18-28, 1994.

[16] M. Hansen, M. Haugland, T. Sinkjær, and N. Donaldson, "Real time foot drop correction using machine learning and natural sensors," *Neuromodulation*, vol. 5, no. 1, pp. 41-53, 2002.

[17] L. Vodovnik, T. Bajd, A. Kralj, F. Gračanin, and P. Strojnik, "Functional electrical stimulation for control of locomotor systems," *Crit. Rev. Bioeng.*, vol. 6, no. 2, pp. 63-131, 1981.

[18] P. Strojnik, A. Kralj, and I. Uršić, "Programmed six-channel electrical stimulator for complex stimulation of leg muscles during walking," *IEEE Trans. Biomed. Eng.*, vol. 26, no. 2, pp. 112-116, 1979.

[19] U. Stanič, R. Aćimović-Janezić, and N. Gros, "Multichannel electrical stimulation for correction of hemiplegic gait. Methodology and preliminary results," *Scand. J. Rehabil. Med.*, vol. 10, no. 2, pp. 75-92, 1978.

[20] A. Kralj, and T. Bajd, *Functional Electrical Stimulation: Standing and walking after spinal cord injury* Boca Raton, Florida: CRC Press, 1989.

[21] A. Kralj, T. Bajd, and R. Turk, "Gait restoration in paraplegic patients: A feasibility demonstration using multichannel surface electrode FES," *J. Rehabil. Res. Dev.*, vol. 20, no. 1, pp. 3-20, 1983.

[22] A. Kralj, T. Bajd, R. Turk, and H. Benko, "Results of FES application to 71 SCI patients," RESNA '87, Meet the Challenge, in *Proc. 10th Annu. Conf. Rehabil. Technol.*, San Jose, CA, USA, pp. 645-647. 1987.

[23] D. Graupe and K. H. Kohn, "Functional neuromuscular stimulator for short-distance ambulation by certain thoracic-level spinal-cord-injured paraplegics," *Surg. Neurol.*, vol. 50, no. 3, pp. 202-207, 1998.

[24] M. Bijak, W. Mayr, M. Rakos, C. Hofer, H. ller, D. Rafolt, M. Reichel, S. Sauermann, C. Schmutterer, E. Unger, M. Russold, and H. Kern, "The Vienna functional electrical stimulation system for restoration of walking functions in spastic paraplegia," *Artif. Organs*, vol. 26, no. 3, pp. 224-227, 2002.

[25] M. R. Popović and T. Keller, "Modular transcutaneous functional electrical stimulation system," *Med. Eng. Phys.*, vol. 27, no. 1, pp. 81-92, 2005.

[26] D. B. Popović and T. Sinkjaer, "Neuromodulation of lower limb monoparesis: functional electrical therapy of walking," *Acta neurochir.*, vol. 97, no. Pt 1, pp. 387-393, 2007.

[27] R. Kobetič, R. J. Triolo, and E. B. Marsolais, "Muscle selection and walking performance of multichannel FES systems for ambulation in paraplegia," *IEEE Trans. Neural Syst. Rehabil. Eng.*, vol. 5, no. 1, pp. 23-29, 1997.

[28] R. Kobetič and E. B. Marsolais, "Synthesis of paraplegic gait with multichannel functional neuromuscular stimulation," *IEEE Trans. Neural Syst. Rehabil. Eng.*, vol. 2, no. 2, pp. 66-79, 1994.

[29] J. J. Daly, K. Roenigk, J. Holcomb, J. M. Rogers, K. Butler, J. Gansen, J. McCabe, E. Fredrickson, E. B. Marsolais, and R. L. Ruff, "A randomized controlled trial of functional neuromuscular stimulation in chronic stroke subjects," *Stroke*, vol. 37, no. 1, pp. 172-178, 2006.

[30] T. E. Johnston, R. R. Betz, B. T. Smith, B. J. Benda, M. J. Mulcahey, R. Davis, T. P. Houdayer, M. A. Pontari, A. Barriskill, and G. H. Creasey, "Implantable FES system for upright mobility and bladder and bowel function for individuals with spinal cord injury," *Spinal Cord*, vol. 43, no. 12, pp. 713-723, 2005.

[31] D. Guiraud, T. Stieglitz, K. P. Koch, J. L. Divoux, and P. Rabischong, "An implantable neuroprosthesis for standing and walking in paraplegia: 5-Year patient follow-up," *J. Neural Eng.*, vol. 3, no. 4, 2006.

[32] V. K. Mushahwar, P. L. Jacobs, R. A. Normann, R. J. Triolo, and N. Kleitman, "New functional electrical stimulation approaches to standing and walking," *J. Neural Eng.*, vol. 4, no. 3, 2007.

[33] A. Dutta, R. Kobetič, and R. J. Triolo, "Ambulation after incomplete spinal cord injury with EMG-triggered functional electrical stimulation," *IEEE Trans. Biomed. Eng.*, vol. 55, no. 2, pp. 791-794, 2008.

[34] D. B. Popović, "Control of walking in disabled humans," *J. Automatic Control*, vol. 13 (supplement) 2003.

[35] H. Gollee and K. J. Hunt, "Nonlinear modeling and control of electrically stimulated muscle: A local model network approach," *Int. J. Control*, vol. 68, no. 6, pp. 1259-1288, 1997.

[36] M. Ferrarin, F. Palazzo, R. Riener, and J. Quintern, "Model-based control of FES-induced single joint movements," *IEEE Trans. Neural Syst. Rehabil. Eng.*, vol. 9, no. 3, pp. 245-257, 2001.

[37] K. J. Hunt, R. P. Jaime, and H. Gollee, "Robust control of electrically-stimulated muscle using polynomial H$_\infty$ design," *Control Eng. Practice*, vol. 9, no. 3, pp. 313-328, 2001.

[38] F. Previdi and E. Carpanzano, "Design of a gain scheduling controller for knee-joint angle control by using functional electrical stimulation," *IEEE Trans. Control Syst. Technol.*, vol. 11, no. 3, pp. 310-324, 2003.

[39] F. Previdi, T. Schauer, S. M. Savaresi, and K. J. Hunt, "Data-driven control design for neuroprostheses: A virtual reference feedback tuning (VRFT) approach," *IEEE Trans. Control Syst. Technol.*, vol. 12, no. 1, pp. 176-182, 2004.

[40] S. Jezernik, R. G. V. Wassink, and T. Keller, "Sliding mode closed-loop control of FES: Controlling the shank movement," *IEEE Trans. Biomed. Eng.*, vol. 51, no. 2, pp. 263-272, 2004.

[41] S. J. Lister, N. B. Jones, S. K. Spurgeon, and J. J. A. Scott, "Simulation of human gait and associated muscle activation strategies using sliding-mode control techniques," *Sim. Mod. Practice Theory*, vol. 14, no. 5, pp. 586-596, 2006.

[42] S. Mohammed, P. Poignet, and D. Guiraud, "Closed loop nonlinear model predictive control applied on paralyzed muscles to restore lower limbs functions," in *Proc. 2006 IEEE/RSJ Int. Conf. Intelli. Robots Syst.*, IROS, Beijing, pp. 259-264, 2006.

[43] T. Fuhr, J. Quintern, R. Riener, and G. Schmidt, " Walking with WALK!," *IEEE Eng. Med. Biol. Mag.,* vol. 27, no. 1, pp. 38-48, 2008.

[44] A. Prochazka, "Comparison of natural and artificial control of movement," *IEEE Trans. Neural Syst. Rehabil. Eng.*, vol. 1, no. 1, pp. 7-17, 1993.

[45] P. C. Sweeney, G. M. Lyons, and P. H. Veltink, "Finite state control of functional electrical stimulation for the rehabilitation of gait," *Med. Biol. Eng. Comput.*, vol. 38, no. 2, pp. 121-126, 2000.

[46] H. M. Franken, P. H. Veltink, and H. K. Boom, "Restoring gait in paraplegics by functional electrical stimulation," *IEEE Eng. Med. Biol. Mag.*, vol. 13, no. 4, pp. 564-570, 1994.

[47] P. H. Veltink, W. De Vries, H. J. Hermens, G. Baardman, M. Ijzerman, S. Heinze, A. V. Nene, G. Zilvold, and H. B. K. Boom, "A comprehensive FES system for mobility restoration in paraplegics," in Pedotti, A., Ferrarin, M., Quintern, J., and Riener, R. (eds.) *Neuroprosthetics: from basic research to clinical application* Berlin-Heidelberg: Sringer Verlag, 1996, pp. 163-169.

[48] "The organization of movement," in Kandel, E. R., Schwartz, J. H., and Jessell, T. M. (eds.) *Principles of neural science* 4 ed. McGraw-Hill, 2000, pp. 653-673.

[49] S. Jonić, T. Janković, V. Gajić, and D. Popović, "Three machine learning techniques for automatic determination of rules to control locomotion," *IEEE Trans. Biomed. Eng.*, vol. 46, no. 3, pp. 300-310, 1999.

[50] Anonymous. MEMS and Sensors (2008, June 4), Available: http://www.analog.com/en/ cat/0,2878,764,00.html.

[51] M. J. Mathie, A. C. F. Coster, N. H. Lovell, and B. G. Celler, "Accelerometry: Providing an integrated, practical method for long-term, ambulatory monitoring of human movement," *Physiol. Measur.*, vol. 25, no. 2, 2004.

[52] H. J. Luinge and P. H. Veltink, "Measuring orientation of human body segments using miniature gyroscopes and accelerometers," *Med. Biol. Eng. Comput.*, vol. 43, no. 2, pp. 273-282, 2005.

[53] R. E. Mayagoitia, A. V. Nene, and P. H. Veltink, "Accelerometer and rate gyroscope measurement of kinematics: an inexpensive alternative to optical motion analysis systems," *J. Biomech.*, vol. 35, no. 4, pp. 537-542, 2002.

[54] S. Mangold, M. R. Popović, and T. Keller, "Muscle activity during normal walking and its relevance for the functional electrical stimulation applications," in *Proc. 7th Vienna Int. Workshop FES*, Vienna, Austria. 2001.

[55] Z. M. Nikolić and D. B. Popović, "Predicting quadriceps muscle activity during gait with an automatic rule determination method," *IEEE Trans. Biomed. Eng.*, vol. 45, no. 8, pp. 1081-1085, 1998.

[56] N. Matsushita, Y. Handa, M. Ichie, and N. Hoshimiya, "Electromyogram analysis and electrical stimulation control of paralyzed wrist and hand," *J. Electromyogr. Kinesiol.*, vol. 5, no. 2, pp. 117-128, 1995.

[57] A. Erdemir, S. McLean, W. Herzog, and A. J. van den Bogert, "Model-based estimation of muscle forces exerted during movements," *Clin. Biomech.*, vol. 22, no. 2, pp. 131-154, 2007.

[58] M. G. Pandy, "Computer modeling and simulation of human movement," *Annu. Rev. Biomed. Eng.*, vol. 3 pp. 245-273, 2001.

[59] D. Popović, R. B. Stein, M. N. Oguztoreli, M. Lebiedowska, and S. Jonić, "Optimal control of walking with functional electrical stimulation: A computer simulation study," *IEEE Trans. Rehabil. Eng.*, vol. 7, no. 1, pp. 69-79, 1999.

[60] R. B. Stein, E. P. Zehr, M. K. Lebiedowska, D. B. Popović, A. Scheiner, and H. J. Chizeck, "Estimating mechanical parameters of leg segments in individuals with and without physical disabilities," *IEEE Trans. Rehabil. Eng.*, vol. 4, no. 3, pp. 201-211, 1996.

[61] D. Popović, M. Radulović, L. Schwirtlich, and N. Jauković, "Automatic vs. hand-controlled walking of paraplegics," *Med. Eng. Phys.*, vol. 25, no. 1, pp. 63-73, 2003.

[62] A. Kostov, B. J. Andrews, D. B. Popović, R. B. Stein, and W. W. Armstrong, "Machine learning in control of functional electrical-stimulation systems for locomotion," *IEEE Trans. Biomed. Eng.*, vol. 42, no. 6, pp. 541-551, 1995.

[63] M. N. Oguztoreli, D. Popović, and R. B. Stein, "Optimal control for musculo-skeletal systems," *J. Automatic Control*, vol. 4 pp. 1-16, 1994.

[64] D. Popović and S. Jonić, "Control of bipedal locomotion assisted with functional electrical stimulation," in *Proc. Am. Control Conf.*, pp. 1238-1242, San Diego, California, 1999.

[65] S. Jonić and D. Popović, "Machine learning for prediction of muscle activations for a rule-based controller," in *Proc. Annu. Int. Conf. IEEE EMBS*, vol. 4, pp. 1781-1784, NJ, United States, 1997.

[66] A. E. Bryson, *Dynamic Optimization*. Menlo Park, CA: Addison Wesley Longman, 1999.

[67] R. Baratta, M. Solomonow, B. H. Zhou, D. Letson, R. Chuinard, and R. D'Ambrosia, "Muscular coactivation. The role of the antagonist musculature in maintaining knee stability," *Am. J. Sports Med.*, vol. 16, no. 2, pp. 113-122, 1988.

[68] Y. K. Thong, M. S. Woolfson, J. A. Crowe, B. R. Hayes-Gill, and D. A. Jones, "Numerical double integration of acceleration measurements in noise," *Measurement*, vol. 36, no. 1, pp. 73-92, 2004.

CHAPTER 2
A New Tool for Designing the Control of Walking in Individuals with Disabilities[*]

Summary–Sensorimotor model (SMM) is an essential component for the design of rules for rule-based control of gait by means of functional electrical stimulation. The SMM comprises sensory part (sensor data) and motor part (muscle activation profiles). The muscle activation profiles are generated by using biomechanical gait simulations. It is important for the simulations to use models that can be customized for an individual with disability. In this chapter, we describe our method for customized modeling and simulations (CMS). The CMS is based on optimal control and uses a reduced musculoskeletal model. The model comprises only the parameters that can be experimentally identified in a given subject. The optimal control is based on static optimization that minimizes tracking errors from desired gait pattern while penalizing total muscle efforts. Importantly, the optimization that we developed is flexible; the tracking errors can be defined in different phase spaces, that is, in terms of segment angles, angular velocities or angular accelerations. Therefore, inputs (desired trajectories) for optimization can be provided by using different gait sensors (e.g., goniometers, gyroscopes, and accelerometers). The outputs from the simulation are: 1) profiles of activation for the muscles involved in leg control, and 2) gait pattern generated when the calculated profiles are applied as inputs to the model. Since the model is customized to the subject, the activations are generated by taking into account the current status of the subject's neuromusculoskeletal system. We implemented the simulations as a user friendly software tool named OptiWalk. OptiWalk is a Windows compatible application developed in Microsoft Visual Studio .NET and Matlab. It integrates a database of subjects, a database of gait patterns, an optimization engine and a graphical user interface. The database of subjects stores model parameters. The database of gait patterns is a set of functional gait patterns recorded from able-bodied subjects walking at a range of gait speeds. The optimization engine implements optimal control. Graphical user interface is responsible for interaction with a user and visualization of simulation inputs and outputs. Typical OptiWalk use case scenario comprises following steps: 1) subject's model parameters are loaded from the database of subjects; 2) a desired gait pattern for the subject is loaded from the database of gait patterns; 3) optimization algorithm is selected and optimization parameters are set; 4) optimal control simulation is started; 5) calculated muscle activation profiles and generated joint angles are plotted; 6) generated gait is animated in the form of a stick figure. The whole process (steps 1–6) can be repeated iteratively and interactively, as shown in the example that we provided, until desired results are obtained. OptiWalk allows testing the feasibility of different gait patterns for a particular disabled individual. Namely, the simulation shows if the subject's muscles are strong enough to generate the desired gait. Additionally, OptiWalk allows testing the minimal plant responses (e.g., minimal muscle strength) that are needed for particular activity. In case a desired gait pattern is feasible, the simulation provides timing and pattern of muscle activation that is necessary to generate the selected gait in a given disabled individual. The calculated muscle activation profiles together with sensor data make up an SMM. The SMM can be used as a knowledge base for machine learning that generates the rules for real-time control of walking.

1. INTRODUCTION

1.1. Musculoskeletal modeling and simulations

Human body can be modeled as a system of rigid segments connected by joints. The system is driven by a set of biological actuators (musculo-tendon units) which produce forces acting on the segments. Both the magnitude and direction of the generated forces depend on the current geometry of the system (musculoskeletal geometry). Therefore, a complete model of the musculoskeletal system has to include three interdependent parts: 1) a model of the mechanical linkage (body segmental dynamics, 2) a model of the actuator (musculo-tendon dynamics), and 3) a description of the musculoskeletal geometry.

The first research efforts in the field of modeling and simulation of human movements were directed towards formulating mathematical models of body segmental dynamics. The goal was to develop methods for setting up equations of motion in the form which is convenient for computer implementation. Pioneering work was done in the mid-seventies by Stepanenko and Vukobratović [1] who used a Newton-Euler approach to dynamics, instead of somewhat more traditional Lagrangian approach, to derive differential equations for spatial open-chain mechanisms. This work was revised by Orin and colleagues [2] for the legs of walking robots. They improved the efficiency by writing the forces and moments in the local link reference frames instead of the inertial frame. Armstrong [3] and Luh *et al.* [4] improved computational efficiency even further by setting up the calculations in an iterative (or recursive) manner. Koozekanani *et al.* [5] applied a recursive free body approach to estimate joint torques associated with observed human postural motion in sagittal plane.

Huston *et al.* [6] used Langrange's form of D'Alambert's principle to develop a full set of governing dynamical equations for a 15 segment 34 degrees-of-freedom (DoF) whole body model. Onyshko and Winter [7] applied Lagrangian mechanics to derive equations of motion for a 7 segment planar model. The model was used to describe and study human gait by implementing forward dynamics simulation. Initial conditions and joint toque histories were used as inputs for the model and the system response (generated gait pattern) was the output. Hatze [8] used the traditional Lagrangian approach to define a comprehensive mathematical model of the human musculoskeletal system. In addition to link-mechanical equations of motion describing the so called body segmental dynamics, the model included musculo-mechanical equations for muscle dynamics. Hatze [9] also reported a simulation of a take-off phase of a long-jump using a 17 segment model driven by 46 muscles.

Marshall *et al.* [10] used a general Newtonian approach to simulate a non-branching N-segment open chain model of the human body. Similarly to the approach of Onyshko and Winter [7], the model was used for direct dynamics simulations of planar movements of upper and lower extremities. Khang and Zajac [11], [12] developed a planar computer model to investigate paraplegic standing induced by functional electrical stimulation (FES). Yamaguchi and Zajac [13] used a three-dimensional 8 DoF model to determine a minimal set of muscles that could approximate able-bodied gait trajectories without requiring either high levels of force or precise control of muscle activation. The muscle stimulation profiles were determined by a combination of dynamic programming and open-loop, trial-and-error adjustment.

Due to ever increasing computational resources, a number of studies introducing large scale musculoskeletal models and various numerical optimization methods were developed and presented in literature [14]. Pandy *et al.* [15] introduced a method termed control vector parameterization [16] in the simulation of large scale musculoskeletal systems. In this approach, muscle excitations are approximated by piecewise linear functions using a set of so called nodal points, which then become the variables in the resulting parameter optimization problem. Anderson and Pandy [17] applied this method for simulation of gait using a three-dimensional 23 DoF musculoskeletal model actuated by 54 muscles. Instead of tracking experimentally recorded data, they used dynamic optimization to predict body motions, ground reaction forces and muscle excitation patterns by minimizing metabolic energy expenditure per unit distance traveled. Neptune *et al.* [18] parameterized muscle excitations by modeling them as block patterns characterized by three parameters: onset, duration and magnitude. They implemented simulated annealing

optimization algorithm for tracking experimentally recorded gait kinematics using a planar 9 DoF model driven by 15 muscles. Control vector parameterization approach in the form of single and multiple shooting was also applied to simulations of cycling (2 DoF, 9 muscles [19]), running (20 DoF, 14 muscles [20]) and vertical jumping (3 DoF, 9 muscles [21]).

Control vector parameterization is computationally expensive method. Control inputs are easily reconstructed from nodal points, but the cost function, system state trajectories and sensitivities have to be calculated by integrating the system equations. Therefore, a number of integrations have to be done in each optimization step. Direct collocation method [22], on the contrary, parameterizes both the system states and the controls. System differential equations are transcribed into a set of algebraic equality constraints. Therefore, there is no need for their explicit integration during optimization. Stelzer and Stryk [23] compared direct collocation and direct shooting in the simulation of human kicking motion for 2 DoF planar leg model actuated by 5 muscles. They reported improvement of about two orders-of-magnitude in numerical efficiency when using direct collocation.

Thelen *et al.* [24] presented a new algorithm named computed muscle control that uses static optimization along with feedforward and feedback control to drive the model toward a set of desired kinematics. The method is computationally efficient since it requires only a single integration of system equations. They applied computed muscle control to drive 3 DoF, 30 muscle model of pedaling. Later, Thelen and Anderson [25] used the same method to compute muscle excitations for one half of a gait cycle for 21 DoF, 92 muscle model. The solution was obtained an order of magnitude faster compared to conventional dynamic optimization. Seth and Pandy [26] presented another computationally efficient two-stage algorithm for calculation of muscle excitations from the observed motion data. The algorithm was based on feedback linearization and linear quadratic tracking. They simulated vertical jumping using 6 DoF, 9 muscle model and reported 3 orders-of-magnitude less CPU time compared to dynamic optimization based on control vector parameterization approach.

1.2. Customized musculoskeletal modeling and simulations for the control of FES

The aforementioned approaches for simulation of human movement use complex and sophisticated musculoskeletal models comprising a number of segments and muscles. The muscles are modeled individually by specifying detailed geometry (e.g., insertion points, via points, pinnation angles) and biomechanical characteristics (e.g., maximal isometric force) for each muscle. Often, muscle models include muscle composition (e.g., ratio of slow and fast fibers) and dynamics of biochemical processes at the cellular level (e.g., Ca^{2+} uptake). These detailed musculoskeletal models are very important since they give crucial insights and conclusions about general biomechanics of human movement [14]. The data from these simulations can assist in understanding individual muscle function and contribution [18], relationship between muscle activity and generated movement kinematics and kinetics, muscle coordination, strategies used by the central nervous system for the control of movement [27] etc.

However, the existing models, being highly sophisticated and detailed, have poor user interface and are generally difficult to work with; large number of parameters, from muscle fiber properties to mechanical parameters of leg segments, have to be specified before starting the simulation. Many of these parameters are difficult and some are even impossible to identify experimentally. As a result, the models are generally not customized for a given individual. Therefore, the existing models are not applicable for designing a real-time control that would lead to a practical FES system for gait restoration. For this specific purpose, a model is needed that is tractable in a practical situation.

A distinction can be made between the attempts to deal with an essentially complete system (human body walking on the ground) and reduced models. Problem could be simplified by reducing the number of DoF in the model by, for example, treating the motion in only one plane at a time, or reducing the number of links in the model. Consequently, attempts to analyze multi-joint structures are often characterized by a search for ways of reducing the number of DoF to a manageable level. The dynamics of motion confined to a plane is much simpler than that in three dimensions. Fortunately, locomotion can often be decomposed into a dominant component in the sagittal plane with much smaller contributions to the progression in the frontal and horizontal planes.

The motor disability caused by an injury or a disease of the central nervous system changes greatly the

response of the sensory-motor systems; the muscles are weaker, reflexes and central control are abnormal and viscoelastic joint properties are altered as well. Therefore, a model that would lead to an effective control of FES has to take into account the current status of the musculoskeletal system of a potential user.

In this chapter, we present a methodology for optimal control of FES for gait restoration based on a reduced model of gait that can be customized for a potential user of FES. The model parameters can be identified experimentally. The approach is implemented and demonstrated as an interactive and user-friendly software tool for biomechanical simulations. The tool starts from the desired trajectory and the user characteristic model parameters and calculates the profiles of muscle activations for the leg muscles. The cost function for optimization is the tracking error from the desired gait pattern and the total muscle efforts.

The simulation inputs (sensory information) and outputs (muscle activation profiles) constitute a sensorimotor model (SMM) of gait. The SMM can be used as a knowledge base for implementation of machine learning (see Chapter 1, Fig. 1.6). The machine learning generates the rules for real-time artificial reflex control of FES (see Chapter 1, Fig. 1.5). Importantly, since the muscle activations are determined by using customized modeling and simulation approach (CMS), the resulting control (i.e., the rules) takes into account the current status of an impaired neuromusculoskeletal system.

2. REDUCED MUSCULOSKELETAL MODEL AND SIMULATION

2.1. *Musculoskeletal model*

In order to obtain the model of manageable complexity that can be customized to a given user, we adopted a number of deliberate simplifications. We reduced the system to a planar musculoskeletal model of one leg (see Fig. 2.1). The model comprises three rigid bodies (thigh, shank, and foot) connected by pin joints (hip, knee and ankle). The joints allow hip and knee flexion/extension and ankle dorsi/plantar
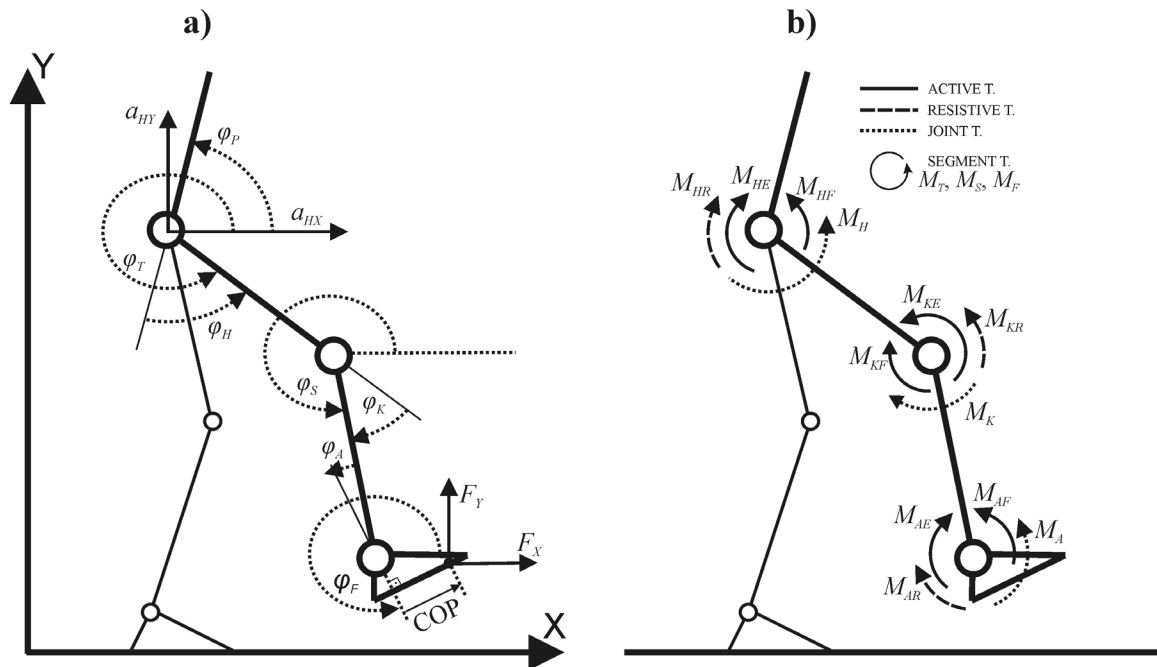
Fig. 2.1. Biomechanical model: a) angles and interface forces (gait pattern signals), and b) torques considered. The notations are: M_{HF}, M_{KF}, M_{AF} are active torques produced by the equivalent flexor muscles in the hip, knee and ankle joints; M_{HE}, M_{KE}, M_{AE} are active torques produced by the equivalent extensor muscles in the hip, knee and ankle joints; M_{HR}, M_{KR}, M_{AR} are resistive (viscoelastic) torques in the hip, knee and ankle joints; M_H, M_K, M_A are the net joint torques; M_T, M_S, M_F are the net torques acting at the thigh, shank and foot segments; φ_P, φ_T, φ_S, φ_F are absolute angles of the pelvis, thigh, shank and foot from horizontal axis; φ_H, φ_K, φ_A are hip, knee and ankle joint angles; F_X, F_Y are horizontal and vertical component of ground reaction force; COP is the position of the center of pressure along the sole of the foot; a_{HX}, a_{HY} are horizontal and vertical acceleration of the hip.

flexion. Although the system is reduced to only one leg, the simulation takes into account the whole body. The influence of the rest of body (trunk/head/arms and the other leg) is represented by the interface forces and torques acting at the hip. The interaction with the ground is modeled by a ground reaction force acting at the sole of the foot in the center of pressure. It is assumed that the center of pressure moves along the sole during the stance phase of gait. The variables prescribing the interaction with the environment (hip inertial information and ground reaction force data) are supplied as inputs for the simulation. The whole system can be regarded as a triple pendulum with the hip being a moving hanging point. Each leg segment is described by four parameters – mass (m), length (L), distance of the center of mass from the proximal joint (d), and moment of inertia about the central axis perpendicular to the sagittal plane (J_C) (see Appendix).

Since identifying the characteristics of individual muscles (geometry and strength) is generally unfeasible, the muscles are not modeled individually. Instead, the groups of muscles were modeled and adopted as actuators driving the model. Namely, an equivalent flexor/extensor muscle substitutes all monoarticular and biarticular muscles that act to flex/extend the joint. Therefore, there are six equivalent muscles in total – a pair of antagonists per joint. They are modeled as nonlinear torque generators. Viscoelastic joint properties reflecting the influence of passive tissues crossing the joints are modeled as nonlinear resistive torques. The models and the parameters for the active and resistive torques are described later.

Importantly, the muscles', viscoelastic joints', and segments' parameters for the model can be experimentally identified. A practical, although not very precise, procedure of determining these parameters is given in Stein *et al.* [28].

Dynamics of the system (see Fig. 2.1) are described by the following matrix equation:

$$\begin{bmatrix} \ddot{\varphi}_T \\ \ddot{\varphi}_S \\ \ddot{\varphi}_F \end{bmatrix} = \mathbf{A}^{-1}(\mathbf{\Phi}) \left(\mathbf{B}(\mathbf{\Phi}) \begin{bmatrix} \dot{\varphi}_T^2 \\ \dot{\varphi}_S^2 \\ \dot{\varphi}_F^2 \end{bmatrix} + \mathbf{C}(\mathbf{\Phi}) + \mathbf{D}(\mathbf{\Phi}) \begin{bmatrix} F_X \\ F_Y \end{bmatrix} + \mathbf{E}(\mathbf{\Phi}) \begin{bmatrix} a_{HX} \\ a_{HY} \end{bmatrix} + \mathbf{T} \begin{bmatrix} M_{HF} - M_{HE} - M_{HR} \\ M_{KF} - M_{KE} - M_{KR} \\ M_{AF} - M_{AE} - M_{AR} \end{bmatrix} \right) \tag{2.1}$$

where $\mathbf{\Phi}=[\varphi_T \; \varphi_S \; \varphi_F]^{\mathrm{T}}$ is a vector of thigh, shank and foot segment angles from the horizontal axis; $[M_H \; M_K \; M_A]^{\mathrm{T}}$ is a vector consisting of hip, knee and ankle joint torques; $[F_X \; F_Y]^{\mathrm{T}}$ is a vector of horizontal and vertical components of ground reaction force; $[a_{HX} \; a_{HY}]^{\mathrm{T}}$ is a vector comprising horizontal and vertical components of hip acceleration; $\mathbf{A}(\mathbf{\Phi})$ is 3 x 3 system mass matrix; $\mathbf{B}(\mathbf{\Phi})$ is 3 x 3 matrix describing centrifugal effects; $\mathbf{C}(\mathbf{\Phi})$ is 3 x 1 vector containing only gravitational terms, $\mathbf{E}(\mathbf{\Phi})$ and $\mathbf{D}(\mathbf{\Phi})$ are 3 x 2 matrices describing the influence of interface forces and torques acting at the hip and the foot-sole, respectively; $\mathbf{T}$ is 3 x 3 matrix describing how the joint torques M_H, M_K, and M_A contribute to total torques M_T, M_S, and M_F acting at the segments. The joint torques in (2.1) are already expressed as sums of active (M_{HF}, M_{KF}, M_{AF}, M_{HE}, M_{KE}, M_{AE}) and resistive torques (M_{HR}, M_{KR}, M_{AR}) [see Fig. 2.1(b)]. The matrices $\mathbf{A}$–$\mathbf{E}$ and $\mathbf{T}$ are given in Appendix.

2.1.1. Model of equivalent muscle

Nonlinear model of muscle dynamics used for joint angle control in this simulation is a modified version of the Hill model. It is a well known tree component multiplicative muscle model used in several other studies [29]–[31]. The active torque (M_a) generated at the joint by the equivalent muscle depends on the activation (u), joint angle (φ) and joint angular velocity ($d\varphi/dt$):

$$M_a = f(\varphi)g(\dot{\varphi})u. \tag{2.2}$$

The function $f(\varphi)$ is maximal isometric torque versus joint angle characteristics of the muscle. The function $g(d\varphi/dt)$ is normalized torque versus joint angular velocity characteristics of the muscle. It is a scaling factor that has the value of 1 under isometric conditions ($d\varphi/dt = 0$). The product of the first two terms in (2.2), that is, $M_{max}(\varphi, d\varphi/dt) = f(\varphi)g(d\varphi/dt)$, represents maximal torque that the muscle can generate for the given joint angle φ and angular velocity $d\varphi/dt$. The variable $u \in [0,1]$ is normalized level of muscle activation (0–muscle is relaxed; 1–muscle is fully activated). It is the control input for the muscle and gives the torque M_a generated by the muscle as the fraction of the maximal torque M_{max}

($M_a = uM_{max}(\varphi, d\varphi/dt)$). We used muscle activation u as the control input for the muscle in order to simplify the problem. The more complete model would include the muscle activation dynamics $a(u)$ [29]. In that case, the term u would be muscle excitation (control input) and the muscle activation (muscle state) would be the output of the low-pass critically damped filter $a(u)$. In Chapter 3 of this thesis we present an algorithm which uses such a complete muscle model.

The function $f(\varphi)$ is modeled by a quadratic curve $F(\varphi)$:

$$f(\varphi) = \begin{cases} F(\varphi), F(\varphi) > 0 \\ 0 \quad , F(\varphi) \leq 0 \end{cases} \quad \wedge \quad F(\varphi) = c_0 + c_1\varphi + c_2\varphi^2. \tag{2.3}$$

The parameters c_i ($i = 0, 1, 2$) give the shape of the profile and represent the best 2nd order fit through experimentally recorded data (isometric tests).

The function $g(d\varphi/dt)$ is simulated by a piecewise linear curve:

$$g(\dot{\varphi}) = \begin{cases} c_4, \quad G(\dot{\varphi}) > c_4 \\ G(\dot{\varphi}), \ 0 \leq G(\dot{\varphi}) \leq c_4 \quad \wedge \quad G(\dot{\varphi}) = 1 + c_3\dot{\varphi}. \\ 0, \quad G(\dot{\varphi}) < 0 \end{cases} \tag{2.4}$$

The parameters c_3 and c_4 are determined experimentally (isokinetic tests) and give the slope and saturation of the profile $g(d\varphi/dt)$, respectively. It is known from the muscle physiology that the muscles can generate higher (lower) forces during eccentric (concentric) contractions compared to isometric conditions. Therefore, the parameter c_3 (the slope) is positive for extensor and negative for flexor equivalent muscle.

2.1.2. Viscoelastic joint properties

Passive joint properties were modeled by a linear viscoelastic term and a nonlinear double exponential term:

$$M_p = d_0(\varphi - \varphi_0) + d_1\dot{\varphi} + d_2 e^{d_3\varphi} - d_4 e^{d_5\varphi}. \tag{2.5}$$

The nonlinear term represents resistive torque around terminal joint positions. The angle φ_0 is the neutral joint position in which the elastic torque is zero. The parameters d_i ($i = 0, 1, 2, 3, 4, 5$) can be estimated by using passive tests (pendulum and pull tests) [28].

2.2. Simulation

Mathematical model given in (2.1) was transformed into a state space form. First, the active (M_{HF}, M_{KF}, M_{AF}, M_{HE}, M_{KE}, M_{AE}) and resistive torques (M_{HR}, M_{KR}, M_{AR}) were expressed by using the equations (2.2) and (2.5), respectively. Then, a vector of state variables comprising segment angles (φ_T, φ_S, φ_F) and segment angular velocities ($d\varphi_T/dt$, $d\varphi_S/dt$, $d\varphi_F/dt$) was introduced. After some rearrangement and grouping, mathematical model in the state-space form was obtained:

$$\dot{x}_1(t) = x_2(t)$$

$$\dot{x}_2(t) = P_2(\mathbf{X}(t), t) + \sum_{i=1}^{6} R_{2,i}(\mathbf{X}(t), t) u_i(t) = A_2(\mathbf{X}(t), \mathbf{U}(t))$$

$$\dot{x}_3(t) = x_4(t)$$

$$\dot{x}_4(t) = P_4(\mathbf{X}(t), t) + \sum_{i=1}^{6} R_{4,i}(\mathbf{X}(t), t) u_i(t) = A_4(\mathbf{X}(t), \mathbf{U}(t)) \tag{2.6}$$

$$\dot{x}_5(t) = x_6(t)$$

$$\dot{x}_6(t) = P_6(\mathbf{X}(t), t) + \sum_{i=1}^{6} R_{6,i}(\mathbf{X}(t), t) u_i(t) = A_6(\mathbf{X}(t), \mathbf{U}(t)).$$

The vector $\mathbf{X} = [x_i]$ ($i = 1, 2, 3, 4, 5, 6$) is vector of state variables. The variables $x_1 = \varphi_F$, $x_2 = d\varphi_F/dt$,

$x_3 = \varphi_S$, $x_4 = d\varphi_S/dt$, $x_5 = \varphi_T$, and $x_6 = d\varphi_T/dt$ are segment angles and angular velocities. The vector $\mathbf{U} = [u_i]$ ($i = 1, 2, 3, 4, 5, 6$) is vector of muscle activations for the six equivalent muscles driving the system. They are the control inputs and their determination is the purpose of the simulation. The terms $P_i(\mathbf{X}, t)$ and $R_{i,j}(\mathbf{X}, t)$ ($i = 2, 4, 6$ and $j = 1, 2, 3, 4, 5, 6$) are nonlinear functions of the system state $\mathbf{X}$ and the variables that are given as inputs for the simulation (i.e., hip accelerations–a_{HX}, a_{HY} and ground reaction force data–F_X, F_Y, COP). Note that the expressions A_i ($i = 2, 4, 6$) express segment angular accelerations dx_i/dt ($i = 2, 4, 6$) as functions of the current system state $\mathbf{X}(t)$ and inputs $\mathbf{U}(t)$.

Discrete form of the model (2.6) can be obtained by using finite difference approximations of the derivatives (i.e., $dx_i/dx \sim [x_i(n+1)-x_i(n)]/h$):

$$x_1(n+1) = x_1(n) + hx_2(n)$$

$$x_2(n+1) = x_2(n) + hP_2(\mathbf{X}(n),n) + h\sum_{i=1}^{6} R_{2,i}(\mathbf{X}(n),n)u_i = B_2(\mathbf{X}(n),\mathbf{U}(n))$$

$$x_3(n+1) = x_3(n) + hx_4(n)$$

$$x_4(n+1) = x_4(n) + hP_4(\mathbf{X}(n),n) + h\sum_{i=1}^{6} R_{4,i}(\mathbf{X}(n),n)u_i = B_4(\mathbf{X}(n),\mathbf{U}(n))$$

$$x_5(n+1) = x_5(n) + hx_6(n)$$

$$x_6(n+1) = x_6(n) + hP_6(\mathbf{X}(n),n) + h\sum_{i=1}^{6} R_{6,i}(\mathbf{X}(n),n)u_i = B_6(\mathbf{X}(n),\mathbf{U}(n)).$$

(2.7)

The parameters h and n denote sampling period and sample number (i.e., simulation step), respectively. Note that the expressions B_i ($i = 2, 4, 6$) predict segment angular velocities x_i ($i = 2, 4, 6$) in the next simulation step (i.e., $n+1$) by using the current system state $\mathbf{X}(n)$ and inputs $\mathbf{U}(n)$.

Finally, the following equations are obtained by incrementing the indices in (2.7) from ($n+1$) to ($n+2$) and then substituting (2.7) in the obtained expressions:

$$x_1(n+2) = x_1(n) + 2hx_2(n) + h^2 P_2(\mathbf{X}(n),n) + h^2 \sum_{i=1}^{6} R_{2,i}(\mathbf{X}(n),n)u_i = C_1(\mathbf{X}(n),\mathbf{U}(n))$$

$$x_3(n+2) = x_3(n) + 2hx_4(n) + h^2 P_4(\mathbf{X}(n),n) + h^2 \sum_{i=1}^{6} R_{4,i}(\mathbf{X}(n),n)u_i = C_3(\mathbf{X}(n),\mathbf{U}(n))$$

(2.8)

$$x_5(n+2) = x_5(n) + 2hx_6(n) + h^2 P_6(\mathbf{X}(n),n) + h^2 \sum_{i=1}^{6} R_{6,i}(\mathbf{X}(n),n)u_i = C_5(\mathbf{X}(n),\mathbf{U}(n)).$$

The expressions C_i ($i = 1, 3, 5$) predict segment angles x_i ($i = 1, 3, 5$) two steps ahead (i.e., $n+2$) from the current simulation step by using the current system state $\mathbf{X}(n)$ and inputs $\mathbf{U}(n)$.

The task of the simulation is to determine muscle activations $u_i(n)$ ($i = 1, 2, 3, 4, 5, 6$) that produce muscle forces adequate to generate desired gait pattern with minimal muscle efforts. The simulation can be formulated as an optimization problem in which the goal is to minimize tracking errors from desired trajectory $\mathbf{X}^*(n)$ and levels of muscle activations. The trajectory $\mathbf{X}^*(n)$ can be expressed equivalently in different phase spaces, that is, it can be given as: c) a set of desired segment angles x_i^* ($i = 1, 3, 5$), 2) a set of desired segment angular velocities x_i^* ($i = 2, 4, 6$), or 3) a set of desired segment angular accelerations dx_i^*/dt ($i = 2, 4, 6$). The expressions C_i ($i = 1, 3, 5$), B_i ($i = 2,4,6$) and A_i ($i = 2, 4, 6$) are used to form the cost functions $C(n)$, $B(n)$ and $A(n)$ for the tracking of trajectories that are given in the phase space of angles, angular velocities or angular accelerations, respectively:

$$\min_{\mathbf{U}(n)} C(n) = \min_{\mathbf{U}(n)} \left[\left(\frac{x_1^*(n+2) - C_1(\mathbf{X}(n), \mathbf{U}(n))}{x_{1MAX}^*} \right)^2 + \left(\frac{x_3^*(n+2) - C_3(\mathbf{X}(n), \mathbf{U}(n))}{x_{3MAX}^*} \right)^2 + \right.$$
$$\left. + \left(\frac{x_5^*(n+2) - C_5(\mathbf{X}(n), \mathbf{U}(n))}{x_{5MAX}^*} \right)^2 + \lambda \sum_{i=1}^{6} u_i^2 \right].$$

(2.9)

$$\min_{\mathbf{U}(n)} B(n) = \min_{\mathbf{U}(n)} \left[\left(\frac{x_2^*(n+1) - B_2(\mathbf{X}(n), \mathbf{U}(n))}{x_{2MAX}^*} \right)^2 + \left(\frac{x_4^*(n+1) - B_4(\mathbf{X}(n), \mathbf{U}(n))}{x_{2MAX}^*} \right)^2 + \right.$$
$$\left. + \left(\frac{x_6^*(n+1) - B_6(\mathbf{X}(n), \mathbf{U}(n))}{x_{6MAX}^*} \right)^2 + \lambda \sum_{i=1}^{6} u_i^2 \right].$$

(2.10)

$$\min_{\mathbf{U}(n)} A(n) = \min_{\mathbf{U}(n)} \left[\left(\frac{\dot{x}_2^*(n) - A_2(\mathbf{X}(n), \mathbf{U}(n))}{\dot{x}_{2MAX}^*} \right)^2 + \left(\frac{\dot{x}_4^*(n) - A_4(\mathbf{X}(n), \mathbf{U}(n))}{\dot{x}_{4MAX}^*} \right)^2 + \right.$$
$$\left. + \left(\frac{\dot{x}_6^*(n) - A_6(\mathbf{X}(n), \mathbf{U}(n))}{\dot{x}_{6MAX}^*} \right)^2 + \lambda \sum_{i=1}^{6} u_i^2 \right].$$

(2.11)

The first three terms in (2.9)–(2.11) are the sum of squares of normalized tracking errors (in different phase spaces) and the last term is the total muscle effort expressed as the sum of squares of muscle activation levels. The parameter λ is the weighting factor. The terms $x_{i,MAX}^*$ ($i = 1, 2, 3, 4, 5, 6$) and $dx_{i,MAX}^*/dt$ ($i = 2, 4, 6$) are maximal values of the respective signals comprising the desired trajectory.

The cost functions (2.9)–(2.11) are nonlinear with respect to muscle activations $\mathbf{U}(n)$. Furthermore, the optimization is subject to constraints due to musculoskeletal physiology. Namely, the joint and segment angles have to be within the physiological ranges of motion. Muscle activation has to be between zero and one. The constraints can be expressed in the following form:

$$U_i^{MIN} \leq u_i(n) \leq U_i^{MAX} \quad i = 1,2,3,4,5,6$$
$$\Phi_F^{MIN} \leq C_1(\mathbf{X}(n), \mathbf{U}(n)) \leq \Phi_F^{MAX}$$
$$\Phi_S^{MIN} \leq C_3(\mathbf{X}(n), \mathbf{U}(n)) \leq \Phi_S^{MAX}$$
$$\Phi_T^{MIN} \leq C_5(\mathbf{X}(n), \mathbf{U}(n)) \leq \Phi_T^{MAX}$$
$$\Phi_H^{MIN} \leq C_5(\mathbf{X}(n), \mathbf{U}(n)) - \pi - \varphi_P(n+2) \leq \Phi_H^{MAX}$$
$$\Phi_K^{MIN} \leq C_5(\mathbf{X}(n), \mathbf{U}(n)) - C_3(\mathbf{X}(n), \mathbf{U}(n)) \leq \Phi_K^{MAX}$$
$$\Phi_A^{MIN} \leq C_1(\mathbf{X}(n), \mathbf{U}(n)) - C_3(\mathbf{X}(n), \mathbf{U}(n)) \leq \Phi_A^{MAX}.$$

(2.12)

The parameters Φ^{MIN} and Φ^{MAX} are minimal and maximal values of the segment (T–thigh, S–shank, F–foot) and joint angles (H–hip, K–knee, A–ankle). The term φ_P is absolute angle of the pelvis from horizontal axis (supplied as input into the simulation). The parameters U_i^{MIN} and U_i^{MAX} ($i = 1, 2, 3, 4, 5, 6$) are minimal and maximal values of activation levels for the six equivalent muscles. The min-max values of the angles and activations can be set on a subject-specific basis (e.g., measured ranges of motion, comfortable muscle activation levels).

Nonlinear programming (NLP) can be used to find a numerical solution of this nonlinear optimization problem with constraints. We used implementation of NLP based on sequential quadratic programming [32]. The outputs from the simulations are: 1) calculated muscle activations, and 2) generated trajectory $X(n)$, that is, segment angles x_i ($i = 1, 3, 5$), angular velocities x_i ($i = 2, 4, 6$) and angular accelerations dx_i/dt ($i = 2, 4, 6$) that are obtained when the calculated activations are applied to the model.

3. INTERACTIVE SIMULATION OF FES ASSISTED GAIT - OPTIWALK

3.1. OptiWalk architecture

The simulation is implemented as an interactive standalone application developed in Microsoft C# .NET 2003 and Matlab 7.4. The application comprises following modules:

- Database of subjects (Microsoft Access database)
- Database of desired gait patterns (Microsoft Access database)
- User interface front-end (developed in C# .NET)
- Optimization engine (developed in Matlab 7.4)

Database of subjects: The database contains model parameters for different subjects. A record in the database comprises parameters c_{ij} ($i = 0, 1, 2, 3, 4$ and $j = 1, 2, 3, 4, 5, 6$) describing six equivalent muscles (index j denotes the muscle), parameters d_{ik} ($i = 0, 1, 2, 3, 4, 5$ and $k = 1, 2, 3$) for the three viscoelastic joint torques (index k denotes the torque) and sets of mechanical parameters in the form of (m, L, d, J_C) for the thigh, shank and foot leg segments. The application integrates the functions for managing the database; the records can be created, stored, modified and deleted. When a record is selected, the parameters from the record are loaded into the application's workspace. As a result, the biomechanical model is customized for the selected subject.

Database of desired gait patterns: This is a repository of gait patterns that can be used as desired trajectories for the simulation. A gait pattern (database record) comprises segment angles ($\varphi_P, \varphi_T, \varphi_S, \varphi_F$), angular velocities ($d\varphi_P/dt, d\varphi_T/dt, d\varphi_S/dt, d\varphi_F/dt$) and accelerations ($d^2\varphi_P/dt^2, d^2\varphi_T/dt^2, d^2\varphi_S/dt^2, d^2\varphi_F/dt^2$), horizontal ($a_{HX}$) and vertical ($a_{HY}$) components of hip acceleration, horizontal (F_X) and vertical (F_Y) components of ground reaction force and trajectory of the center of pressure (COP) along the sole of the foot [see Fig. 2.1(a)]. The signals describe desired movement of the leg in the sagittal plane (angles, angular velocities, and angular acceleration) and interaction of the leg with the rest of the body (hip accelerations) and the ground (ground reaction forces). The gait patterns for the database are recorded from able bodied subjects. Recordings can be done in a gait lab by using camera based motion capture system and a built-in force plate. The OptiWalk application integrates the functions for managing the database; the records can be created, stored, and deleted. A gait pattern can be imported in the database from a Matlab file containing the gait pattern signals. Typically, the signals are calculated from the motion capture data by using motion analysis software (e.g., Visual3D, C-Motion, USA). The calculated data are exported to Matlab, saved as a Matlab file and then imported into the application.

User interface front-end: This is the central module of the application that is responsible for handling user requests, managing the databases, transferring data to and from the optimization engine and visualizing the simulation inputs and outputs. Graphical user interface is organized as a sequence of four tabs: *Model parameters*, *Desired gait pattern*, *Optimization* and *Visualization*. The tabs correspond to the typical sequence of steps in using the application: 1) select a model, 2) select a desired gait pattern, 3) run simulation, and 4) visualize generated gait pattern.

Optimization engine: This is a set of Matlab functions implementing the simulation. The Matlab functions are organized and compiled into a .NET component for easy integration with the other application modules [33]. The inputs for the optimization engine are model parameters and a desired gait pattern selected from the database of subjects and database of gait patterns, respectively. The outputs are calculated muscle activations for the six equivalent muscles and generated gait pattern.

The structure of the OptiWalk application and the dataflow between the components is depicted in Fig 2.2. Both development environments (.NET 2.0 and Matlab 7.4) used for OptiWalk implementation are essentially cross platform technologies. Therefore, although developed and tested under Windows XP, OptiWalk could be easily adapted to run under other operating systems (e.g., Linux).

3.2. OptiWalk scenario

Flowchart showing a typical sequence of steps in using the application is given in Fig. 2.3. First, a subject is selected from the database of subjects. This will load model parameters into the application workspace. Next, a desired gait pattern for the subject is selected from the database of gait patterns. This
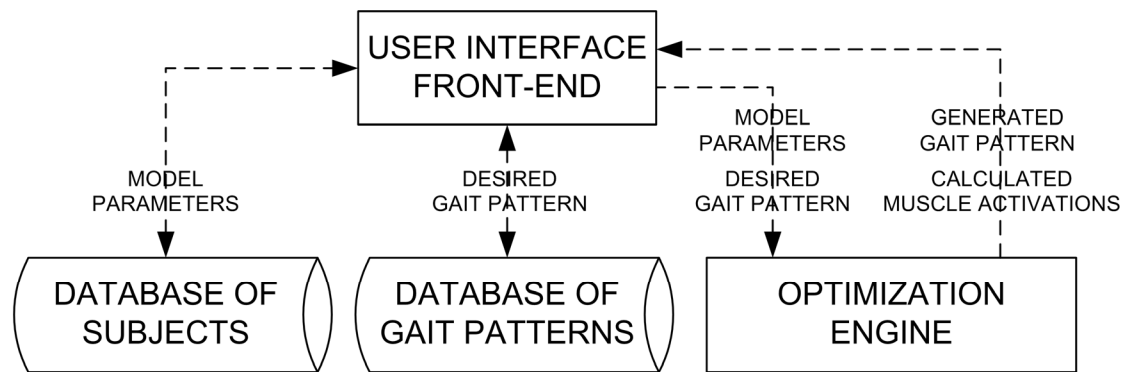
Fig. 2.2. OptiWalk structure. OptiWalk comprises four modules: database of subjects, database of gait patterns, optimization engine and user interface front-end. Dashed lines represent the dataflow between the modules. Note that some lines are bidirectional (two arrows) and some lines are unidirectional (one arrow).
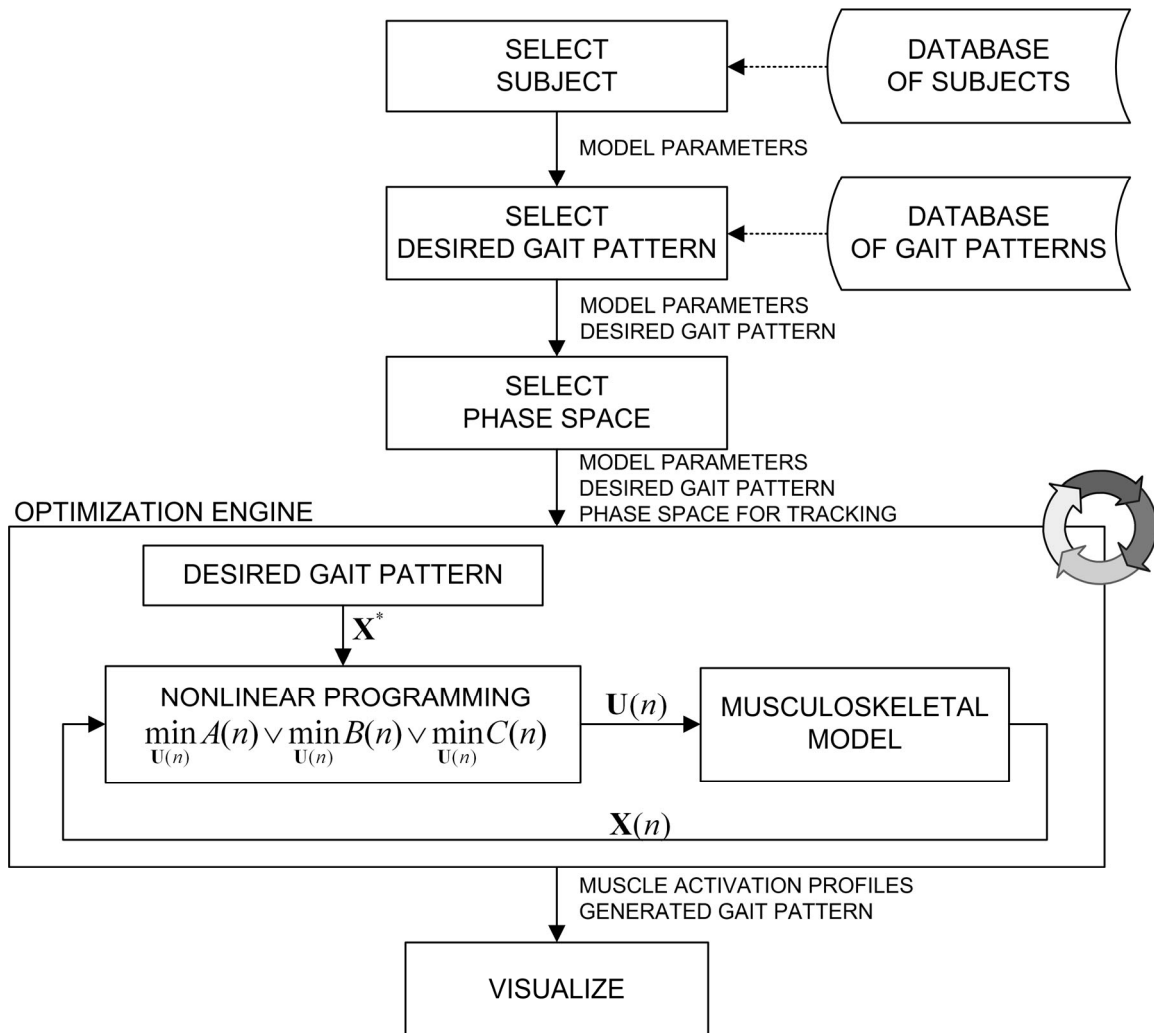
Fig. 2.3. OptiWalk flowchart. The boxes represent typical steps in using the application. User selects a subject, a desired gait pattern for the subject and a phase space for the tracking. Using these parameters as inputs, the simulation is started. In each step n, optimal control $\mathbf{U}(n)$ is determined by minimizing the tracking errors from the desired gait pattern $\mathbf{X}^*(n)$ while penalizing the total muscle efforts. The cost function ($A(n)$, $B(n)$, or $C(n)$) used for optimization depends on the selected phase space. The calculated muscle activations and generated gait pattern are visualized.

will load gait kinetics and kinematics to be used as desired trajectory for the simulation. Then, a phase space for the tracking is chosen. The selection of the phase space determines the cost function that is used for optimization. Simulation is started. Muscle activations are calculated on a sample by sample basis in a forward dynamics manner. In each simulation step, optimal control is determined by minimizing the selected cost function. The control calculated in the current step is applied to the model, a new state of the system is obtained, the state is fed back to the optimizer and the simulation proceeds in the next step. The process repeats until the end of the desired gait pattern. The simulation outputs muscle activation profiles and a generated gait pattern. The generated gait is animated in the form of a stick figure.

3.3. Example

Here, we present the case for a hemiplegic subject with moderate spasticity, weak hip muscles and the rest of the muscles that are almost normal torque generators. Model parameters are loaded into the application's workspace by selecting the subject's name from the list of subjects stored in the database. The model appears in the *Model Parameters* tab of the application's main window (see Fig. 2.4). The tab comprises user interface (UI) elements organized in groups. Text fields in the group *General Data* contain general-purpose information about the model (e.g., model name, creation date, comment). UI
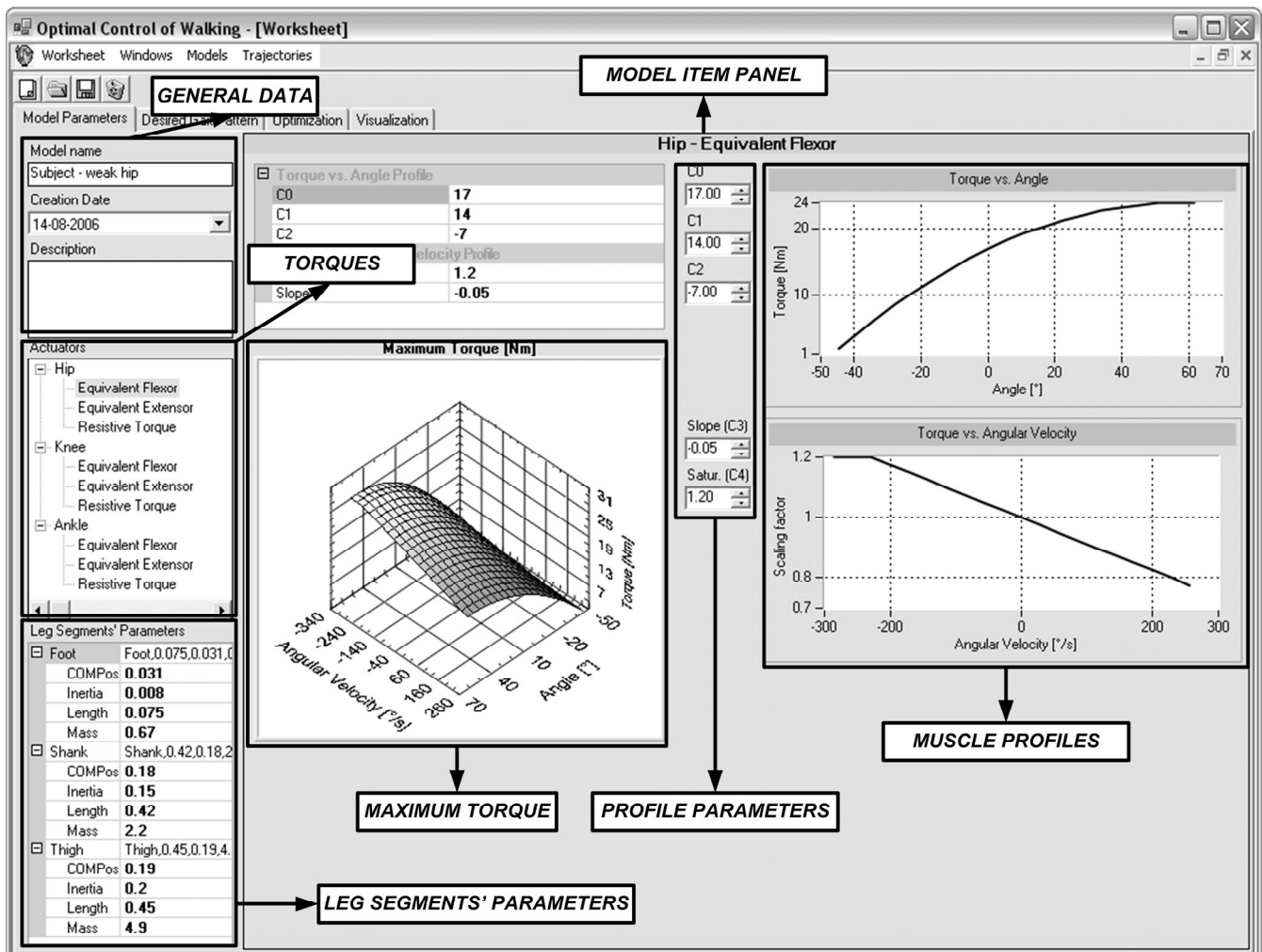
Fig. 2.4 *Model parameters* tab. The tab shows model parameters for the selected subject. User interface element *Torques* shows model joints, equivalent muscles actuating the joints, and passive elastic joint torques. Parameters describing the currently selected muscle (*Equivalent Hip Flexor*) are shown in *Model Item Panel*. Muscle torque vs. joint angle and normalized muscle torque vs. joint angular velocity profiles (*Muscle Profiles*) as well as maximal muscle torque over the angle vs. angular velocity plane (*Maximum Torque*) are plotted. The parameters c_i (i=0,1,2,3,4) for the profiles (*Profile Parameters*) are given in the numerical up-down controls. If dimensions are not written explicitly, the parameters have dimensions from the International System of Units (SI). Note that the maximal torque that can be generated by the hip flexor muscle in this particular subject is 25 Nm.

element *Torques* shows the joints (*Hip*, *Knee* and *Ankle*), corresponding equivalent muscles (*Equivalent Flexor*, *Equivalent Extensor*) and viscoelastic joint torques (*Resistive Torque*). If one of the items is selected by a mouse click, parameters describing the selected item appear in *Model Item Panel* area and the name of the item is shown on the top of the panel (*Hip - Equivalent Flexor*). Mechanical parameters of the leg are shown in UI element *Leg Segments' Parameters*. Mass of the segment (*Mass*), length of the segment (*Length*), distance of the center of mass of the segment from the proximal joint (*COMPos*) and segment's moment of inertia about the central axis perpendicular to the sagittal plane (*Inertia*) are given for each segment (*Thigh*, *Shank* and *Foot*).

In Fig. 2.4, equivalent hip flexor muscle is currently selected in *Torques* list. Thereby, its parameters are shown in *Model Item Panel*. Muscle torque versus joint angle [$f(\varphi)$ in (2.3)] and normalized muscle torque versus joint angular velocity [$g(d\varphi/dt)$ in (2.4)] profiles are plotted (*Muscle Profiles*). Maximal torque [i.e., $M_{max}=f(\varphi)g(d\varphi/dt)$] that the muscle can generate over the operating range of the joint (i.e., angle x angular velocity plane) is depicted as a surface plot (*Maximal Torque*). The parameters c_i ($i = 0,1,2,3,4$) of the profiles $f(\varphi)$ and $g(d\varphi/dt)$ are shown in interactive up-down numerical controls located next to the corresponding plots (*Profile Parameters*). If the parameters are modified (e.g., by clicking the arrows), the plots are immediately updated to reflect the changes. It can be seen from Fig. 2.4 that, in this particular subject, maximal torque that the hip flexor muscle can generate is about 25 Nm.

After the model parameters have been loaded, next step in OptiWalk use case scenario (see Fig. 2.3) is to select a desired gait pattern for the subject. Our first goal was to check if it would be possible to generate walking at a gait speed that is close to normal. Therefore, a gait pattern (*gait pattern A*) recorded from an able-bodied individual walking at the gait speed of 1.2 m/s was selected from the database of desired gait patterns. We recorded the pattern in the gait lab at the Center for Sensory Motor Interaction, Aalborg University, Denmark. Camera based motion capture system (8 ProReflex MCU240 cameras, Qualisys, SE) and an AMTI force plate (OR6-5, Advanced Mechanical Technology, USA) were used to record gait kinetics and kinematics. Passive retro-reflective markers were placed on the right leg and pelvis following the recommendations for the human motion analysis software (Visual3D, C-Motion, USA) that was used for processing the motion capture data. The gait pattern signals [see Fig. 2.1(a)] were calculated and exported as Matlab data file. The file is then imported in OptiWalk and saved in the database as *gait pattern A*.

Gait pattern A is loaded into the application's workspace and shown in *Desired Gait Pattern* tab of the application's main window (see Fig. 2.5). Text fields grouped under *General Data* contain general-purpose information about the pattern (i.e., name, creation date, sampling period and comment). The plots on the right show absolute angles (φ_P, φ_T, φ_S, φ_F) of the leg segments in sagittal plane measured from horizontal axis. The rest of the gait pattern signals (i.e., angular accelerations, angular velocities, ground reaction force data, and hip accelerations) can be inspected by activating the corresponding push button (*Signal Selector Panel*). The cursors (vertical dashed lines) mark the section of the gait pattern that is selected for simulation. One gait stride is selected in Fig. 2.5.

The model parameters and desired gait pattern shown in Figs. 2.4 and 2.5 respectively are inputs for optimization. *Optimization* tab (see Fig. 2.6) controls the simulation: 1) optimization algorithm (e.g., dynamic programming, static optimization) and a phase space for the tracking can be selected, 2) optimization parameters can be set (e.g., weighting factor λ in (2.9)-(2.11), min-max constraints in (2.12) for the angles and activations, maximum number of cost function evaluations, termination tolerance etc), and 3) the simulation can be started and results plotted. In this example, we selected static optimization as the algorithm and segment angles as the targets (phase space) for the tracking. The simulation lasted 21 seconds. The results are shown in Fig. 2.6. Panels on the left depict desired and generated joint angles. Panels on the right are calculated muscle activations for the six equivalent muscles acting at the hip, knee and ankle joints. The top part of each panel shows flexor and the bottom part extensor activity. The simulation calculates quantitative measures for the quality of tracking and estimates for the total muscle efforts. Difference between the desired and generated joint angles is tracking error. Mean and maximum absolute tracking errors and their standard deviations are calculated for each joint angle. The total muscle effort is estimated by summing up the levels of muscle activations over the whole activation profile for
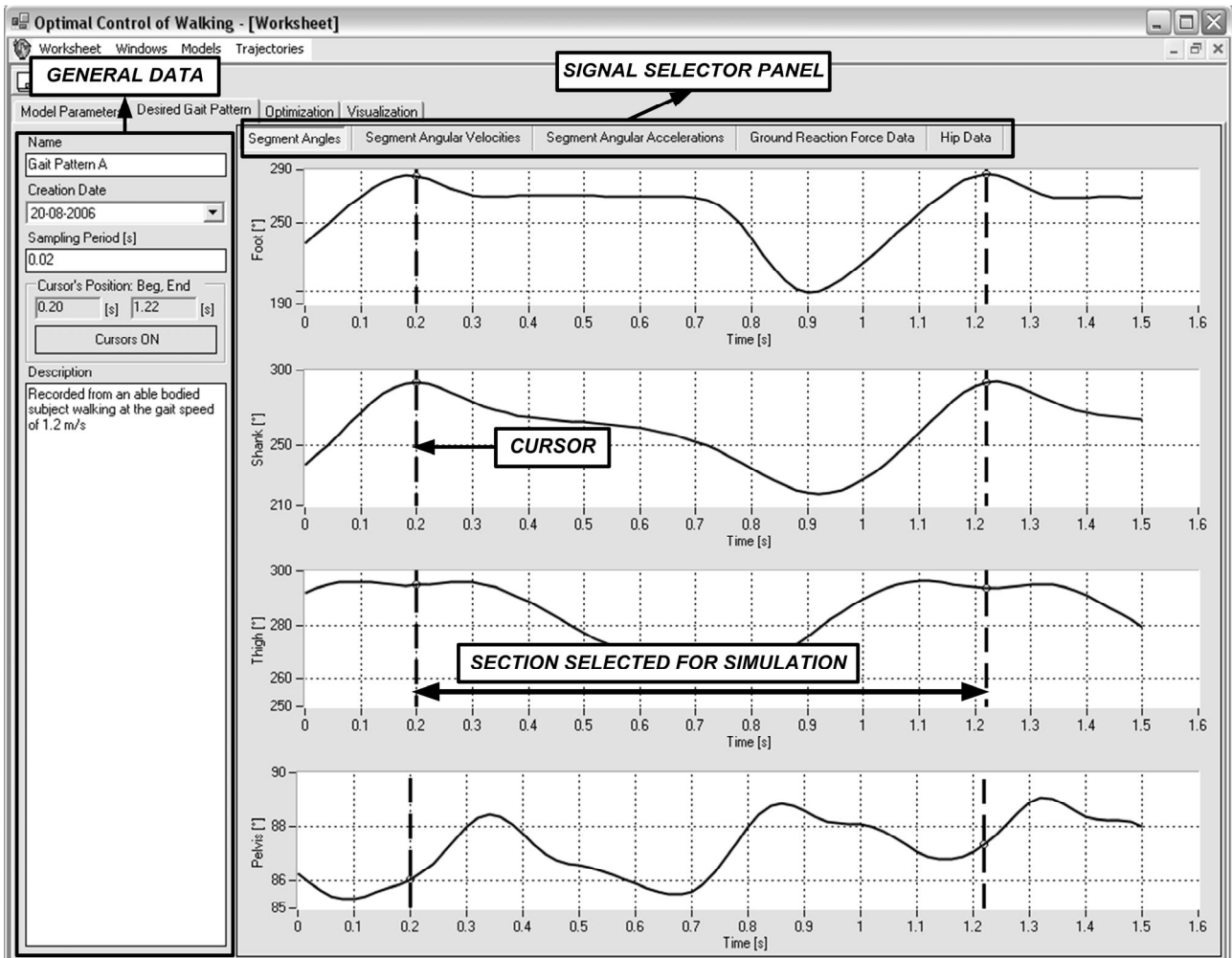
Fig. 2.5. *Desired Gait Pattern* tab. The tab shows kinematic signals (segment angles, angular velocities, angular accelerations, hip accelerations) and kinetic signals (ground reaction force data) that together constitute a desired gait pattern (simulation input). The gait pattern shown in the figure was recorded from an able-bodied subject walking at a gait speed of 1.2 m/s (*gait pattern A*). Absolute segment angles of the pelvis, thigh, shank and foot in the sagittal plane measured from the horizontal axis are plotted. The cursors (dashed vertical lines) mark the section of the gait pattern (i.e., one gait stride) that will be used for the simulation.
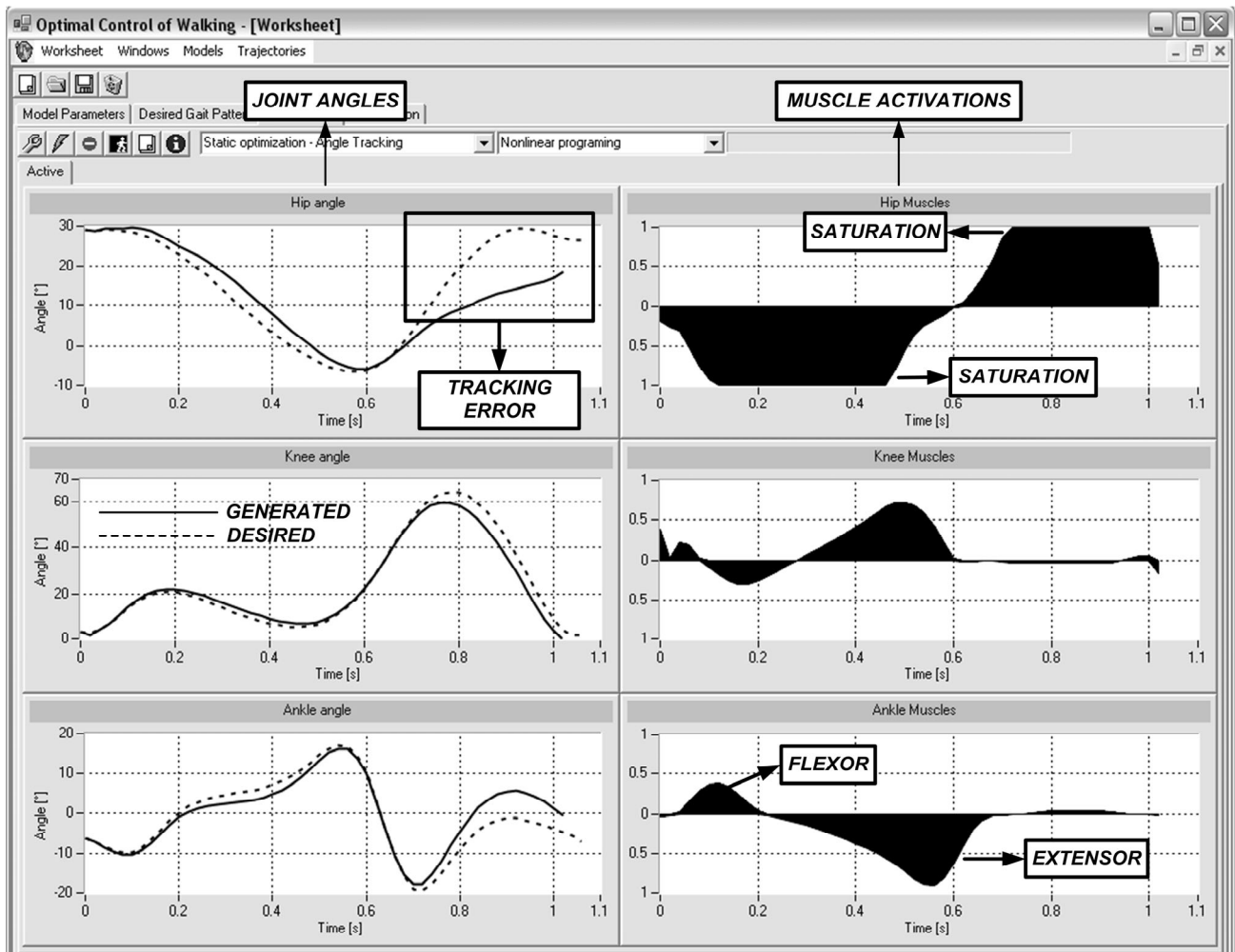
Fig. 2.6. *Optimization* tab. The tab handles the set up of various optimization parameters, controls the simulation and plots the results. The panels on the left show desired (dashed lines) and generated (continuous lines) hip, knee and ankle joint angles (from top to bottom). The panels on the right are normalized muscle activations (0 – muscle relaxed, 1 – muscle fully activated). The top and bottom part of each panel show flexor and extensor activity, respectively. The figure presents simulation results for the model and desired gait pattern from Figs. 2.4 and 2.5, respectively. The largest tracking error is observed in the hip joint angle during the swing phase of the gait stride. The hip flexor muscle is saturated (equals one) during that period. Therefore, the subject's muscles are not strong enough to generate the desired gait.
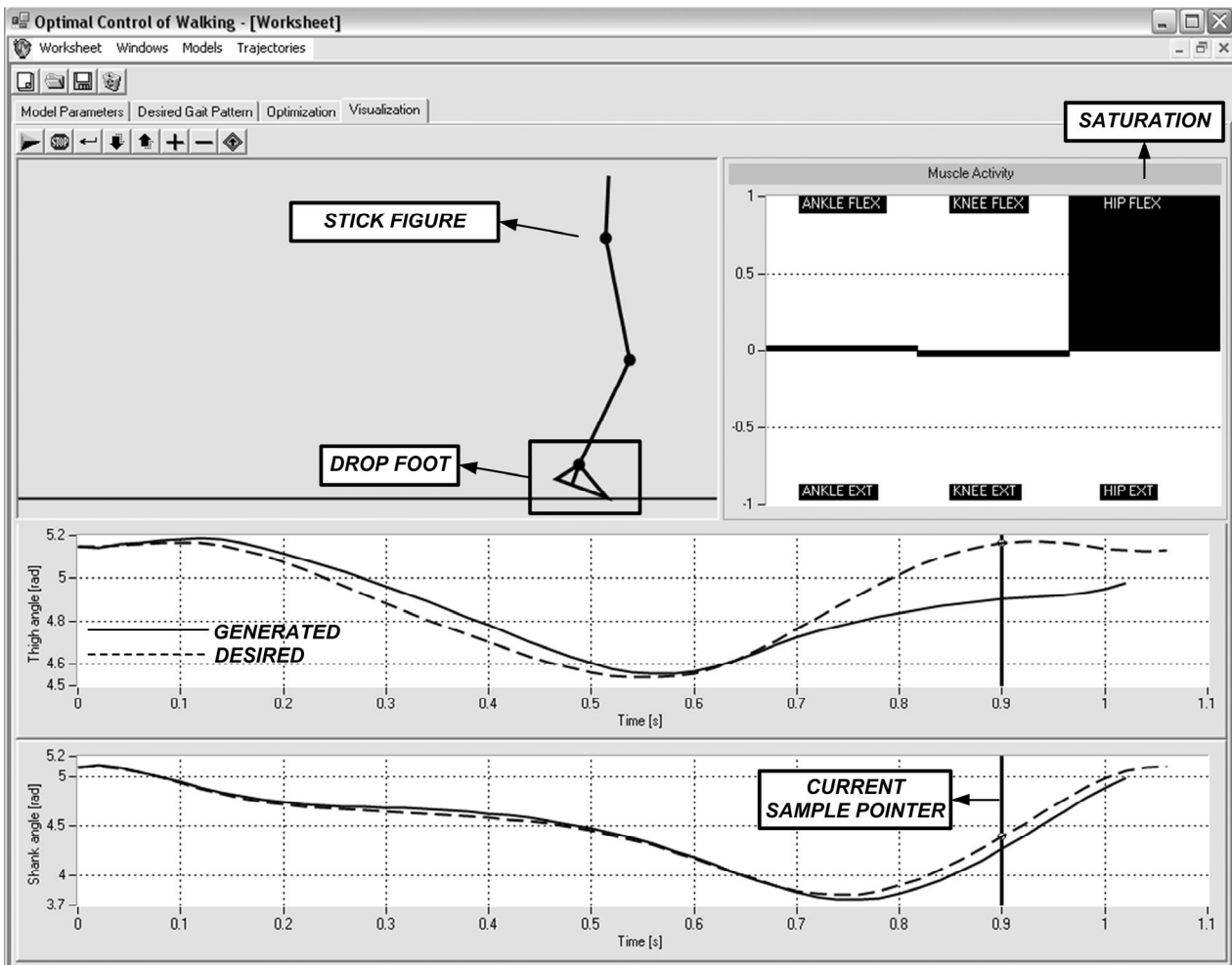
Fig. 2.7. *Visualization* tab. The tab animates the gait pattern that was generated in the simulation. The gait is visualized in the form of a stick figure. The panel with vertical bars shows the momentary levels of muscle activity. The top bars are for the flexors and the bottom bars are for the extensors. The lower panels plot selected gait signals. Thigh and shank segment angles are plotted. The vertical cursor (*Current Sample Pointer*) marks the signal sample corresponding to the current animation time. The figure shows a snapshot of the swing phase of the gait. The hip flexor muscle is too weak to produce the necessary amount of hip flexion and, as a consequence, the subject's foot strikes the floor.

the muscle. This "net" activity is computed for each muscle, joint ("net" activity of the antagonistic muscle pair) and the profile in total ("net" activity of the six muscles). The numerical measures for the quality of tracking and muscle efforts can be used to compare the results of different simulations.

The following can be seen by analyzing the results shown in Fig. 2.6. The tracking error is visible in all joint angles. The largest deviation from the desired angle is noticeable in the hip during the swing phase of the gait stride. Simultaneously, during the same period, the muscle activation for the hip flexor muscle goes into saturation (equals one). Therefore, the muscle is maximally active but the thigh is still far below the desired trajectory. The final conclusion is that the subject's hip flexor muscle is not strong enough to generate the desired gait.

The last step in the typical OptiWalk scenario is to visualize the simulation results in *Visualization* tab (see Fig. 2.7). The tab is divided into three areas: 1) panel for animation of the generated gait pattern in the form of a stick figure, 2) panel with vertical bars that show the activity of the equivalent muscles and 3) panel for plotting various kinetic and kinematic signals characterizing the generated gait (e.g., joint torques, powers, segment angles etc). The panels are synchronized – as the stick figure moves during the animation, the bars for the muscle activity are updated, and *Current Sample Pointer* marks the signal value corresponding to the current animation time.

Animation of walking generated in this example demonstrated the practical consequences of the simulation results that are shown in Fig. 2.6 (tracking errors, saturations). Since the hip flexor muscle was
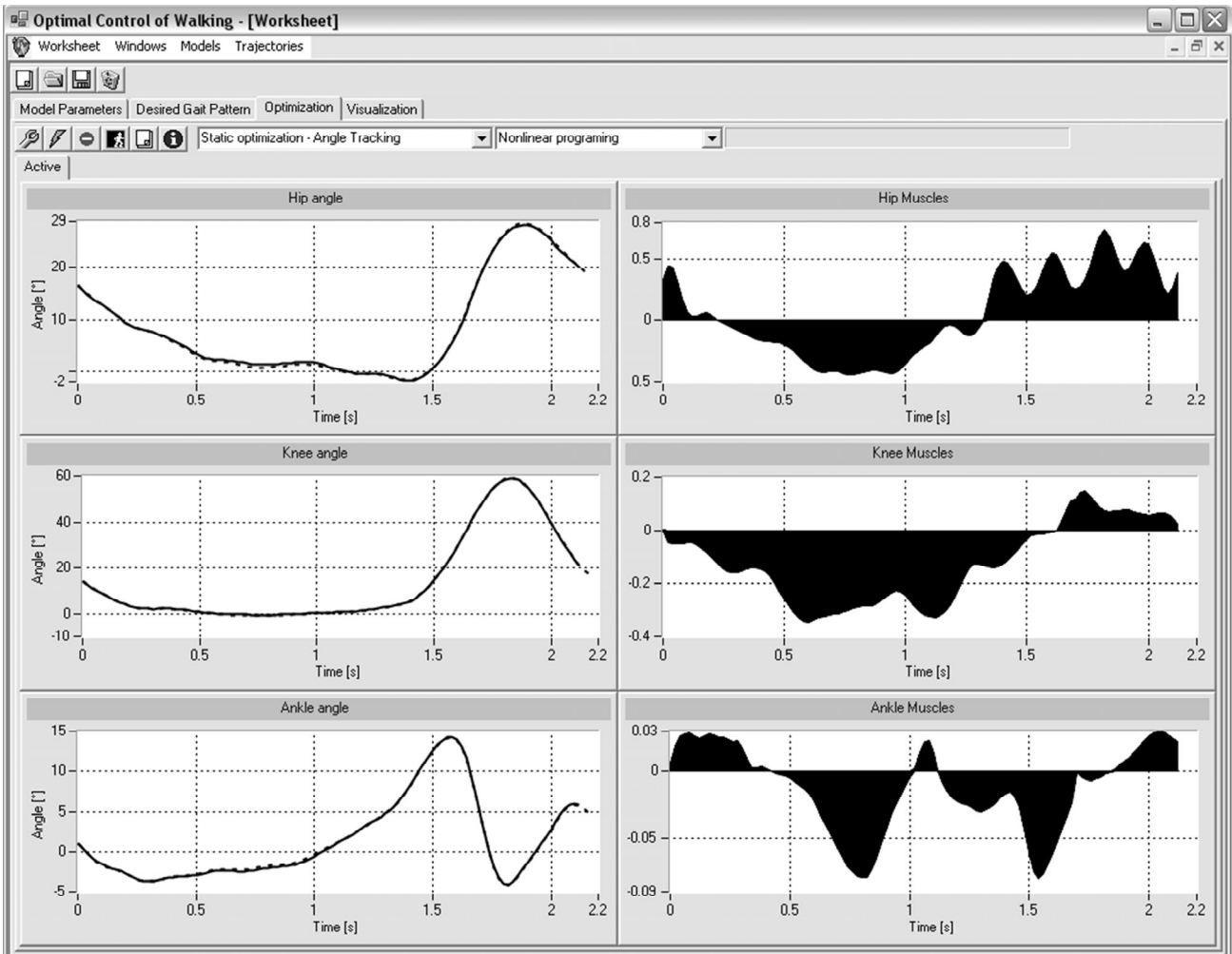
Fig. 2.8. Simulation results (*Optimization* tab) for the same subject (see Fig. 2.4) and new gait pattern (*gait pattern B*). Gait pattern recorded from an able bodied subject walking slowly (~ 0.25 m/s) was selected from the database of desired gait patterns. The simulation was implemented with the same parameters (optimization algorithm, phase space) as the previous one. Note that the tracking errors are now negligible and muscle activations did not saturate. Therefore, the selected pattern is feasible. The calculated muscle activation profiles can be used for designing the control of FES.

not strong enough to generate an appropriate amount of hip flexion, the subject's foot actually strikes the ground, during the swing phase of the gait stride. Therefore, *gait pattern A* showed to be unfeasible for this particular subject. That is to say that the gait pattern was too demanding with respect to the current capabilities of the subject's neuromusculoskeletal system.

Importantly, the flexibility of OptiWalk can be used to find a gait pattern that will lead to simulation results that are satisfactory. We selected *gait pattern B* from the database of gait patterns to be the new desired gait for the subject. The pattern was recorded in the same able-bodied individual as the *gait pattern A*. However, this time the individual was instructed to walk very slowly (~ 0.25 m/s). *Gait pattern B* was used as input for the new simulation. The simulation was implemented with the same parameters (e.g., optimization algorithm, phase space) as the previous one. The results are shown in Fig. 2.8. Notice that this time the tracking error was very small and the muscle activations did not saturate. *Visualization* tab confirmed that the generated gait looked normally. Therefore, *gait pattern B* is feasible and can be adopted as the desired gait to be generated by means of FES in the selected subject. The muscle activation profiles from Fig. 2.8 can be used for designing the control of FES that would result with the desired gait in the selected subject.

4. DISCUSSION

The immediate question that one can ask is why we developed a new simulation model although there are many simulation methods that are already developed and presented in literature. Several sophisticated software tools for modeling, simulation and analysis of human motion are available. Some packages, such as, SIMM (MusculoGraphics Inc., US) or AnyBody (AnyBody Technology A/S, DK) are commercial and some are in the public domain (e.g., OpenSim [34] and HuMAns [35]). However, these tools implement complex musculoskeletal models that are not applicable for the control of FES that would be convenient for implementation within a practical system.

The reasons are following: 1) in reality it is not possible to determine with sufficient precision parameters that are instrumental for the implementation of this methods, 2) the response of muscles that are activated by electrical stimulation does not correspond to the activities found in healthy individuals, 3) injury or disease greatly modifies the sensory-motor circuitry in individuals who should use assistive technology, 4) the parameters of the plant change with time, and 5) assistive systems control only parts of the system, while most of the plant is under preserved biological control.

All of the considerations influenced the design of the tool presented in this chapter. We use a model that is reduced to the form in which with acceptable precision one can determine the parameters. Namely, the response of the muscles and mechanical parameters of leg segments and joints can be experimentally identified. The model is customized to reflect the current status of the subject's neuromusculoskeletal system. Therefore, the controls (muscle activation profiles) are determined by taking into account the weaker muscles as well as other constraints induced by the disability (e.g., spasticity – through increased joint stiffness).

OptiWalk tool integrates a database of desired gait patterns. The gait patterns are recorded from able-bodied individuals walking at a range of gait speeds (from very slow to normal). Therefore, the database comprises functional patterns that require different levels of muscle efforts to be generated. Initially, a low-effort pattern can be selected for the subject and later, as the subject improves in performance, more demanding patterns can be simulated and used as the target gait to be restored by means of FES.

There is a database of model parameters. It is likely that the biomechanical parameters for the subject will change. This is because walking with the assistive system will contribute to changes in the sensory-motor system responses. Since the model parameters in OptiWalk are easily accessible and editable, the model can be opened anytime, parameters changed and saved in the database. Furthermore, the updated model can be simulated and a new set of muscle activation profiles determined. Therefore, the control of FES is updated to reflect the latest changes in the properties of sensory-motor structures.

Muscle activation profiles determined by the tool are intended to be used for the design of an FES controller based on artificial reflex control (see Chapter 1, Fig. 1.5). The control is mimicking biological mechanisms; thereby, the human can relatively easy adapt his voluntary control over the non-paralyzed parts of the body. The main application of the new tool is envisioned in the clinical environment by a technical person.

OptiWalk was designed to be a user friendly application. As a result, it is quite easy to manage the models and gait patterns and to set up and run the simulations. This makes OptiWalk a very flexible and powerful tool for conducting customized biomechanical gait simulations. For example, a number of different gait patterns can be simulated for a given subject (model). The simulations will show which patterns that can be generated by the subject's musculoskeletal system. By comparing the simulation results (e.g., tracking errors and muscle efforts), the most suitable gait pattern can be selected from the set of feasible ones. For the selected gait pattern, the simulation determines the timing and profile of muscle activations that are necessary to generate the pattern in the selected subject. The profiles can be used to design the control of FES for the subject.

Furthermore, the tool allows the analysis of minimum plant responses needed for desired activity. Namely, for the given gait pattern, the model parameters (e.g., muscle strength, passive joint stiffness) could be changed iteratively until desired simulation results are obtained (e.g., tracking errors within prescribed limits). These plant responses could then be eventually built as a result of the appropriate training or addition of some orthotic device (e.g., joint stabilization).

The model presented was primarily developed for the assistance of hemiplegic individuals where only one side of the body will be externally controlled. Controlling one leg in early phase of hemiplegia while walking was shown to be a valuable method for training of the neural circuits that likely promotes changes in cortical excitability and cortical plasticity; thereby, potentially allowing the user to walk after the training without the assistive system [36]. The use of the same control in paraplegic individuals is likely still not good enough because of the major problem of balance that requires the use of hand supports over the walker or similar assists, that is, major change of the plant and transformation to quadrupedal walking.

The developed model and optimization algorithms are sufficiently flexible to allow the testing of various sensors to be used in the sensory-driven FES of walking. The equations (2.9)-(2.11) can be used to implement the tracking in different phase spaces. Since the tracking errors are expressed in terms of angular velocities or angular accelerations, the data from gyroscopes or accelerometers respectively can be used directly as the inputs for the simulation. This is an interesting possibility since these sensors, made in microelectromechanical technologies, are practical and convenient for daily application.

The main purpose of the tool is to enable the efficient generation of sensorimotor models (SMMs) by using customized modeling and simulation (CMS) approach (see Chapter 1, Fig. 1.7). The muscle activation profiles calculated by the simulation together with the sensor data that are used as inputs for the simulation make up an SMM (for the selected gait pattern and the subject). The SMM is intended to be used for the design of rule-based control of FES (see Chapter 1, Fig. 1.6).

OptiWalk was developed in order to: 1) allow the testing of our CMS approach on a number of examples, 2) act as a common environment in which all further developments would be integrated, and 3) potentially evolve into a clinical tool for designing rule-based control of FES customized to the user.

5. APPENDIX

The matrices from equation (2.1) are:

$$\mathbf{A}(\mathbf{\Phi}) = \begin{bmatrix} J_{CT} + m_F L_T^2 + m_S L_T^2 + m_T d_T^2 & (m_F L_S L_T + m_S d_S L_T)\cos(\varphi_T - \varphi_S) & m_F d_F L_T \cos(\varphi_T - \varphi_F) \\ (m_F L_S L_T + m_S d_S L_T)\cos(\varphi_T - \varphi_S) & J_{CS} + m_F L_S^2 + m_S d_S^2 & m_F d_F L_S \cos(\varphi_S - \varphi_F) \\ m_F d_F L_T \cos(\varphi_T - \varphi_F) & m_F d_F L_S \cos(\varphi_S - \varphi_F) & J_{CF} + m_F d_F^2 \end{bmatrix}$$

$$\mathbf{B}(\mathbf{\Phi}) = \begin{bmatrix} 0 & -(m_F L_S L_T + m_S d_S L_T)\sin(\varphi_T - \varphi_S) & -m_F d_F L_T \sin(\varphi_T - \varphi_F) \\ (m_F L_S L_T + m_S d_S L_T)\sin(\varphi_T - \varphi_S) & 0 & -m_F d_F L_S \sin(\varphi_S - \varphi_F) \\ m_F d_F L_T \sin(\varphi_T - \varphi_F) & m_F d_F L_S \sin(\varphi_S - \varphi_F) & 0 \end{bmatrix}$$

$$\mathbf{C}(\mathbf{\Phi}) = \begin{bmatrix} -g(m_S L_T + m_F L_T + m_T d_T)\cos(\varphi_T) \\ -g(m_F L_S + m_S d_S)\cos(\varphi_S) \\ -gm_F d_F \cos(\varphi_F) \end{bmatrix} \quad \mathbf{D}(\mathbf{\Phi}) = \begin{bmatrix} -L_T \sin(\varphi_T) & L_T \cos(\varphi_T) \\ -L_S \sin(\varphi_S) & L_S \cos(\varphi_S) \\ CF2CP_y - d_F \sin(\varphi_F) & d_F \cos(\varphi_F) - CF2CP_x \end{bmatrix}$$

$$\mathbf{E}(\mathbf{\Phi}) = \begin{bmatrix} (m_S L_T + m_F L_T + m_T d_T)\sin(\varphi_T) & -(m_S L_T + m_F L_T + m_T d_T)\cos(\varphi_T) \\ (m_F L_S + m_S d_S)\sin(\varphi_S) & -(m_F L_S + m_S d_S)\cos(\varphi_S) \\ m_F d_F \sin(\varphi_F) & -m_F d_F \cos(\varphi_F) \end{bmatrix}$$

$$\mathbf{T} = \begin{bmatrix} 1 & 1 & 0 \\ 0 & -1 & -1 \\ 0 & 0 & 1 \end{bmatrix}$$

The notations are given in the following table:

J_{CT}, J_{CS}, J_{CF}	moments of inertia of the thigh, shank and foot about the central axes perpendicular to the sagittal plane
L_T, L_S, L_F	lengths of the thigh, shank and foot
d_T, d_S, d_F	distances from the proximal joint to the center of the mass for the thigh, shank and foot
m_T, m_S, m_F	masses of the thigh, shank and foot
g	gravitational acceleration
$\varphi_T, \varphi_S, \varphi_F$	angles of the thigh, shank and foot from horizontal axis
$CF2CP_y, CF2CP_x$	distances between the center of mass of the foot and the center of pressure along the vertical and horizontal axis

REFERENCES

[1] Y. Stepanenko and M. Vukobratović, "Dynamics of articulated open chain active mechanisms," *Math. Biosci.*, vol. 28, no. 1-2, pp. 137-170, 1976.

[2] D. E. Orin, R. B. Mcghee, M. Vukobratović, and G. Hartoch, "Kinematic and kinetic-analysis of open-chain linkages utilizing Newton-Euler methods," *Math. Biosci.*, vol. 43, no. 1-2, pp. 107-130, 1979.

[3] W. W. Armstrong, "Recursive solution to the equations of motion of an n-link manipulator," in *Proc. 5th World Congr., Theory of Machines, Mechanisms*, vol. 2, pp.1343 - 1346, 1979 2008.

[4] J. Y. S. Luh, M. W. Walker, and R. P. C. Paul, "On-line computational scheme for mechanical manipulators," *J. Dyn. Sys. Meas. Control,* vol. 102, no. 2, pp. 69-76, 1980.

[5] S. H. Koozekanani, K. Barin, R. B. McGhee, and H. T. Chang, "A Recursive Free-Body Approach to Computer Simulation of Human Postural Dynamics," *IEEE Trans., Biomed. Eng.*, vol. 30, no. 12, pp. 787-792, 1983.

[6] R. L. Huston, C. E. Passerello, R. E. Hessel, and M. W. Harlow, "On human body dynamics," *Ann. Biomed. Eng.*, vol. 4, no. 1, pp. 25-43, 1976.

[7] S. Onyshko and D. A. Winter, "A mathematical-model for the dynamics of human locomotion," *J. Biomech.*, vol. 13, no. 4, pp. 361-368, 1980.

[8] H. Hatze, "Complete set of control equations for human musculoskeletal system," *J. Biomech.*, vol. 10, no. 11-1, pp. 799-805, 1977.

[9] H. Hatze, "A comprehensive model for human motion simulation and its application to the take-off phase of the long jump," *J. Biomech.*, vol. 14, no. 3, pp. 135-142, 1981.

[10] R. N. Marshall, R. K. Jensen, and G. A. Wood, "A general Newtonian simulation of an n-segment open-chain model," *J. Biomech.*, vol. 18, no. 5, pp. 359-367, 1985.

[11] G. Khang and F. E. Zajac, "Paraplegic standing controlled by functional neuromuscular stimulation. II. Computer simulation studies," *IEEE Trans., Biomed. Eng.*, vol. 36, no. 9, pp. 885-894, 1989.

[12] G. Khang and F. E. Zajac, "Paraplegic standing controlled by functional neuromuscular stimulation. I. Computer model and control-system design," *IEEE Trans., Biomed. Eng.*, vol. 36, no. 9, pp. 873-884, 1989.

[13] G. T. Yamaguchi and F. E. Zajac, "Restoring unassisted natural gait to paraplegics via functional neuromuscular stimulation - a computer-simulation study," *IEEE Trans., Biomed. Eng.*, vol. 37, no. 9, pp. 886-902, 1990.

[14] A. Erdemir, S. McLean, W. Herzog, and A. J. van den Bogert, "Model-based estimation of muscle forces exerted during movements," *Clin. Biomech.*, vol. 22, no. 2, pp. 131-154, 2007.

[15] M. G. Pandy, F. C. Anderson, and D. G. Hull, "A parameter optimization approach for the optimal control of large-scale musculoskeletal systems," *J. Biomech. Eng.*, vol. 114, no. 4, pp. 450-460, 1992.

[16] C. J. Goh and K. L. Teo, "Control parameterization: a unified approach to optimal control problems with general constraints," *Automatica*, vol. 24, no. 1, pp. 3-18, 1988.

[17] F. C. Anderson and M. G. Pandy, "Dynamic optimization of human walking," *J. Biomech. Eng.*, vol. 123, no. 5, pp. 381-390, 2001.

[18] R. R. Neptune, S. A. Kautz, and F. E. Zajac, "Contributions of the individual ankle plantar flexors to support, forward progression and swing initiation during walking," *J. Biomech.*, vol. 34, no. 11, pp. 1387-1398, 2001.

[19] R. R. Neptune, "Optimization algorithm performance in determining optimal controls in human movement analyses," *J. Biomech. Eng.*, vol. 121, no. 2, pp. 249-252, 1999.

[20] R. R. Neptune, I. C. Wright, and A. J. V. Bogert, "A method for numerical simulation of single limb ground contact events: application to heel-toe running," *Comp. Meth. Biomech. Biomed. Eng.*, vol. 3, no. 4, pp. 321-334, 2000.

[21] T. Spagele, A. Kistner, and A. Gollhofer, "Modeling, simulation and optimization of a human vertical jump," *J. Biomech.*, vol. 32, no. 5, pp. 521-530, 1999.

[22] O. Von Stryk, "Numerical solution of optimal control problems by direct collocation," in Bulirsch, R., Miele, A., Stoer, J., and Well, K.-H., (eds.), *Optimal Control, Calculus of Variations, Optimal Control Theory and Numerical Methods*, Birkhauser, International Series of Numerical Mathematics 111, Basel 1993.

[23] M. Stelzer and O. Von Stryk, "Efficient forward dynamics simulation and optimization of human body dynamics," *ZAMM Zeitschrift fur Angewandte Mathematik und Mechanik*, vol. 86, no. 10, pp. 828-840, 2006.

[24] D. G. Thelen, F. C. Anderson, and S. L. Delp, "Generating dynamic simulations of movement using computed muscle control," *J. Biomech.*, vol. 36, no. 3, pp. 321-328, 2003.

[25] D. G. Thelen and F. C. Anderson, "Using computed muscle control to generate forward dynamic simulations of human walking from experimental data," *J. Biomech.*, vol. 39, no. 6, pp. 1107-1115, 2006.

[26] A. Seth and M. G. Pandy, "A neuromusculoskeletal tracking method for estimating individual muscle forces in human movement," *J. Biomech.*, vol. 40, no. 2, pp. 356-366, 2007.

[27] F. E. Zajac, R. R. Neptune, and S. A. Kautz, "Biomechanics and muscle coordination of human walking: Part II: Lessons from dynamical simulations and clinical implications," *Gait Posture*, vol. 17, no. 1, pp. 1-17, Feb.2003.

[28] R. B. Stein, E. P. Zehr, M. K. Lebiedowska, D. B. Popovic, A. Scheiner, and H. J. Chizeck, "Estimating mechanical parameters of leg segments in individuals with and without physical disabilities," *IEEE Trans. Neural Syst. Rehabil. Eng.*, vol. 4, no. 3, pp. 201-211, 1996.

[29] P. H. Veltink, H. J. Chizeck, P. E. Crago, and A. Elbialy, "Nonlinear joint angle control for artificially stimulated muscle," *IEEE Trans. Biomed. Eng.*, vol. 39, no. 4, pp. 368-380, 1992.

[30] G. Shue, P. E. Crago, and H. J. Chizeck, "Muscle-joint models incorporating activation dynamics, moment-angle, and moment-velocity properties," *IEEE Trans. Biomed. Eng.*, vol. 42, no. 2, pp. 212-223, 1995.

[31] D. Popović, R. B. Stein, M. N. Oguztoreli, M. Lebiedowska, and S. Jonić, "Optimal control of walking with functional electrical stimulation: A computer simulation study," *IEEE Trans. Neural Syst. Rehabil. Eng.*, vol. 7, no. 1, pp. 69-79, 1999.

[32] Anonymous (accessed on June 4th 2008). MATLAB Optimization Toolbox User's guide. Available online at: http://www.mathworks.com/access/helpdesk/help/pdf_doc/optim/optim_tb.pdf.

[33] Anonymous (accessed on June 4th 2008). MATLAB Builder NE User's guide. Available online at: http://www.mathworks.com/access/helpdesk/help/pdf_doc/dotnetbuilder/dotnetbuilder.pdf.

[34] S. L. Delp, S. L. Delp, F. C. Anderson, A. S. Arnold, P. Loan, A. Habib, C. T. John, E. Guendelman, and D. G. Thelen, "OpenSim: Open-Source Software to Create and Analyze Dynamic Simulations of Movement," *IEEE Trans. Biomed. Eng.*, vol. 54, no. 11, pp. 1940-1950, 2007.

[35] Anonymous (accessed on June 4th 2008). The HuMAnS toolbox, a homogeneous framework for motion capture, analysis and simulation. Available online at: http://www.inrialpes.fr/bipop/software/humans/index.html. 2008.

[36] D. Popović, "Functional Electrical Therapy of walking for neurorehabilitation in hemiplegic individuals" in *Motor Control (11 suppl.): Proc. Prog. Motor Control*, Santos, Brazil, pp. 1087-1640, 2007.

CHAPTER 3
Control of Multichannel Electrical Stimulation of Paretic Leg in Individuals with Hemiplegia: Moving-Window Dynamic Optimization[*]

Summary–The rules for rule-based controller are computer generated from a sensorimotor model (SMM) of gait by using machine learning. The SMM comprises sensory component (sensor data) and motor component (muscle excitations) that are used as inputs and target outputs for machine learning, respectively. As a result, sensor data are incorporated into inputs (feedback) and muscle excitations become the outputs (feedforward commands) of the generated rule-based controller. Since the goal is to design a practical system, both components of the SMM have to be in the proper form: 1) sensor data should be acquired by using a set of gait sensors suitable for daily application, and 2) muscle excitation profiles should be convenient for implementation by an electronic stimulator. The goal of this study was to develop simulation methods for generation of the motor component of the SMM in the form appropriate for simple implementation. We present here a new moving-window dynamic optimization (MWDO) method for biomechanical gait simulations. The MWDO leads to piecewise constant muscle excitation profiles. This type of excitation profiles was adopted since it has uniform and simple structure that is convenient for implementation of rule-based control of pulsatile electrical stimulation. Moreover, the method uses dynamic optimization and therefore takes into account muscle activation dynamics. MWDO was validated within the user customized sagittal plane model representing the foot, shank, and thigh interfacing the body by the equivalent force and torque. Input data for the validation were recorded from an able-bodied subject walking at various gait speeds (0.4–1.4 m/s). The cost function for optimization was the weighted sum of excitation levels and squares of tracking errors from the desired trajectory. The permissible margin for tracking errors was set at ±1 SDJA (standard deviation of joint angles) based on the typical variability of joint angles during normal walking of healthy individuals. Estimation of excitation profiles for one gait cycle using MWDO takes less than 25 minutes within Matlab environment on a PC computer. The simulation was proven to be robust across the range of gait speeds.

1. INTRODUCTION

The rules for rule-based control of functional electrical stimulation (FES) are computer generated from the sensorimotor model (SMM) of gait. The SMM comprises sensor data and muscle excitation profiles. The sensor data are used as inputs and the excitation profiles as target outputs for machine learning (see Chapter 1, Fig. 1.6). As a result, a real-time controller is generated and its inputs (feedback) and outputs (feedforward commands) are created from the sensory and motor components of the SMM, respectively (see Chapter 1, Fig. 1.8). Since our goal is to develop a practical system, both components have to be in the proper form: 1) sensors data have to be acquired by using gait sensors suitable for daily application, and 2) muscle excitation profiles should be convenient for implementation by an electronic stimulator. The muscle excitations can be generated by using customized modeling and simulations (see Fig. 3.1). The goal of this study was to develop simulation methods for generation of the motor component of the SMM in the form appropriate for simple implementation.

In principle, muscle excitation is a signal which could have an arbitrary shape; normalized excitation levels are allowed to change freely between 0 (no excitation) and 1 (full excitation). However, FES systems for walking use pulsatile electrical stimulation with a typical frequency of about 20–25 pulses per second. Therefore, the activity can only be changed when a new stimulation is provided, that is, every 40 to 50 ms. Considering the aforementioned characteristics, we adopted the profile in the form of a piecewise constant signal (PWC) comprising constant-amplitude segments (CASs) of equal duration ($\geq$ 50 ms) to be the suitable output from the simulation (see Fig. 3.2). Since the excitation profile is adopted to be PWC, the simulation should include muscle activation dynamics. The activation dynamics, in terms of engineering, operate as a low pass filter. Hence, smooth transitions in the muscle force follow abrupt changes in the intensity of muscle excitation levels [1], [2], [3].

We describe here a new method for customized modeling and simulations based on dynamic optimization (DO). The method meets the above-mentioned requirements. We based the simulation on DO since it is a flexible method for implementation of optimal control subject to constraints given by differential and/or algebraic equations [4]. The simulation that we developed was named moving-window dynamic optimization (MWDO).

We present the performances of the MWDO method. The MWDO was validated within the user customized sagittal plane model representing the foot, shank, and thigh interfacing the body by the equivalent force and torque. The outputs of MWDO are intended to be used for rule-based control of multichannel surface FES for assisting paretic leg of individuals with hemiplegia. The study took into consideration the control of the knee and ankle joints due to the fact that the envisioned assistive system will activate the shank and thigh muscles. Since the control signals for the model were constrained to be
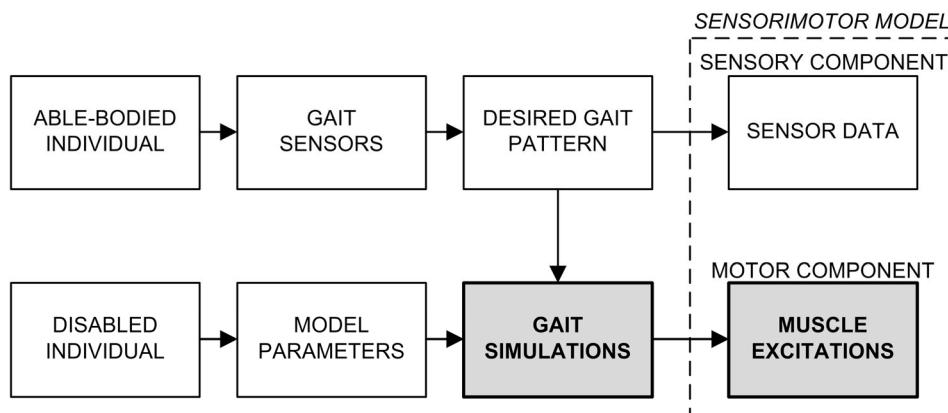
Fig. 3.1. Customized modeling and simulation (CMS) approach. Desired gait pattern is recorded from an able-bodied individual. Model parameters are experimentally identified from a disabled subject. Using a model customized to the subject, biomechanical gait simulations determine muscle excitations that are adequate to generate the desired gait. The output from the CMS is an SMM. The shaded boxes are the steps of the CMS that were in the focus of this study. The goal of the study was to generate the motor component (muscle excitations) of the SMM in the form appropriate for simple implementation.

PIECEWISE CONSTANT MUSCLE EXCITATION SIGNAL u_i
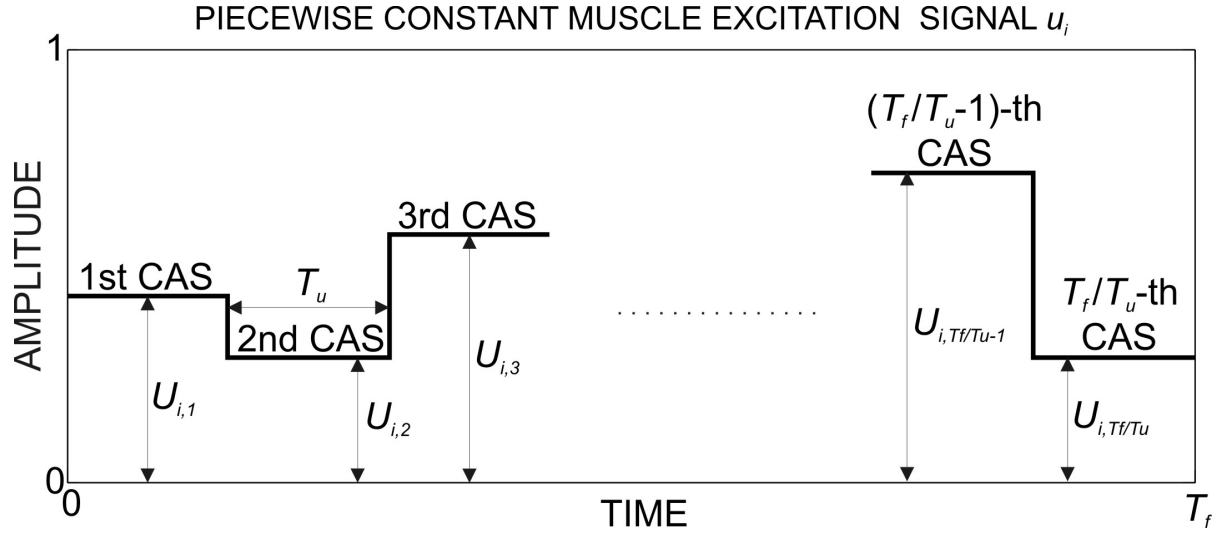
Fig. 3.2. The sketch of the intensity of stimulation (muscle excitation) in the form of piecewise constant signals. The signal u_i is a sequence of constant-amplitude segments (CASs) of equal durations. The CASs are numbered from 1st to T_f/T_u-th. Parameters T_f and T_u are simulation duration and CAS duration, respectively. Parameter $U_{ij}, j = 1,2,…,T_f/T_u$ is the amplitude of the j-th CAS of the signal u_i. The signal is normalized to the interval 0 (no excitation) and 1 (maximum excitation).

PWC, the question was if the application of MWDO would result in good tracking of the desired trajectories. Therefore, we tested the MWDO using many gait patterns recorded at a range of gait speeds that are of interest in rehabilitation of individuals with hemiplegia. It was assumed that tracking was satisfactory if the tracking errors were within ±1 SDJA (standard deviation of joint angles in normal gait). SDJA was based on typical inter-subject variability of joint angles during normal walking of healthy individuals. Reference profiles for SDJA in the knee and ankle joint angles over a gait stride were taken from [5]. SDJA was in the range of 3.2–7.6° and 2.6–6.9° for the knee and ankle joint angles, respectively.

2. METHODS

2.1. Model

The biomechanical model used in this study was designed for a particular application: restoration of hemiplegic gait by means of a four-channel FES with surface electrodes. The model comprised three rigid bodies – thigh, shank and foot – connected by pin joints which allowed rotation in the sagittal plane (see Fig. 3.3). The knee and ankle joints permit flexion/extension and dorsi/plantar flexion, respectively. Each of the joints was driven by a pair of equivalent muscles representing all the muscles that contribute to joint flexion or extension. A three compartment multiplicative Hill based model was used for the muscles. The influence of passive tissues crossing the joints was modeled by nonlinear resistive torques. The envisioned FES system will activate knee flexors/extensors and ankle flexors/extensors of the affected leg of a hemiplegic patient. The hip joint control was not considered in the simulation because the potential users control this joint to a large extent and it is very difficult to control hip movement with surface stimulation. Therefore, the model of the whole leg presented in Chapter 2 (see Fig. 2.1) was further reduced for the purpose of this study.

The following equation describes the system dynamics:

$$\begin{bmatrix} \ddot{\varphi}_S \\ \ddot{\varphi}_F \end{bmatrix} = \mathbf{A}^{-1}(\mathbf{\Phi})\left(\mathbf{B}(\mathbf{\Phi})\begin{bmatrix} \dot{\varphi}_S^2 \\ \dot{\varphi}_F^2 \end{bmatrix} + \mathbf{C}(\mathbf{\Phi}) + \mathbf{D}(\mathbf{\Phi})\begin{bmatrix} F_X \\ F_Y \end{bmatrix} + \mathbf{E}(\mathbf{\Phi})\begin{bmatrix} a_{KX} \\ a_{KY} \end{bmatrix} + \mathbf{T}\begin{bmatrix} M_K \\ M_A \end{bmatrix} \right) \tag{3.1}$$

where $\mathbf{\Phi} = [\varphi_S \; \varphi_F]^{\mathrm{T}}$ is a vector consisting of shank and foot segment angles from horizontal axis; $[M_K \; M_A]^{\mathrm{T}}$ is a vector comprising knee and ankle joint torques; $[F_X \; F_Y]^{\mathrm{T}}$ is a vector consisting of horizontal and vertical ground reaction forces; $[a_{KX} \; a_{KY}]^{\mathrm{T}}$ is a vector comprising horizontal and vertical components of knee acceleration; $\mathbf{A}(\mathbf{\Phi})$ is 2 x 2 system mass matrix; $\mathbf{B}(\mathbf{\Phi})$ is 2 x 2 matrix describing centrifugal
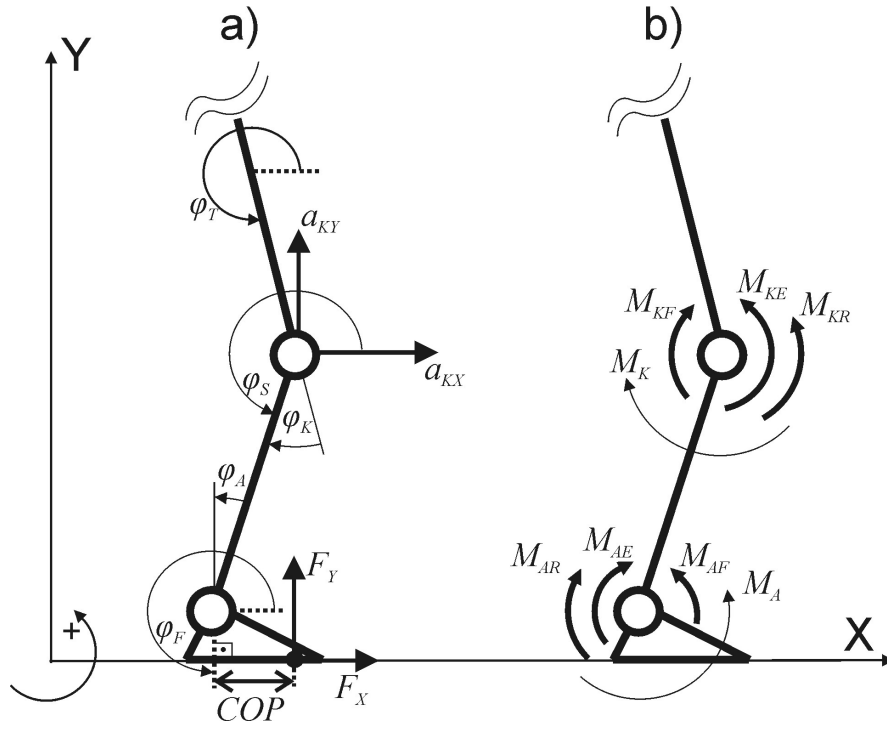
Fig. 3.3. Biomechanical model: a) definition of angles, accelerations and forces; and b) definition of considered torques. The thick links and circles represent segments and joints that are part of the model. The notations are: φ_T, φ_S, φ_F – angles of the thigh, shank and foot from horizontal axis; φ_K, φ_A – knee and ankle joint angles; a_{KX}, a_{KY} – horizontal and vertical components of knee accelerations; F_X, F_Y – horizontal and vertical components of ground reaction force; COP – trajectory of the center of pressure along the sole of the foot; M_{AF}, M_{AE}, M_{KF}, M_{KE} – torques generated by the equivalent ankle flexor, ankle extensor, knee flexor and knee extensor muscles; M_{AR}, M_{KR} – resistive ankle and knee joint torques; M_A, M_K – total torques acting at the ankle and knee joints.

effects; $\mathbf{C(\Phi)}$ is 2 x 1 vector of gravitational terms; $\mathbf{E(\Phi)}$ and $\mathbf{D(\Phi)}$ are 2 x 2 matrices describing the influence of interface forces and torques acting at the knee and the sole of the foot respectively; and $\mathbf{T}$ is 2 x 2 matrix describing how the joint torques contribute to total torques acting at the segments. The matrices and notations are given in Appendix.

Mathematical model in the state-space form was derived from (3.1). First, a vector of state variables comprising segment angles, segment angular velocities, and muscle activations was introduced. Then, the joint torques M_K and M_A were expressed as the sums of active and resistive torques produced by the equivalent muscles and the passive tissue, respectively (see Appendix). Finally, after some regrouping of the terms, the following nonlinear equations in the state-space form were obtained:

$$\dot{x}_i = \begin{cases} (u_i - x_i)[u_i / \tau_{act} + (1-u_i)/\tau_{deact}], & u_i \geq x_i \\ (u_i - x_i)/\tau_{deact}, & u_i < x_i \end{cases}, i = 1, 2, 3, 4; \tag{3.2}$$

$$\dot{x}_5 = x_6; \quad \dot{x}_6 = P_6(\mathbf{X},t) + \sum_{i=1}^{4} R_{6,i}(\mathbf{X},t)x_i; \quad \dot{x}_7 = x_8; \quad \dot{x}_8 = P_8(\mathbf{X},t) + \sum_{i=1}^{4} R_{8,i}(\mathbf{X},t)x_i. \tag{3.3}$$

The vector $\mathbf{X} = [x_i]$ (i = 1, 2,…, 8) is the vector of state variables. The variables $x_i \in [0,1]$ (i = 1, 2, 3, 4) are normalized muscle activations which give the current level of activation of the equivalent muscles. The maximal activation corresponding to maximally contracted muscle was assumed to be 1, while the resting muscle was described with the activation value 0. The variables $x_5 = \varphi_F$, $x_6 = d\varphi_F/dt$, $x_7 = \varphi_S$, and $x_8 = d\varphi_S/dt$ are segment angles and segment angular velocities. Equation (3.3) models the skeletal dynamics. The terms $P_i(\mathbf{X},t)$ and $R_{i,j}(\mathbf{X},t)$ (i = 6, 8 and j = 1, 2, 3, 4) are nonlinear functions of the system states (i.e., segment angles and angular velocities) and simulation inputs (i.e., ground reaction forces, knee acceleration). Equation (3.2) models muscle activation dynamics. Parameters τ_{act} and τ_{deact} are time constants for muscle activation and deactivation, respectively. The vector $\mathbf{U} = [u_i]$ (i = 1, 2, 3, 4) is the vector of control inputs driving the behavior of the system. The signals $u_i \in [0,1]$, (i = 1, 2, 3, 4) are

normalized levels of excitations for the equivalent ankle flexor, ankle extensor, knee flexor and knee extensor muscle, respectively.

2.2. Moving-window dynamic optimization

The goal was to determine the muscle excitations u_i to be the piecewise constant (PWC) signals having constant-amplitude segments (CASs) of equal duration (see Fig. 3.2), while the generated trajectory remains within the preset tolerance from the desired trajectory. Since CAS duration was predefined, the variables that needed to be determined were the amplitudes U_{ij} of the j-th CAS of the PWC signal u_i:

$$U_{ij}, i = 1,2,3,4 \wedge j = 1,2,\ldots,T_f / T_u. \tag{3.4}$$

The parameters T_f and T_u are simulation duration and CAS duration, respectively. We applied new iterative algorithm to calculate the parameters U_{ij}. In each iteration n, starting at $n = 1$, the amplitudes of the n-th CASs of the control signals were determined (i.e., parameters U_{in}, $i = 1, 2, 3, 4$).

The time window TW_n spanning K consecutive CASs starting from the n-th CAS was defined:

$$TW_n = [(n-1)T_u, (n+K-1)T_u]. \tag{3.5}$$

This was followed by optimization over the interval TW_n:

$$\min_{\substack{U_{ij}, i=1,2,3,4 \wedge \\ j=n,n+1,\ldots n+K-1}} \int_{t=(n-1)T_u}^{(n+K-1)T_u} \left\{ \lambda_{TE}\left[\left(\frac{\varphi_F^*(t) - x_5(t)}{\varphi_{F\max}^*} \right)^2 + \left(\frac{\varphi_S^*(t) - x_7(t)}{\varphi_{S\max}^*} \right)^2 \right] + \lambda_U \sum_{i=1}^{4} u_i^2(t) \right\} dt$$

$$s.t. \tag{3.6}$$

$$\dot{\mathbf{X}} = \mathbf{f}(\mathbf{X}, t, \mathbf{U}); \quad U_{ij} \in [0,1].$$

The notations φ_S^*, φ_F^*, $\varphi_{S\max}^*$ and $\varphi_{F\max}^*$ are for the desired shank and foot segment angles and their maximal values, respectively. The first two terms in the cost function are the sum of squares of normalized tracking errors from the desired trajectory and the last term is the sum of squares of muscle excitations. The parameters λ_{TE} and λ_U are the factors setting the relative weights of tracking error versus total excitation in the overall cost function. The term $\mathbf{f}(\mathbf{X}, t, \mathbf{U})$ represents the mathematical model of the system given by (3.2) and (3.3).

Equation (3.6) represents a nonlinear parameter optimization problem in which 4*K unknown design variables U_{ij}, $i = 1, 2, 3, 4$ and $j = n, n+1,\ldots, n+K-1$; have to be determined. Consequently, we solved (3.6) by applying nonlinear programming based on sequential quadratic programming [6].

After determining the optimal values, the amplitudes of the n-th CASs of the control signals (i.e., U_{in}, $i = 1, 2, 3, 4$) were stored while the rest of the values were discarded. Then, the controls u_i were applied to the system with the amplitudes equal to the calculated optimal CAS amplitudes U_{in} and the system equations were integrated over the duration of one CAS, that is, over the time interval $[(n-1)T_u, nT_u]$. Final system state obtained by the integration was used as the initial condition for integration in the next iteration.

Described procedure was repeated after incrementing the iteration number, effectively shifting the window TW_n given by (3.5) for one CAS duration towards the end of the input gait pattern as shown in Fig. 3.4.

MWDO simulations were implemented in Matlab 7.1 on a standard PC platform (Pentium dual-core processor at 2 GHz). The program (*.mat) is available on the request from the authors.

2.3. Collecting the input data

Input data (desired gait patterns) for presented simulations have been recorded from a male able-bodied subject (30 yrs; H = 1.74 m; M = 75 kg) in the Gait Laboratory at the Center for Sensory Motor Interaction, Aalborg University, by using the methods described in [7]. The laboratory is equipped with a camera based motion capture system (8 ProReflex MCU240 cameras, Qualisys, SE) and a single AMTI force plate (OR6-5, Advanced Mechanical Technology, USA). The data were acquired at 100 samples per second using PCI-DAS1602/12 DAQ board (Measurement Computing Corporation, USA). During the
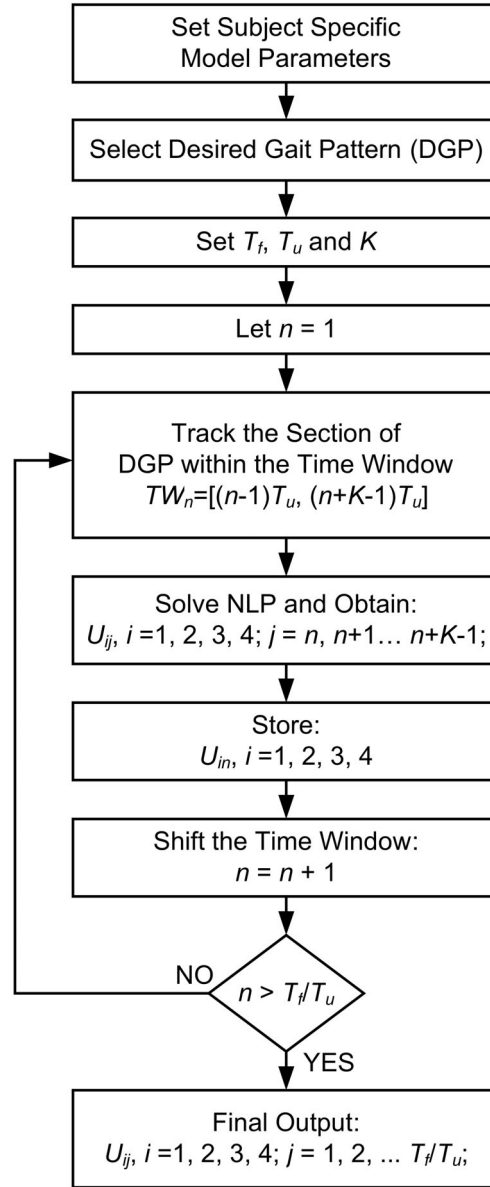
```
┌─────────────────────────┐
│   Set Subject Specific   │
│    Model Parameters      │
└─────────────────────────┘
            │
            ▼
┌─────────────────────────┐
│ Select Desired Gait     │
│ Pattern (DGP)           │
└─────────────────────────┘
            │
            ▼
┌─────────────────────────┐
│  Set Tf, Tu and K        │
└─────────────────────────┘
            │
            ▼
┌─────────────────────────┐
│  Let n = 1               │
└─────────────────────────┘
            │
            ▼
┌─────────────────────────┐
│  Track the Section of    │
│  DGP within the Time     │
│  Window                  │
│  TWn=[(n-1)Tu, (n+K-1)Tu]│
└─────────────────────────┘
            │
            ▼
┌─────────────────────────┐
│  Solve NLP and Obtain:   │
│  Uij, i =1, 2, 3, 4;     │
│  j = n, n+1… n+K-1;      │
└─────────────────────────┘
            │
            ▼
┌─────────────────────────┐
│  Store:                  │
│  Uin, i =1, 2, 3, 4      │
└─────────────────────────┘
            │
            ▼
┌─────────────────────────┐
│  Shift the Time Window:  │
│  n = n + 1               │
└─────────────────────────┘
            │
            ▼
      ◇ n > Tf/Tu ◇  NO
            │ YES
            ▼
┌─────────────────────────┐
│  Final Output:           │
│  Uij, i =1, 2, 3, 4;     │
│  j = 1, 2, ... Tf/Tu;    │
└─────────────────────────┘
```

Fig. 3.4. Moving-window dynamic optimization. The parameters are: T_u, T_f – CAS duration and simulation duration; TW_n – moving time window for optimization; K – the length ($K \cdot T_u$) of the optimization window TW_n; n – iteration number; U_{ij} – the amplitude of the j-th CAS of the signal u_i; NLP – nonlinear programming. The parameters are depicted in Fig. 3.2 and explained in the text.

acquisition, the subject walked at four gait speeds (0.4, 0.8, 1 and 1.4 m/s), making ten walking trials at each of the speeds. Thigh angle, knee and ankle joint angles, knee acceleration, ground reaction force and trajectory of the center of pressure along the sole of the foot [see Fig. 3.3(a)] were calculated from the camera and the force plate data using a software for the analysis of human motion (Visual3D, C-Motion, USA). The signals were low-pass filtered by a 2nd order dual-pass Butterworth filter at a cutoff frequency of 6 Hz [5].

The quality of tracking was assessed by calculating the mean values (MEAN$_{TE}$), standard deviations (STD$_{TE}$), and maximum values (MAX$_{TE}$) of the absolute tracking errors. The absolute tracking error in the i-th sample $TE(i)$ was defined as absolute value of the difference between the i-th sample of generated joint angle (φ_K, φ_A) and the i-th sample of desired joint angle (φ_K^*, φ_A^*):

$$TE\varphi_K(i) = \left|\varphi_K(i) - \varphi_K^*(i)\right|, \quad TE\varphi_A(i) = \left|\varphi_A(i) - \varphi_A^*(i)\right|. \tag{3.7}$$

The inertial and muscle parameters for the biomechanical model were determined by using a Kin-Com machine (KC2, Isokinetic International, USA) and the techniques described in [8].

THIGH ANGLE [°]

NORMALIZED GROUND REACTION FORCES
VERTICAL ·········· HORIZONTAL

JOINT ANGLES [°]
KNEE ANGLE ·········· ANKLE ANGLE

COP [m]

TIME [s]

KNEE ACCELERATION [m/s²]
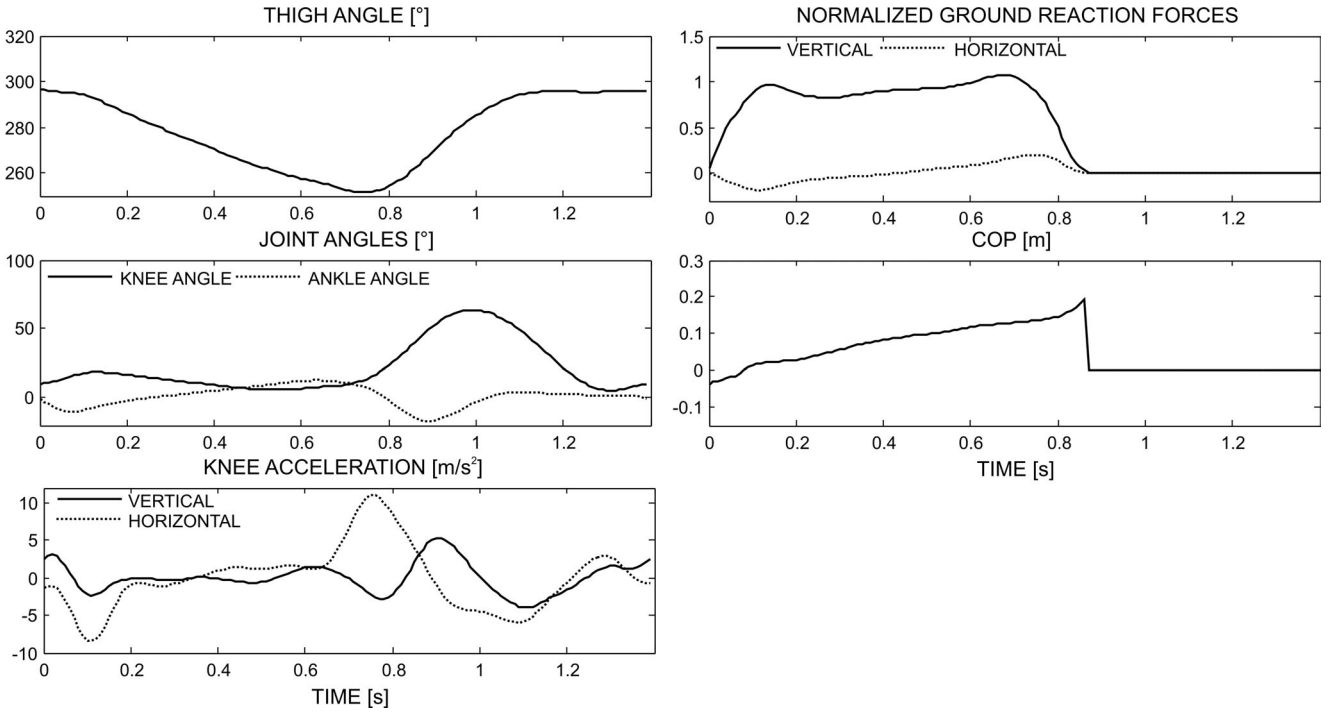VERTICAL
HORIZONTAL

TIME [s]

Fig. 3.5. Input data for simulation. The plots show one gait stride starting with the right heel strike recorded at the gait speed of 1 m/s. Ground reaction forces are normalized to body weight. The set of signals constitutes a desired gait pattern for the simulation. The signals are defined in Fig. 3.3(a).

TABLE I

PARAMETERS FOR THE BIOMECHANICAL MODEL

S	$J_{CS} = 0.09$ kg·m²	$m_S = 3.5$ kg		$d_S = 0.19$ m		$L_S = 0.415$ m
F	$J_{CF} = 0.02$ kg·m²	$m_F = 1.08$ kg		$d_F = 0.04$ m		$L_F = 0.088$ m
AF	$c_{10} = 59.1$	$c_{11} = -29$	$c_{12} = -110$	$c_{13} = 0.055$		$c_{14} = 1.15$
AE	$c_{20} = 135.1$	$c_{21} = 90.44$	$c_{22} = -250.2$	$c_{23} = 0.04$		$c_{24} = 1.4$
AR	$d_{10} = 9.8$	$d_{11} = 0.6$	$d_{12} = 3.5$	$d_{13} = 5.8$	$d_{14} = 0.7$	$d_{15} = -7.99$
KF	$c_{30} = 79.1$	$c_{31} = 2.3$	$c_{32} = -5.11$	$c_{33} = 0.04$		$c_{34} = 1.3$
KE	$c_{40} = 27.55$	$c_{41} = 199.55$	$c_{42} = -90.38$	$c_{43} = 0.05$		$c_{44} = 1.5$
KR	$d_{20} = 8.5$	$d_{21} = 0.55$	$d_{22} = 0.003$	$d_{23} = 4.41$	$d_{24} = 60.58$	$d_{25} = -27.21$

Legend: S, F – shank and foot; K, A – knee and ankle joints; F, E – equivalent flexor and extensor; R – resistive joint torque. Parameters are defined in Appendix.

3. RESULTS

Here we show one example in details and the summary results for all of the collected input data. Data similar to the ones shown in Fig. 3.5 were used as the desired gait patterns for the simulations. The figure shows a sample of the recordings at the gait speed of 1 m/s which starts with the right heel strike. The parameters determining the model of the leg are in Table I.

Parameters for MWDO were set to the following values: $T_u = 50$ ms and $K = 5$. The simulation using the desired gait pattern from Fig. 3.5 lasted approximately 9 minutes. Simulation results are given in Fig. 3.6. The figure shows the calculated muscle excitation profiles and the joint angles that would be obtained if these profiles are applied. The generated angles are superimposed onto the desired angles in order to show the quality of tracking. The tracking errors were within the prescribed error margin of ±1 SDJA.

By using the same model (Table I) and optimization parameters ($T_u = 50$ ms, $K = 5$), we simulated all of the 40 gait strides that were recorded. Stride duration was in the range of 1.1–2.4 s for the gait speeds considered in this study. The corresponding simulation durations were from 4 to 25 minutes. The overall mean and maximum absolute tracking errors and their standard deviations for the knee and ankle joint angles were $\text{MEAN}_{TE}(\varphi_K) = 0.55°$, $\text{STD}_{TE}(\varphi_K) = 0.72°$, $\text{MAX}_{TE}(\varphi_K) = 3.91°$, $\text{MEAN}_{TE}(\varphi_A) = 0.59°$,
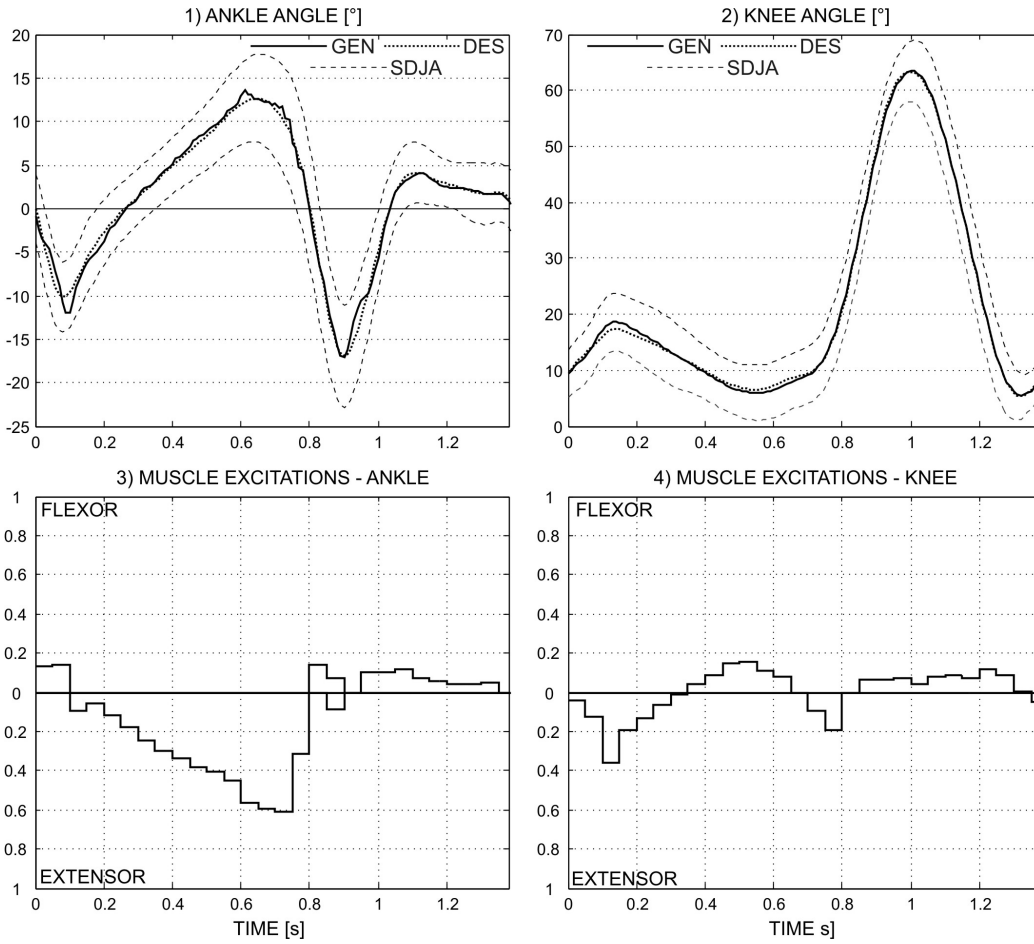
Fig. 3.6. Joint angles (panels 1 and 2) and muscle excitations (panels 3 and 4) obtained by setting the parameters for MWDO to: $T_u = 50$ ms and $K = 5$. The excitation profiles are PWC signals having CASs of equal duration (50 ms). The panels 3 and 4 include the excitation for both flexor muscles (upper part), and the extensors (lower part). Generated angles (GEN), desired angles (DES), and SDJA profiles (taken from [5]) are represented by continuous, dotted and dashed lines, respectively. Notice that the tracking errors are within the margins of ±1 SDJA.

$\text{STD}_{\text{TE}}(\varphi_A) = 0.64°$, and $\text{MAX}_{\text{TE}}(\varphi_A) = 4.69°$. The tracking errors were within the allowable margins of ±1 SDJA in all conducted simulations.

In order to test the generality of the algorithm, we used the same model parameters (Table I) and input data shown in Fig. 3.5, and then varied the optimization parameters. For this test, we selected CAS durations of 50, 100 and 150 ms and for each value of CAS duration we used different lengths of the optimization window ($K = 2,3,4,5$). We tested at least two simulations for each value of K.

Fig. 3.7 shows simulation results for $T_u = 100$ ms and $K = 3$. In this case, the simulation lasted for about 7 minutes. The generated muscle excitations are PWC signals comprising CASs which are twice as long as the CASs of the signals in Fig. 3.6. Consequently, the mean and maximum ankle angle tracking errors increased ($\text{MEAN}_{\text{TE}}(\varphi_A) = 1.1°$, $\text{MAX}_{\text{TE}}(\varphi_A) = 3.8°$), compared to the errors obtained in Fig. 3.6 ($\text{MEAN}_{\text{TE}}(\varphi_A) = 0.52°$, $\text{MAX}_{\text{TE}}(\varphi_A) = 2.4°$). Although the errors are now larger, they are still within ±1 SDJA from the desired joint angles. Overall, in only two cases the generated angles deviated from the desired trajectories for more than ±1 SDJA. These were two out of five simulations with $T_u = 150$ ms and $K = 2$.

In general, longer CAS duration leads to coarser profiles and thereby produces larger tracking errors as it can be seen by comparing Figs. 3.6 and 3.7. For the constant CAS, increasing the value of K decreased tracking errors and increased simulation duration. This was due to the fact that longer optimization window was being used for calculating each of the CAS amplitudes. For example, the lowest mean ankle and knee joint angle tracking errors ($\text{MEAN}_{\text{TE}}(\varphi_A) = 0.52°$, $\text{MEAN}_{\text{TE}}(\varphi_K) = 0.42°$) were obtained for $T_u = 50$ ms and $K = 5$; the simulation lasted approximately 9 minutes. The shortest simulation duration of about 1 minute was obtained for $T_u = 100$ ms and $K = 2$, but the mean tracking errors were higher
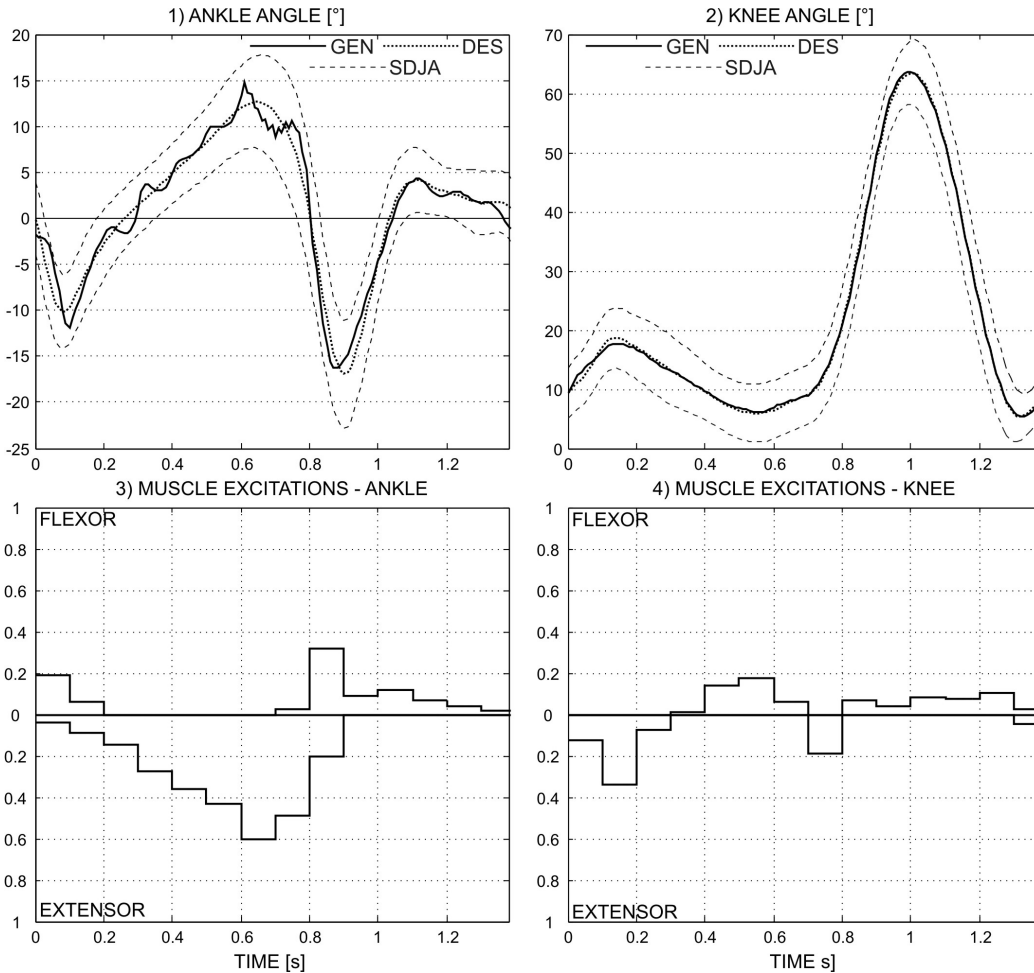
Fig. 3.7. Joint angles (panels 1 and 2) and muscle excitations (panels 3 and 4) obtained by setting the parameters for MWDO to: T_u = 100 ms and K = 3. The panels 3 and 4 include the excitation for both flexor muscles (upper part), and the extensors (lower part). Generated angles (GEN), desired angles (DES), and SDJA profiles (taken from [5]) are represented by continuous, dotted and dashed lines, respectively. Notice that the muscle excitations have CASs which are twice as long as the CASs in the signals from Fig. 3.6. Consequently, the tracking errors are larger (particularly at the ankle joint); however, they are still within the permissible range (±1 SDJA).

(MEAN$_{TE}(\varphi_A)$ = 1.56°, MEAN$_{TE}(\varphi_K)$ = 0.84°).

In addition, we calculated the torques generated at the joints and by the muscles. Overall, the torques from the simulation were within the range reported in literature for the normal gait at the same gait speeds [5].

4. DISCUSSION

We developed a novel method for generation of muscle excitations to be used for the synthesis of rule-based control for assisting gait in individuals with hemiplegia. The biomechanical model and the optimization algorithm were developed with the purpose of designing a practical FES system with four stimulation channels applied to one leg of an individual with compromised walking. The biomechanical model reduction allows identification of the parameters; thereby customization of simulation to the potential user.

The task of the simulation was to calculate the controls which, although constrained to be PWC, generate a gait pattern that is tracking the desired one within the adopted error margin. The question was if MWDO would be able to meet the performance requirements stated in the introduction. The ability of MWDO to generate the excitation profiles for a number of gait patterns recorded at different gait speeds was tested. In addition, the profiles were shaped using a range of CAS durations. The analysis shows that this task was accomplished: the tracking errors were within the acceptable margins. Furthermore, although PWC stimulation was applied, the torques generated by the muscles were smooth and within the

range of joint torques reported in literature.

Importantly, MWDO generates excitation profiles that have uniform and simple structure. The excitations are stair-like and similar to the profiles typically used in FES. They are convenient for straightforward implementation and execution by a programmable stimulator. The profiles could be transferred to the stimulator and used directly as an initial stimulation sequence for the individual with hemiplegia. This could be an alternative to manual adjustment of the stimulation parameters using trial-and-error procedure. Since the CAS duration is predefined and equal, the profile is completely defined by an array of CAS amplitudes. These are the only data that need to be transferred to and stored by a programmable stimulator. This minimizes the memory requirements and allows efficient management of the stimulation parameters.

Finally, the excitation profiles calculated by MWDO can be used as the target outputs for machine learning generating the rules for rule-based control of FES. Importantly, MWDO generates the profiles which are PWC and thereby convenient for application of machine learning. Namely, in addition to the powerful machine learning techniques which are able to interpolate nonlinear functions of arbitrary complexity (e.g., radial basis artificial neural networks and multilayer perceptrons [9], [10]), the more specialized techniques that approximate PWC functions could be used for the mapping (e.g., classification and regression trees [9], inductive learning [11]). The latter are especially desirable since they belong to the class of so called symbolic techniques and generate the rules in the form of decision trees or production logic formulas. Both of these structures are human readable (IF-THEN-ELSE) and easy to implement by transcribing them directly into analogous constructs of a high level programming language (e.g., if {} else {} construct in C programming language).

On a more general level, this study demonstrated the advantages of the new optimization method. MWDO method is flexible; the profiles can be shaped by using the parameter T_u (CAS duration). As explained earlier, this controls the tradeoff between the coarseness of the profiles and the magnitude of the tracking errors. Coarser profiles have fewer transitions in excitation levels per gait stride, and thereby they are likely to generate fewer and simpler rules for rule-based control. This flexibility of MWDO is an important feature that can be used to design an optimal set of rules through trial and error. The best combination of values for the parameters T_u and K will depend on the specific case and desired simulation goals (e.g., tolerable tracking errors and maximum excitation levels). Once set, the parameters are held constant during the simulation. MWDO can be modified to allow the values of the parameters T_u and/or K to change adaptively during the simulation according to a preset criterion such as, for example, maximum allowed tracking error over the current optimization window. However, that would significantly increase the complexity of the optimization algorithm. Moreover, it would compromise the basic idea of the algorithm, that is, the generation of simple and uniform excitation profiles.

Another important feature of the new method is related to the time needed for the simulation. Our method breaks up a complex optimization task into a number of smaller ones which are easier to solve (see Fig. 3.4). We obtained the simulation times which were between 1 and 25 minutes by using a standard PC machine. This is important because in clinical applications, the power production of muscles can be low due to atrophy or other impairments. Hence, the simulation can result with large tracking errors and the generated gait can show to be inadequate [12]. Therefore, several gait patterns possibly at different gait speeds need to be tested for the potential user before a suitable one is selected [7].

5. APPENDIX

The matrices from equation (3.1) are:

$$\mathbf{A}(\mathbf{\Phi}) = \begin{bmatrix} J_{CS} + m_F L_S^2 + m_S d_S^2 & m_F d_F L_S \cos(\varphi_S - \varphi_F) \\ m_F d_F L_S \cos(\varphi_S - \varphi_F) & J_{CF} + m_F d_F^2 \end{bmatrix};$$

$$\mathbf{B}(\mathbf{\Phi}) = \begin{bmatrix} 0 & -m_F d_F L_S \sin(\varphi_S - \varphi_F) \\ m_F d_F L_S \sin(\varphi_S - \varphi_F) & 0 \end{bmatrix};$$

$$\mathbf{C}(\mathbf{\Phi}) = \begin{bmatrix} -g(m_S d_S + m_F L_S)\cos\varphi_S \\ -gm_F d_F \cos\varphi_F \end{bmatrix};$$

$$\mathbf{D}(\mathbf{\Phi}) = \begin{bmatrix} -L_S \sin\varphi_S & L_S \cos\varphi_S \\ CF2CP_y - d_F \sin\varphi_F & d_F \cos\varphi_F - CF2CP_x \end{bmatrix};$$ (A3.1)

$$\mathbf{E}(\mathbf{\Phi}) = \begin{bmatrix} (m_S d_S + m_F L_S)\sin\varphi_S & -(m_S d_S + m_F L_S)\cos\varphi_S \\ m_F d_F \sin\varphi_F & -m_F d_F \cos\varphi_F \end{bmatrix};$$

$$\mathbf{T} = \begin{bmatrix} -1 & -1 \\ 0 & 1 \end{bmatrix}.$$

The notations are:

S, F	shank and foot segments;
CS, CF	centers of the mass of the shank and foot;
J_{CS}, J_{CF}	moments of inertia of the shank and foot about the central axes perpendicular to the sagittal plane;
L_S, L_F	lengths of the shank and foot;
d_S, d_F	distances of the proximal joint to the center of the mass for the shank and foot;
m_S, m_F	masses of the shank and foot;
g	gravitational acceleration;
φ_S, φ_F	absolute angles of the shank and foot from horizontal axis;
$CF2CP_x$	distance between the center of mass of the foot (CF) and the center of pressure (CP) along the horizontal axis;
$CF2CP_y$	distance between the center of mass of the foot and the center of pressure along the vertical axis.

The total torques at the joints comprised active torques generated by the equivalent muscles and resistive torque resulting from elastic tissues crossing the joints [see Fig. 3.3(b)]:

$$M_K = M_{KF} - M_{KE} - M_{KR}; \quad M_A = M_{AF} - M_{AE} - M_{AR}.$$ (A3.2)

The equations for the active torques at the ankle joint have the following form:

$$M_{AF} = (c_{10} + c_{11}\varphi_A + c_{12}\varphi_A^2)g_{AF}(\dot{\varphi}_A)x_1; \quad M_{AE} = (c_{20} + c_{21}\varphi_A + c_{22}\varphi_A^2)g_{AE}(\dot{\varphi}_A)x_2.$$ (A3.3)

The variable φ_A is the ankle joint angle in radians. The signals $x_i \in [0,1]$ ($i = 1, 2$) are normalized levels of activation of the equivalent ankle flexor and extensor muscle, respectively. The parameters c_{ik} ($i = 1, 2$ and $k = 0, 1, 2$) determine the maximum isometric torque versus joint angle characteristic for the muscles. They are obtained as the best quadratic fit through experimentally collected data. The terms g_{AF} and g_{AE} are normalized torque versus joint angular velocity characteristics for the flexor and extensor, respectively:

$$g_{AF}(\dot{\varphi}_A) = \begin{cases} c_{14}, & \dot{\varphi}_A < (1 - c_{14})/c_{13} \\ 1 - c_{13}\dot{\varphi}_A, & (1 - c_{14})/c_{13} \leq \dot{\varphi}_A < 1/c_{13} \\ 0, & 1/c_{13} \leq \dot{\varphi}_A \end{cases}$$

$$g_{AE}(\dot{\varphi}_A) = \begin{cases} 0, & \dot{\varphi}_A < -1/c_{23} \\ 1 + c_{23}\dot{\varphi}_A, & -1/c_{23} \leq \dot{\varphi}_A < (c_{24}-1)/c_{23} \\ c_{24}, & (c_{24}-1)/c_{23} \leq \dot{\varphi}_A. \end{cases} \qquad (A3.4)$$

The parameters c_{ik} ($i = 1, 2$ and $k = 3, 4$) determine the slopes and the saturation levels of the profiles. The parameters in (A3.3) and (A3.4) can be determined by using isometric and isokinetic muscle tests. Resistive torque at the ankle joint is given by:

$$M_{AR} = d_{10}(\varphi_A - \varphi_{A0}) + d_{11}\dot{\varphi}_A + d_{12}e^{d_{13}\varphi_A} - d_{14}e^{d_{15}\varphi_A}. \qquad (A3.5)$$

The angle φ_{A0} is the neutral position for the ankle joint. The first two terms model viscoelastic properties of the joint while the other terms represent nonlinear exponential torque around the terminal joint positions. The passive tests such as pull and pendulum experiments are used to estimate the parameters in (A3.5). The equations for the active and resistive torques at the knee have the same form. Importantly, the model parameters c_{ik} ($i = 1, 2, 3, 4$ and $k = 0, 1, 2, 3, 4$; index i denotes the muscle) and d_{ik} ($i = 1, 2$ and $k = 0, 1, 2, 3, 4, 5$; index i denotes the joint) are user specific. The techniques for determining these parameters are described in detail in [8]. Detailed explanation of the equations (A3.3)–(A3.5) and the corresponding parameters can be found in Chapter 2.

Muscle activation dynamics can be modeled by relating the time rate of change of activation (dx_i/dt) to activation (x_i) and excitation (u_i) [2], [3]:

$$\dot{x}_i = \begin{cases} (u_i - x_i)[u_i/\tau_{act} + (1-u_i)/\tau_{deact}], & u_i \geq x_i \\ (u_i - x_i)/\tau_{deact}, & u_i < x_i \end{cases}, \quad i = 1, 2, 3, 4. \qquad (A3.6)$$

where, the parameters τ_{act} and τ_{deact} are time constants for activation and deactivation, respectively. The values of 20 and 60 ms were adopted for activation and deactivation, respectively [2]. The muscle excitations $u_i \in [0,1]$ ($i = 1, 2, 3, 4$) are the control inputs for the system. Their determination is the purpose of the simulation.

REFERENCES

[1] P. H. Veltink, H. J. Chizeck, P. E. Crago, and A. Elbialy, "Nonlinear joint angle control for artificially stimulated muscle," *IEEE Trans. Biomed. Eng.*, vol. 39, no. 4, pp. 368-380, 1992.

[2] C. C. Raasch, F. E. Zajac, B. M. Ma, and W. S. Levine, "Muscle coordination of maximum-speed pedaling," *J. Biomech.*, vol. 30, no. 6, pp. 595-602, 1997.

[3] D. G. Thelen, F. C. Anderson, and S. L. Delp, "Generating dynamic simulations of movement using computed muscle control," *J. Biomech.*, vol. 36, no. 3, pp. 321-328, 2003.

[4] A. E. Bryson, *Dynamic Optimization*. Menlo Park, CA: Addison Wesley Longman, 1999.

[5] D. A. Winter, *Biomechanics and Motor Control of Human Movement: Normal, Elderly and Pathological*, 2nd ed., Waterloo, Ontario, Canada: University of Waterloo Press, 1991.

[6] Anonymous (accessed on June 4th 2008). MATLAB Optimization Toolbox User's guide. Available online at: http://www.mathworks.com/access/helpdesk/help/pdf_doc/optim/optim_tb.pdf.

[7] S. Došen and D. B. Popović, "Accelerometers and Force Sensing Resistors for Optimal Control of Walking of a Hemiplegic," *IEEE Trans. Biomed. Eng.*, vol. 55, no. 8, pp. 1973-1984, 2008.

[8] R. B. Stein, E. P. Zehr, M. K. Lebiedowska, D. B. Popovic, A. Scheiner, and H. J. Chizeck, "Estimating mechanical parameters of leg segments in individuals with and without physical disabilities," *IEEE Trans. Rehabil. Eng.*, vol. 4, no. 3, pp. 201-211, 1996.

[9] B. W. Heller, P. H. Veltink, N. J. M. Rijkhoff, W. L. C. Rutten, and B. J. Andrews, "Reconstructing muscle activation during normal walking - a comparison of symbolic and connectionist machine learning techniques," *Biol. Cybern.*, vol. 69, no. 4, pp. 327-335, 1993.

[10] S. Jonić, T. Janković, V. Gajić, and D. Popović, "Three machine learning techniques for automatic determination of rules to control locomotion," *IEEE Trans. Biomed. Eng.*, vol. 46, no. 3, pp. 300-310, 1999.

[11] Z. M. Nikolić and D. B. Popović, "Predicting quadriceps muscle activity during gait with an automatic rule determination method," *IEEE Trans. Biomed. Eng.*, vol. 45, no. 8, pp. 1081-1085, 1998.

[12] D. Popović, R. B. Stein, M. N. Oguztoreli, M. Lebiedowska, and S. Jonić, "Optimal control of walking with functional electrical stimulation: A computer simulation study," *IEEE Trans. Rehabil. Eng.*, vol. 7, no. 1, pp. 69-79, 1999.

CHAPTER 4
Accelerometers and Force Sensing Resistors for Optimal Control of Walking of a Hemiplegic[*]

Summary–Rule-based controller for gait restoration by means of functional electrical stimulation (FES) is created from a sensorimotor model (SMM) of gait by implementation of supervised machine learning. The SMM comprises: 1) sensor data recorded by a set of gait sensors, and 2) muscle activation profiles calculated by using customized modeling and simulations. The sensor data are used as inputs and the muscle activations as target outputs for machine learning. As a result, a rule-based controller is generated and its inputs (feedback) and outputs (feedforward commands) are created from the sensory and motor components of the SMM, respectively. Therefore, gait sensors that are used to acquire the sensor data for the SMM provide also the real-time feedback for the controller. In order for the system to be practical, the feedback has to comprise sensors that are convenient for daily use. Accelerometers made in microelectromechanical technology and piezoresistive force sensing resistors (FSRs) are possible choice. In order to generate the motor component of the SMM by using the selected sensors, a method for biomechanical gait simulations that computes muscle activations from the data recorded by the sensors has to be developed. In this chapter, we describe an optimal controller for gait simulations which uses accelerometers and FSRs for the control of walking of hemiplegic individuals. The data from four dual-axis accelerometers and four FSRs were inputs, while six muscle activation profiles were outputs. The controller includes two stages: 1) estimating the target gait pattern using artificial neural networks; and 2) optimal control minimizing the tracking errors (from the estimated gait pattern) and muscle efforts. The second stage uses a reduced model that can be customized for an individual with a disability. The controller was tested using data collected from six healthy subjects walking at five gait speeds (0.6–1.4 m/s). The average root mean square errors (RMSE) normalized by the peak-to-peak value of the target signals (NRMSE) were below 6%, 7%, 8% and 3% for estimation of joint angles, hip acceleration, ground reaction force and movement of the center of pressure, respectively. Using the estimated data as inputs, the simulation generated the target healthy-like gait patterns and reproducible muscle activation profiles in 90% of 300 tested gait trials. Overall tracking NRMSE was between 2% and 9%. The optimal controller was developed for testing the feasibility of healthy-like gait patterns in hemiplegic individuals, and for generating SMMs which are required for the synthesis of a sensory-driven rule-based control of walking assisted by FES.

1. INTRODUCTION

Rule-based controller for gait restoration by means of functional electrical stimulation (FES) is created by applying supervised machine learning to a sensorimotor model (SMM) of gait (see Chapter 1, Fig. 1.6). The SMM comprises sensory component (sensor data) and motor component (muscle activation profiles). The sensor data from the SMM are used as inputs and the muscle activations as target outputs for machine learning. As a result, a rule-based controller is generated and its inputs (feedback) and outputs (feedforward commands) are created from the sensory and motor components of the SMM, respectively (see Chapter 1, Fig. 1.8). Chapters 2 and 3 describe the methods for creating the motor component of the SMM. Importantly, the simulation presented in Chapter 3 outputs the profiles that are convenient for implementation. Analogously, the goal of this study was to generate the sensory component of the SMM in the form that leads to a practical system for gait restoration (see Fig. 4.1).

Sensor data for the SMM are acquired by using a set of gait sensors. As explained, the same sensors will provide the real-time feedback for the rule-based controller. In order for the system to be practical, the feedback has to comprise sensors that are convenient for daily use. Hence, the following tasks need to be implemented within the customized modeling and simulation approach (see Fig. 4.1): 1) a set of practical sensors (i.e., easy to don and doff, small and energy efficient, and robust) has to be selected, and 2) a simulation method that uses data from the selected sensors to calculate muscle activations has to be developed. This will allow collecting and simulating a number of examples (gait strides), thereby creating a large knowledge base (sensorimotor model) for machine learning. Such a comprehensive SMM that captures inherent variability of human gait [1] is crucial for designing a robust rule-based controller.

The practical sensory system could include a variety of hardware, such as force sensing resistors (FSRs), and accelerometers or gyroscopes made in microelectromechanical system (MEMS) technology [2]. One simple configuration could comprise a set of multi-axis accelerometers and piezoresistive force sensors since neither is expensive, yet sufficiently reliable and robust [3].

In Chapters 2 and 3, we described biomechanical simulations of gait that use optimal control and a fully customized model of an individual with a disability [4]–[6]. The input for the simulations was a desired gait pattern comprising joint angles, hip accelerations, and ground reaction forces. The data were recorded in a gait laboratory by using a camera based motion capture system and a force plate.

The optimization algorithm that we developed in Chapter 2 allows tracking of desired trajectories to be implemented in different phase spaces (see Chapter 2, equations 2.9–2.11). If the tracking error is formulated in terms of angular accelerations instead of joint angles (see Chapter 2, equation 2.11), the data from accelerometers could be used directly as inputs for the simulation. This was our initial attempt to eliminate the cameras and/or goniometers and to use a practical set of sensors for recording the gait pattern. However, doing so showed that the tracking of accelerations caused data to drift in the joint
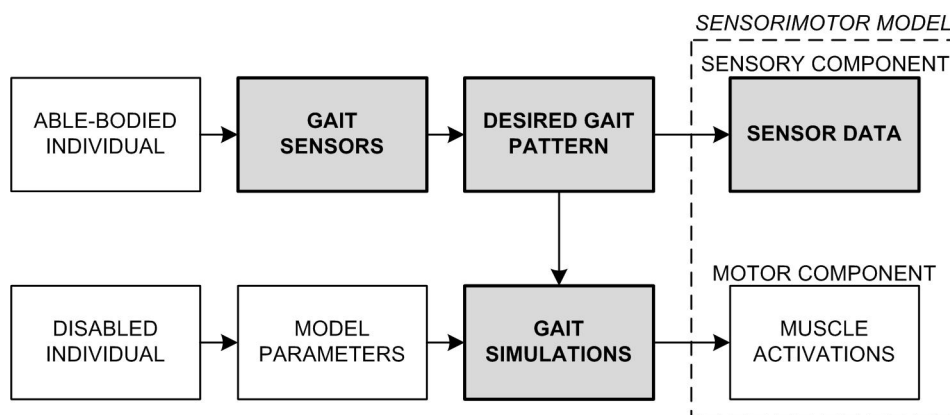

Fig. 4.1. Customized modeling and simulation (CMS) approach. Desired gait pattern is recorded from an able-bodied individual. Model parameters are experimentally identified from a disabled subject. Using a model customized to the subject, biomechanical gait simulations determine muscle activations that are adequate to generate the desired gait. The output from the CMS is an SMM. The shaded boxes are the steps of the CMS that were in the focus of this study. The goal of the study was to generate the sensory component of the SMM in the form that will lead to a practical system for rule-based control of gait.

angle domain, meaning that the simulation was not convergent (see Fig. 4.2). This divergence was likely due to instability of numerical integration [7], [8].

Since the optimization in the angular acceleration phase space showed to be infeasible, and the data from the practical sensory system was confirmed to be reproducible, we decided to develop a method for transforming data from accelerometers and FSRs into a format that leads to the optimal control which converges. Several promising methods were described for calculating joint and/or segment angles from the signals recorded by MEMS sensors. These methods, however, typically used more sensors (e.g., several accelerometers per leg segment [9], accelerometers and gyroscopes [10], magnetic sensors [11]) and/or fairly complex processing [12]. Schepers *et al.* [13] developed a system for ambulatory assessment of ankle and foot dynamics, which integrates the measurement of the GRF with that of foot movement. The system showed to be accurate and reliable but it used three inertial sensors and two six-degrees-of-freedom force sensors to obtain the data for just one leg segment. Moreover, the simulation that we developed requires hip acceleration, and the problem of its measurement was not addressed adequately in literature.

Machine learning was used for estimation of gait kinematics and dynamics. Sepulveda *et al.* [14] used two artificial neural networks (ANN) to map electromyography to joint angles and torques. Goulermas *et al.* [15] evaluated eight different regression techniques for the prediction of segmental angles of the thigh, shank and foot from sagittal plane angular velocities and linear accelerations of the footwear. Savelberg *et al.* [16] applied a feed-forward ANN to map insole pressures and ground reaction forces. They used pressure values from 8 areas under the foot to estimate horizontal component of the GRF.

In this chapter, we present a new procedure for data processing: the estimation of target gait patterns
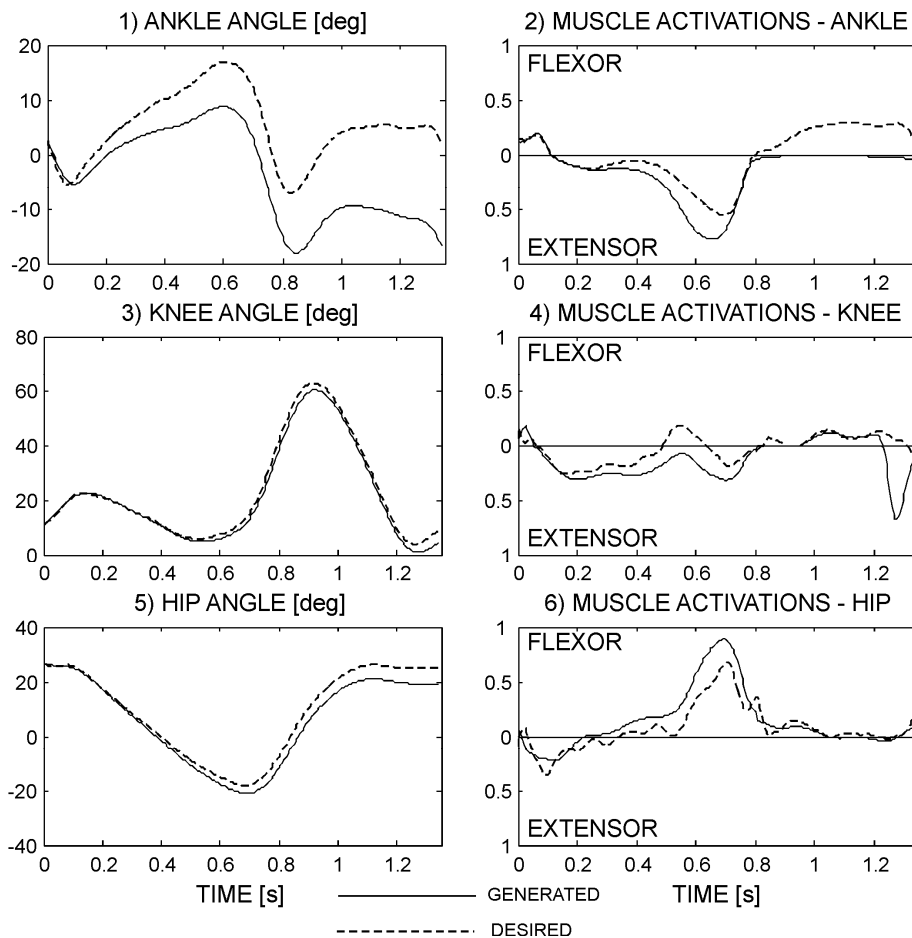

Fig. 4.2. Typical simulation results when the optimization is done in the phase space of angular accelerations. Plots 1, 3, and 5 show the joint angles. The dashed and continuous lines represent desired and generated joint angles, respectively. Drift from the desired trajectories is evident in all of the generated joint angles. Plots 2, 4, and 6 represent normalized muscle activations (0 – relaxed muscle; 1 – maximally contracted muscle). The continuous lines represent activations generated in the simulation while the dashed lines show desired activations that would produce ideal trajectory tracking. Notice that generated muscle activations differ from desired ones.
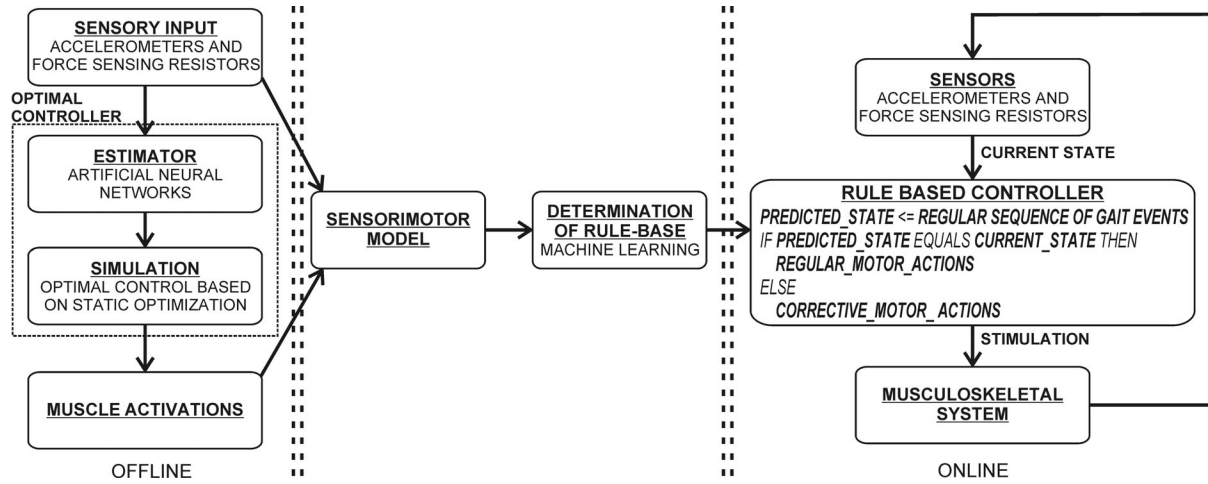
Fig. 4.3. Design and application of a Rule Based Controller (RBC) for FES. Sensorimotor model (SMM) for training of the RBC is created offline by using an optimal controller which receives the input data from the sensors convenient for daily use. Once the SMM is created, the RBC is designed through implementation of machine learning by using the SMM as a knowledge base. Finally, in the online application of RBC, the inputs are supplied by the same sensors used for SMM generation, while the outputs are stimulation patterns customized to the user of the FES system. The controller implements Artificial Reflex Control which is described as a pseudo code within the block "Rule Based Controller". The concept of artificial reflex control is described in detail in Chapter 1 (see Fig. 1.5). Here we present the methods for implementing the steps shown in the left part of the figure.

TABLE I
SUBJECTS PARTICIPATED IN THE STUDY

Subject	Sex	Age	Height [m]	Mass [kg]
1	female	28	1.65	50
2	female	23	1.70	55
3	male	25	1.71	71
4	male	31	1.76	75
5	male	30	1.73	78
6	male	27	1.83	95

from the outputs of accelerometers and FSRs based on machine learning. Then, we show how this transformed data is integrated into the optimal control for generating muscle activation profiles by minimizing tracking errors from the estimated target trajectory and total muscle efforts. The result is an optimal controller that uses data from a practical set of sensors as inputs and generates patterns of activations for the muscles controlling the leg. The controller uses the parameters which characterize the potential user of an FES system. As a result, by using the optimal controller simulations, it is possible to test the feasibility of tracking the target, healthy-like gait pattern; but, by the muscular system of an individual with a physical impairment (decreased muscle output). In this way, an SMM is created comprising sensors data from a practical system and muscle activation profiles that are user customized. The SMM can be used for the design of a real-time rule-based control of walking in individuals with hemiplegia. The flowchart depicting the design of such a controller is given in Fig. 4.3. Both, the estimator and the optimization were implemented using MATLAB 7.0 on a standard PC platform.

2. METHODS

2.1. Subjects

Six able-bodied volunteers participated in the study. All subjects signed a consent form approved by the local ethical committee. The subject data are summarized in Table I. In order to test the performance of the optimal controller under different conditions, we have chosen subjects from both genders with varying biomechanical characteristics.

2.2. Data collection

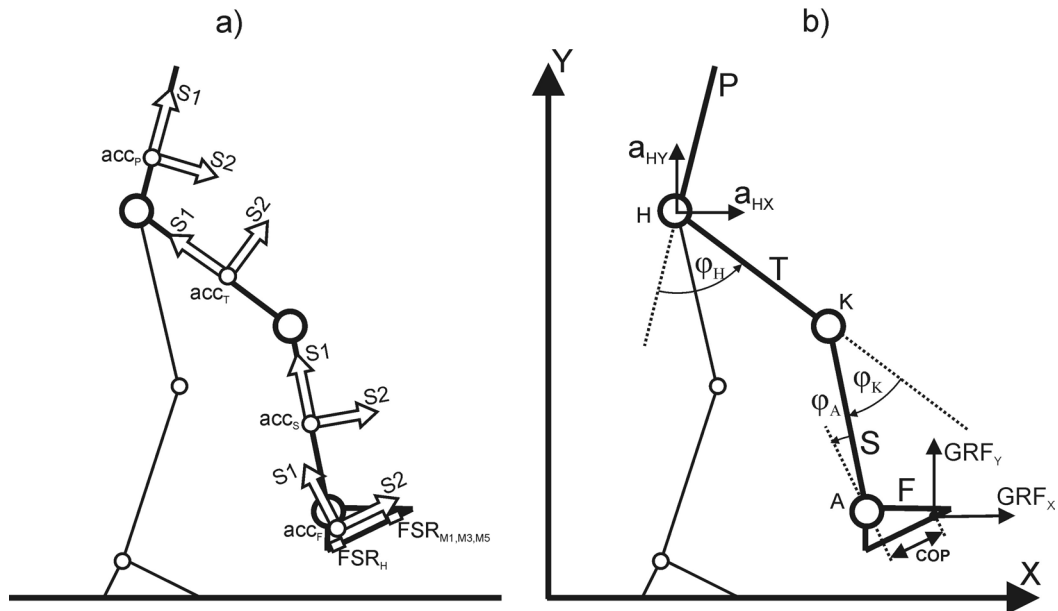We used two measurement systems in parallel: 1) a laboratory-fixed camera based motion capture

Fig. 4.4. (a) Placement of the sensors providing the input data for the estimator. Legend: acc_P, acc_T, acc_S, acc_F – accelerometers positioned on the pelvis (P), thigh (T), shank (S) and foot (F); S1, S2 – lengthwise and perpendicularly oriented sensitive axes of the accelerometers; FSR_H, $FSR_{M1,M3,M5}$ – force sensing resistors placed underneath the heel and the first (M1), third (M3) and fifth (M5) metatarsal bones. (b) Definition of signals representing the target outputs of the estimator (i.e. target gait pattern signals). Legend: φ_H, φ_K, φ_A – hip (H), knee (K) and ankle (A) joint angles; a_{HX}, a_{HY} – horizontal and vertical acceleration of the hip; GRF_X, GRF_Y – horizontal and vertical ground reaction force; COP – position of the center of pressure on the sole of the foot.

system (8 ProReflex MCU240 cameras, Qualisys, SE) with an AMTI force plate (OR6-5, Advanced Mechanical Technology, US), and 2) a mobile system based on accelerometers and FSRs developed at the Center for Sensory-Motor Interaction, Aalborg University.

The subject's pelvis and right leg were instrumented with four FSRs (Interlink Electronics, USA) and four dual-axis accelerometers ADXL203 (Analog Devices, USA). The FSRs, which had 2.5 cm in diameter and 0.3 mm in thickness, were placed under the first, third and fifth metatarsal bones as well as under the heel. They measured the pressure applied to the surface of the sensors. The accelerometers, one per leg segment, were secured on the pelvis, thigh, shank and the foot. They were placed laterally and along the midline of the segments, halfway between the joints. The sensors were oriented so that their sensitive axes were in the sagittal plane. The axes S1 and S2 pointed lengthwise and perpendicular to the leg segments, respectively [see Fig. 4.4(a)]. The accelerometers measured net acceleration due to movement and gravity in the directions of the sensitive axes. The signals from the sensors were acquired by using a DAQ-6024E acquisition card (National Instruments, USA) and a standard PC compatible laptop computer.

The data from the cameras and the force plate were acquired by using a PC compatible desktop computer equipped with Qualisys Track Manager data acquisition software (Qualisys, SE) and PCI-DAS1602/12 DAQ board (Measurement Computing Corporation, USA) ensuring synchronized acquisition from the cameras and the force plate. Reflective markers were placed on the anatomical landmarks of the subject's right leg and pelvis according to the manufacturer's guidelines. Raw motion data (i.e., marker trajectories and signals from the force plate) were processed using Visual3D software for the analysis of human movement (C-Motion, USA). The gait pattern signals (hip accelerations, joint angles, GRF and position of the center of pressure (COP) on the sole of the foot) defined in Fig. 4.4(b) were calculated from the motion capture data.

In order to synchronize two acquisition systems (i.e., the laptop and desktop computers), a digital output from the DAQ card in the laptop computer was used for triggering the camera system. All the data were acquired at 200 samples per second. Joint angles obtained by the camera system and signals from accelerometers were low-pass filtered by a second order dual-pass Butterworth filter at a cutoff frequency of 6 Hz [17]. Ground reaction force data and signals from FSRs were low-pass filtered by a second order dual-pass Butterworth filter at a cutoff frequency of 30 Hz [18].

The subjects were instructed to walk in a gait laboratory along a marked pathway in synchrony with a metronome at five different speeds (0.6, 0.8, 1, 1.2 and 1.4 m/s). Before we started recording at the particular gait speed subject walked five times for practice. Then, subject walked ten times at the given gait speed and ten strides in each trial were recorded by the accelerometers and FSRs. However, only two of the ten strides were simultaneously captured by the cameras due to the limited volume available for camera precision. Ground reaction force data were recorded in one step due to the single force plate available.

2.3. Estimation

The estimator, used as the first stage of the optimal controller, included 8 ANNs. A separate estimator was trained for every subject by using their collected data. The inputs into the estimator were the data from the accelerometers and FSRs while the target outputs were the gait pattern signals recorded by the camera system and the force plate. A separate feed-forward backpropagation ANN was trained for estimating each of the target signals [see Fig. 4.4(b)]. We chose networks with uniform and relatively simple structure; all of the networks had one output neuron and one hidden layer with 10 neurons. A hyperbolic tangent sigmoid function was selected as the transfer function for the neurons.

We prepared training and testing data sets for each of the subjects. Only the data from the strides which were recorded simultaneously by both measurement systems (i.e., mobile system and cameras/force plate) could be used for training and testing the estimator. The data from five randomly chosen gait trials at the gait speeds of 0.8 and 1.2 m/s formed the training data sets. In total, 20 strides (i.e., 2 gait speeds x 5 trials per speed x 2 strides per trial) were used for training the ANNs estimating joint angles and hip accelerations, while 10 steps (i.e., 2 gait speeds x 5 trials per speed x 1 step per trial) were used for training the ANNs for estimation of GRF data. The data from all of the gait speeds not used in the training formed the testing data sets. In total, the sets included 80 strides for testing the ANNs estimating kinematics and 40 steps for testing the ANNs estimating GRF data.

Signals from both outputs [i.e., S1 and S2 in Fig. 4.4(a)] of two accelerometers, placed on the neighboring segments, were used as inputs into the network estimating the joint angle between the segments. The objective was that the ANN would learn how to extract the orientation information from the gravity related component in the accelerometers' outputs. When used for estimating joint angles, signals from the accelerometers were low-pass filtered by a dual-pass Butterworth filter at a cutoff frequency of 3 Hz. This was done in order to filter out higher frequency movement-related components. Data from the accelerometers placed on the pelvis and thigh were used as inputs for estimating the horizontal and vertical hip accelerations.

Signals from FSRs were inputs for the ANNs estimating GRF data. We noticed significant inter and intra-trial variability of the signals coming from the FSRs placed under the metatarsal bones. Instead of using them individually, we made an average and used this aggregated signal, as well as the signal coming from the heel FSR, as inputs for the ANN (i.e., two input signals in total).

It was demonstrated in [19] that the estimation precision of machine learning can be increased if preceding signal values are applied as inputs into the network in addition to the momentary values; that is, if the input signals are considered as time series. In this study, we used momentary values and preceding values at 100 ms and 200 ms for estimating the joint angles and hip accelerations. Momentary values and preceding values at 25 ms and 50 ms were used for estimation of GRF data.

We trained the networks with the Levenberg-Marquardt backpropagation algorithm [20]. All the input and target signals were scaled to the interval [-1, 1] prior to the training. Training was done over 100 epochs and lasted less then 40 seconds for each of the target signals. The list of networks needed for the complete estimation of a gait pattern is given in Table II.

The output signals calculated by the networks were low-pass filtered using a dual-pass Butterworth filter at a cut off frequency of 4 Hz for the angles, and 6 Hz for the other signals. The values of 4 Hz and 6 Hz were selected through trial and error procedure as the values which gave the lowest estimation errors.

We assessed the quality of estimation by several measures. The cross correlation coefficient (CCC) was calculated as a standard measure of overall similarity between the estimated and target signals. A CCC of 0.9 was selected as the minimum threshold for "good" estimation. The root mean square error (RMSE)

TABLE II
THE SET OF ARTIFICIAL NEURAL NETWORKS FOR ESTIMATING THE GAIT PATTERN

Target signal	Number of inputs	Input signals
φ_H	12	acc_{PS1} (0, 100, 200), acc_{PS2} (0, 100, 200) acc_{TS1} (0, 100, 200), acc_{TS2} (0, 100, 200)
φ_K	12	acc_{TS1} (0, 100, 200), acc_{TS2} (0, 100, 200) acc_{SS1} (0, 100, 200), acc_{SS2} (0, 100, 200)
φ_A	12	acc_{SS1} (0, 100, 200), acc_{SS2} (0, 100, 200) acc_{FS1} (0, 100, 200), acc_{FS2} (0, 100, 200)
a_{HY}	12	acc_{PS1} (0, 100, 200), acc_{PS2} (0, 100, 200) acc_{TS1} (0, 100, 200), acc_{TS2} (0, 100, 200)
a_{HX}	12	acc_{PS1} (0, 100, 200), acc_{PS2} (0, 100, 200) acc_{TS1} (0, 100, 200), acc_{TS2} (0, 100, 200)
GRF_Y	6	FSRh (0, 25, 50), FSRm (0, 25, 50)
GRF_X	6	FSRh (0, 25, 50), FSRm (0, 25, 50)
COP	6	FSRh (0, 25, 50), FSRm (0, 25, 50)

Legend: acc_{PS1}, acc_{PS2}, acc_{TS1}, acc_{TS2}, acc_{SS1}, acc_{SS2}, acc_{FS1}, acc_{FS2} – outputs of the perpendicular (S2) and lengthwise (S1) oriented sensitive axes of accelerometers placed on the pelvis (P), thigh (T), shank (S) and the foot (F); (0, 100, 200) – momentary and preceding values at 100 and 200 ms; (0, 25, 50) – momentary and preceding values at 25 and 50 ms; FSRh – signal from the FSR positioned underneath the heel; FSRm – average of the signals from the FSRs positioned underneath the metatarsal bones.

was used to analyze the average difference in the values of the two signals. In order to compare results between trials and across different gait speeds, we calculated normalized RMSE (NRMSE) as the ratio between RMSE and peak-to-peak value of the target signal. The quality was assessed for both training and testing data sets.

2.4. Simulation

The simulation, used as the second stage of the optimal controller, was based on a reduced model of gait described in detail in Chapter 2. The model can be customized for the hemiplegic individual who uses an FES system. The leg was modeled as a planar three segment linkage of rigid bodies connected by pin joints that allow rotation in the sagittal plane. Each of the joints was driven by a pair of equivalent muscles representing all the muscles that contribute to joint flexion or extension. A three compartment multiplicative Hill based model was used for the muscles. The influence of passive tissues crossing the joints was modeled by nonlinear resistive torques.

The input into the simulation was the estimated desired gait pattern (output of the estimator) and a set of user specific model parameters. The outputs of the simulation were: 1) activations of the equivalent muscles around the hip, knee and ankle joints, and 2) hip, knee and ankle joint angles generated when the muscle activations were applied to the system. The cost function for optimal control was the sum of squares of the normalized tracking errors (from the joint angles of the estimated target gait pattern) and a term penalizing the total muscle effort. Detailed descriptions of the model and the optimization algorithm were given in Chapter 2 (see equations 2.1–2.11) and published in [4] and [6]. The model was validated in the studies by Popović *et al.* [5], [6].

The overall performance of the controller (i.e., estimation + simulation) was assessed by analyzing the convergence of the simulation, smoothness and reproducibility of calculated muscle activation profiles, and the size of the tracking errors. There were three gait patterns of interest for the assessment of the quality of tracking: joint angles recorded by the cameras (i.e., target angles), the angles predicted by the estimator (i.e., estimated target angles) and actually used (instead of the target angles) as desired trajectories for the tracking, and joint angles generated by the simulation (i.e., generated angles). Deviations of generated gait pattern from the estimated and target patterns were assessed by calculating normalized root mean square tracking error (NRMSTE) from estimated ($NRMSTE_E$) and target joint angles ($NRMSTE_T$), respectively. $NRMSTE_E$ was defined as RMSE between generated and estimated angles, normalized by the peak-to-peak value of the estimated angles. Hence, $NRMSTE_E$ is the average tracking error made by the simulation. $NRMSTE_T$ was defined as RMSE between generated and target

TABLE III
PARAMETERS FOR THE BIOMECHANICAL MODEL (SUBJECT 4, TABLE I)

T	$J_{CT} = 0.16$ kg·m^2; $m_T = 7.1$ kg; $d_T = 0.163$ m; $L_T = 0.391$ m		
S	$J_{CS} = 0.056$ kg·m^2; $m_S = 4$ kg; $d_S = 0.181$ m; $L_S = 0.423$ m		
F	$J_{CF} = 0.008$ kg·m^2; $m_F = 0.7$ kg; $d_F = 0.031$ m; $L_F = 0.061$ m		
AF	$c_{10} = 65$	$c_{11} = -25$	$c_{12} = -150$
	$c_{13} = 0.05$	$c_{14} = 1.2$	
AE	$c_{20} = 140.4$	$c_{21} = 140.84$	$c_{22} = -310.8$
	$c_{23} = 0.04$	$c_{24} = 1.5$	
AR	$d_{10} = 10$	$d_{11} = 0.6$	$d_{12} = 1.7$
	$d_{13} = 7.3$	$d_{14} = 1.05$	$d_{15} = -4.99$
KF	$c_{30} = 85.6$	$c_{31} = 1.54$	$c_{32} = -9.24$
	$c_{33} = 0.06$	$c_{34} = 1.2$	
KE	$c_{40} = 35.45$	$c_{41} = 220.67$	$c_{42} = -115.77$
	$c_{43} = 0.05$	$c_{44} = 1.4$	
KR	$d_{20} = 9$	$d_{21} = 0.5$	$d_{22} = 0.002$
	$d_{23} = 5.02$	$d_{24} = 50.61$	$d_{25} = -29.32$
HF	$c_{50} = 110$	$c_{51} = -30$	$c_{52} = -60$
	$c_{53} = 0.06$	$c_{54} = 1.2$	
HE	$c_{60} = 150.4$	$c_{61} = 71.84$	$c_{62} = -23.8$
	$c_{63} = 0.04$	$c_{64} = 1.4$	
HR	$d_{30} = 10$	$d_{31} = 0.6$	$d_{32} = 0.04$
	$d_{33} = 5.9$	$d_{34} = 3.05$	$d_{35} = -4.99$

Legend: T, S, F – thigh, shank and foot; H, K, A – hip, knee and ankle joints; F, E – equivalent flexor and extensor; R – resistive joint torque. Parameters are defined in Chapter 2.

angles, normalized by the peak-to-peak value of the target angles. Therefore, NRMSTE$_T$ includes both the error made by the estimator and the tracking error generated in the simulation. This is the overall average tracking error made by the optimal controller.

The minimum threshold for "good" tracking of the target gait patterns was defined by using the reference data for the inter-subject standard deviations in the joint angles (ISSD) for normal gait at slow and normal gait speeds (i.e., a measure of normal gait variability). The maximum values of ISSD normalized by the peak to peak value of the respective angles are 17, 14 and 19% for the ankle, knee and hip joint angles, respectively [1]. Therefore, a generated gait pattern was classified as being "close" to the target pattern if the maximum tracking errors from the target angles, normalized by the peak to peak value of the target angles (NMAXTE$_T$), were below these reference upper limits; gait patterns not classified as "close" were omitted from the resulting sensorimotor model.

3. RESULTS

Here, we demonstrate a characteristic example (Subject 4, Table I) and a summary for the group of subjects considered in the study. The muscle and inertial parameters for the model were identified experimentally (Table III) by using the methods described in [21], and a KinCom machine (KC2, Isokinetic International, US) in our Laboratory at Aalborg University. The estimator for the subject was created by the above-mentioned methods.

Fig. 4.5 shows the input sensory data [see Fig. 4.5(a)] and muscle activations [see Fig. 4.5(b)] calculated by the optimal controller. The sensory signals were recorded in one of the gait trials made at the gait speed of 1 m/s. Notice that the muscle activation profiles are consistent throughout the trial for all of the muscles; the characteristic shapes repeat from stride to stride with similar amplitude and timing (relative to the stride duration). The levels of activation correspond to the muscle strength that is characteristic for the potential user; hence, the actual muscle strength is taken into account. In addition, the profiles demonstrate stride to stride variability which is present in the input sensory data as well.

While Fig. 4.5 demonstrates inputs and final outputs of the optimal controller, the intermediate processing step of estimating the target gait pattern is illustrated in Fig. 4.6. Estimated signals were obtained by applying the data from Fig. 4.5(a) to the inputs of the ANNs (listed in Table II). Target values in Fig. 4.6 are shown for only that section of the trial which was recorded by the cameras and the
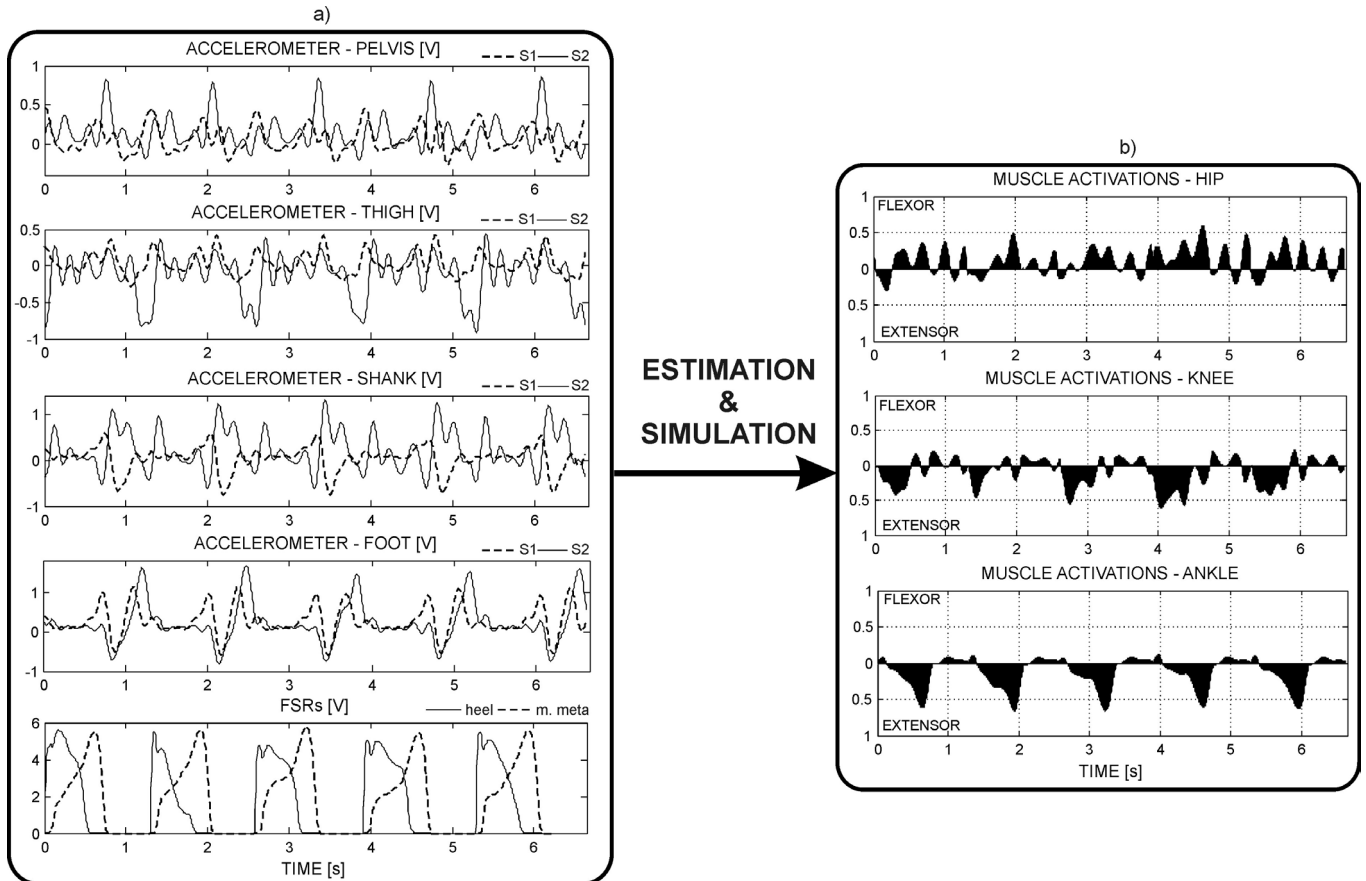
Fig. 4.5. (a) Inputs and (b) outputs of the optimal controller. (a) Data recorded by the sensory system from subject 4 (Table I) at the gait speed of 1 m/s. Labels S1 and S2 denote the outputs from the two sensitive axes of the accelerometers. *Heel* represents the signal from the FSR positioned under the heel and *m. meta* is the average of the signals from the FSRs under the metatarsal bones. Five strides are shown starting with the right heel contact. The offsets were subtracted from each of the accelerometer signals prior to plotting. (b) Normalized muscle activations (0–muscle relaxed, 1–muscle maximally contracted) calculated by the optimal controller from the sensory data given in (a). Notice that the activation profiles have characteristic shape that varies from stride to stride.

force plate.

Summary statistics (Table IV) show the quality of estimation over the testing data recorded from the subject. Table IV gives the average values of RMSE, NRMSE and CCC over each of the gait speeds for all of the estimated signals. Notice that the data from the gait speeds of 0.6, 1 and 1.4 m/s were not used for the training.

Fig. 4.7 demonstrates reproducibility of the simulation. Three consecutive strides from three different trials (i.e., 9 strides in total) at the gait speed of 1 m/s were used as inputs for the optimal controller. The resulting muscle activation profiles are plotted. The gait strides are normalized (0-100%) in order to show them on the same graph. Fig. 4.7 shows that the controller generated similar muscle activation profiles for different gait trials made by the same subject at the same gait speed. In addition to being similar and reproducible, muscle activations are in accordance with the expected activity of different muscles in different phases of the gait cycle (e.g., the ankle flexor is active at the beginning of stance to slow down foot drop, the knee extensor is active throughout the stance phase, the ankle extensor activity peaks at push off, etc.)

The overall statistics (i.e., average CCC, RMSE and NRMSE over all of the gait speeds) for all of the estimators made in the study are in Table V.

By applying the optimal controller using the same model parameters (Table III) and estimators for different subjects, we simulated all of the trials recorded in the study (i.e., 6 subjects x 50 gait trials = 300 gait trials); the simulation converged in 96% of the cases. Using the NMAXTE_T criterion, we could classify 94% of the converged cases as "good" tracking. Therefore, we could suggest that the optimal controller generated the target healthy-like gait in 90% of all the tested gait trials. The NRMSTE_E and

HIP ANGLE [deg]
CCC = 0.993 RMSE = 2.04°

NORMALIZED VERTICAL GRF
CCC = 0.992 RMSE = 0.05

HORIZONTAL HIP ACCELERATION [m/s^2]
CCC = 0.984 RMSE = 0.29 m/s^2

KNEE ANGLE [deg]
CCC = 0.998 RMSE = 1.04°

NORMALIZED HORIZONTAL GRF
CCC = 0.99 RMSE = 0.02

VERTICAL HIP ACCELERATION [m/s^2]
CCC = 0.983 RMSE = 0.27 m/s^2

ANKLE ANGLE [deg]
CCC = 0.981 RMSE = 1.33°

COP [m]
CCC = 0.996 RMSE = 0.0066 m

TIME [s]
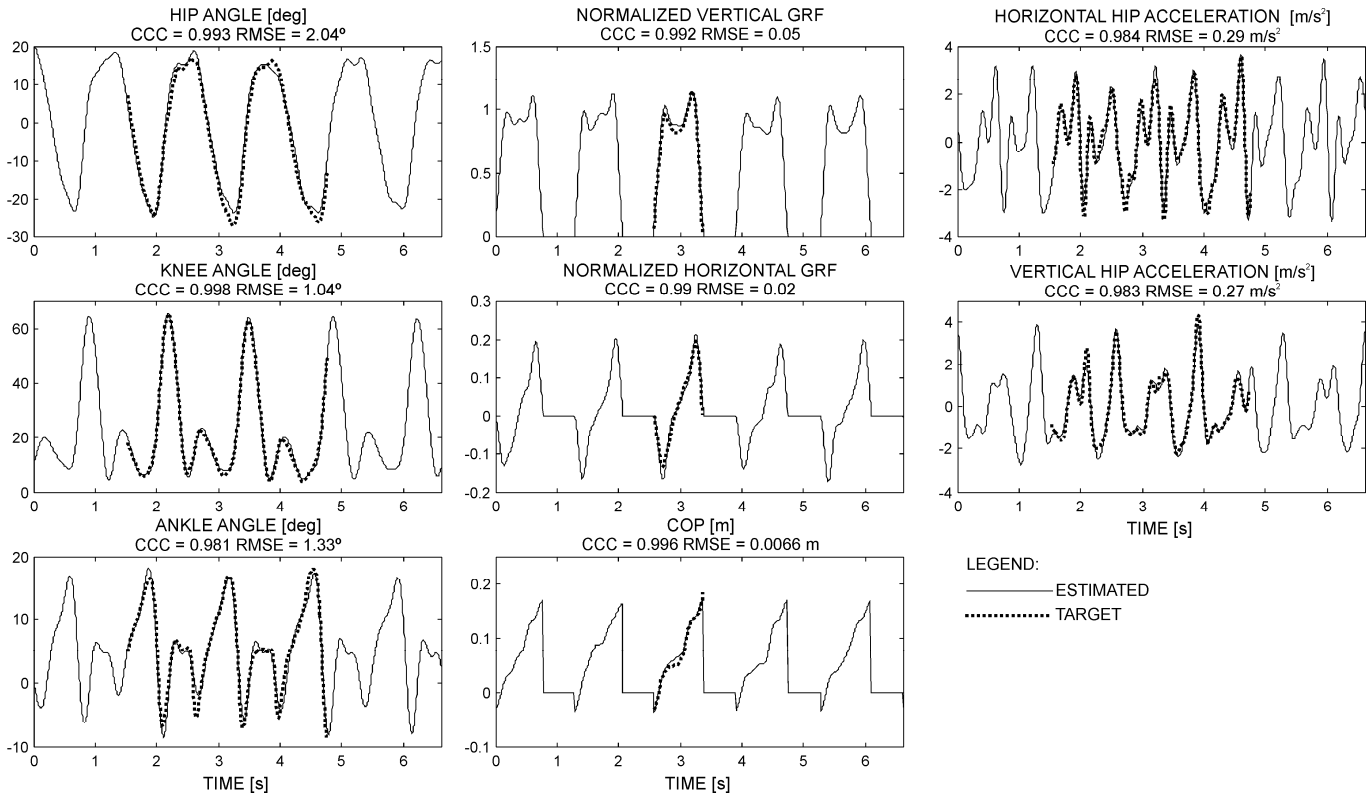
LEGEND:
———— ESTIMATED
············· TARGET

Fig. 4.6 Gait pattern obtained by applying the sensory data given in Fig. 4.5(a) to the inputs of the estimator for the subject 4 (Table I). The continuous lines are estimated while the dotted lines are target signals. The target signals are only available for the section of the trial which was recorded by the cameras/force plate. GRF is normalized by the body weight. The figure demonstrates that it is possible to estimate all of the signals that make up the gait pattern with sufficient precision. Notice that the data from the trials made at this gait speed were not used for training the estimator.

$NRMSTE_T$ for the generated patterns were below 2% and 9% respectively.

As a peripheral study, we tested the ability of the estimators to generalize between the subjects. An estimator trained for one subject was tested by using the testing data set of other subjects. We found that the estimator was applicable as long as the subjects were anthropometrically similar and of the same sex (e.g., subjects 1 and 2, subjects 4 and 5). When the subjects were of different sex or of significantly different height and/or weight (e.g., subjects 3 and 6), the results were poor (CCC < 0.7). For example, between similar subjects 3 and 4 and subjects 4 and 5, horizontal and vertical components of the GRF and movement of the COP could be estimated with an average CCC of about 0.94. The best result in the estimation of joint angles is obtained for the knee angle (CCC ~ 0.95) while the hip and ankle angle could be estimated with the lower CCC of about 0.92. CCC values for estimating the hip accelerations were around 0.91.

4. DISCUSSION

The results presented in the paper demonstrate that the optimal controller generated target healthy like gait patterns in the most of the tested cases. The error made by the estimator was the main cause of divergent simulations and simulations that converged but resulted in the abnormal gait patterns. The divergence and abnormal gait patterns followed the incorrect estimates of the kinematics and dynamics. These estimates affected the torque profiles, ultimately leading to instability in the simulation. The controller, however, is more sensitive to the estimation errors in the stance phase than in the swing phase.

It is important to state again the goals of this simulation: to build a knowledge base (sensorimotor model) that will be used for the design of a rule-based real-time control of the walking. In that sense, perfectly tracking the target gait pattern was not a requirement. The average inter-subject standard deviations in the joint angles for normal gait at slow and normal gait speeds, normalized by the peak to peak value of the respective angles, are 12%, 9% and 15% for the ankle, knee and hip joint angles, respectively [1]. Taking this into account, the maximum value of 9% for $NRMSTE_T$, being an estimate of

TABLE IV
SUMMARY STATISTICS FOR THE PRECISION OF
ESTIMATION OF THE GAIT PATTERNS FOR THE SUBJECT 4 (TABLE I)

Targets	Walking Speeds				
	0.6 m/s	0.8 m/s	1 m/s	1.2 m/s	1.4 m/s
	RMSE (std)	RMSE (std)	RMSE (std)	RMSE (std)	RMSE (std)
φ_A [deg]	1.59 (0.39)	1.62 (0.11)	1.56 (0.15)	1.48 (0.12)	1.64 (0.16)
φ_K [deg]	1.28 (0.15)	1.25 (0.12)	1.18 (0.18)	1.19 (0.18)	1.21 (0.23)
φ_H [deg]	2.23 (0.94)	3.60 (0.57)	2.62 (1.07)	1.31 (0.15)	1.46 (0.37)
a_{HX} [m/s^2]	0.46 (0.08)	0.38 (0.02)	0.39 (0.08)	0.39 (0.06)	0.36 (0.05)
a_{HY} [m/s^2]	0.31 (0.05)	0.26 (0.03)	0.29 (0.04)	0.29 (0.04)	0.39 (0.06)
COP [mm]	6.9 (2.8)	5.94 (2.4)	6.1 (2.3)	4.0 (1.2)	3.8 (0.5)
GRF$_Y$ [N]	38.3 (8.1)	29.7 (8.7)	34.4 (8.6)	42.9 (9.6)	61.9 (14.3)
GRF$_X$ [N]	11.6 (3.7)	14.3 (2.8)	16.8 (6.3)	16.4 (3.2)	11.7 (1.3)
	NRMSE (std) [%]	NRMSE (std) [%]	NRMSE (std) [%]	NRMSE (std) [%]	NRMSE (std) [%]
φ_A	5.6 (1.4)	5.5 (0.4)	5.2 (0.5)	4.7 (0.4)	5.0 (0.5)
φ_K	2.3 (0.3)	2.2 (0.2)	1.9 (0.3)	1.8 (0.3)	1.9 (0.3)
φ_H	5.4 (2.3)	8.1 (1.3)	5.8 (2.4)	2.6 (0.3)	2.8 (0.7)
a_{HX}	8.4 (1.4)	6.0 (0.3)	4.7 (0.9)	4.6 (0.7)	4.0 (0.6)
a_{HY}	6.8 (1.1)	5.3 (0.5)	4.5 (0.6)	3.7 (0.5)	3.8 (0.5)
COP	3.1 (1.3)	2.7 (1.1)	2.8 (1.0)	1.9 (0.6)	1.8 (0.2)
GRF$_Y$	5.4 (1.1)	4.1 (1.2)	4.4 (1.1)	5.2 (1.2)	7.2 (1.7)
GRF$_X$	7.0 (2.2)	6.5 (1.3)	6.5 (2.5)	5.0 (1.0)	3.3 (0.4)
	CCC (std)	CCC (std)	CCC (std)	CCC (std)	CCC (std)
φ_A	0.973 (0.012)	0.974 (0.008)	0.977 (0.005)	0.981 (0.002)	0.980 (0.004)
φ_K	0.997 (0.001)	0.997 (0.000)	0.998 (0.000)	0.998 (0.001)	0.998 (0.001)
φ_H	0.992 (0.002)	0.991 (0.001)	0.994 (0.003)	0.998 (0.001)	0.997 (0.001)
a_{HX}	0.913 (0.023)	0.965 (0.001)	0.978 (0.008)	0.985 (0.005)	0.987 (0.003)
a_{HY}	0.917 (0.042)	0.961 (0.009)	0.978 (0.008)	0.990 (0.002)	0.991 (0.003)
COP	0.993 (0.007)	0.995 (0.005)	0.997 (0.002)	0.998 (0.001)	0.998 (0.000)
GRF$_Y$	0.985 (0.008)	0.988 (0.008)	0.988 (0.005)	0.977 (0.008)	0.969 (0.021)
GRF$_X$	0.982 (0.008)	0.985 (0.006)	0.985 (0.013)	0.988 (0.006)	0.994 (0.002)

Legend: CCC, RMSE, NRMSE – average cross correlation coefficient, root mean square error, and normalized RMSE; std – standard deviation.

TABLE V
SUMMARY STATISTICS FOR THE PRECISION OF ESTIMATION OF
GAIT PATTERNS FOR ALL THE SUBJECTS AND ACROSS ALL THE SPEEDS

Targets	CCC (std)	RMSE (std)	NRMSE (std) [%]
φ_A	0.973 (0.019)	2.07 (0.79) deg	5.9 (1.9)
φ_K	0.997 (0.003)	1.43 (0.53) deg	2.4 (0.8)
φ_H	0.993 (0.004)	1.91 (0.79) deg	4.5 (1.7)
a_{HX}	0.958 (0.025)	0.47 (0.16) m/s^2	6.1 (1.7)
a_{HY}	0.965 (0.030)	0.36 (0.17) m/s^2	5.1 (1.6)
COP	0.996 (0.005)	5.8 (2.7) mm	2.8 (1.3)
GRF$_Y$	0.968 (0.032)	41.9 (18.2) N	6.0 (2.3)
GRF$_X$	0.977 (0.026)	15.7 (8.1) N	7.5 (3.9)

Legend: CCC, RMSE, NRMSE – average cross correlation coefficient, root mean square error and normalized RMSE; std – standard deviation.
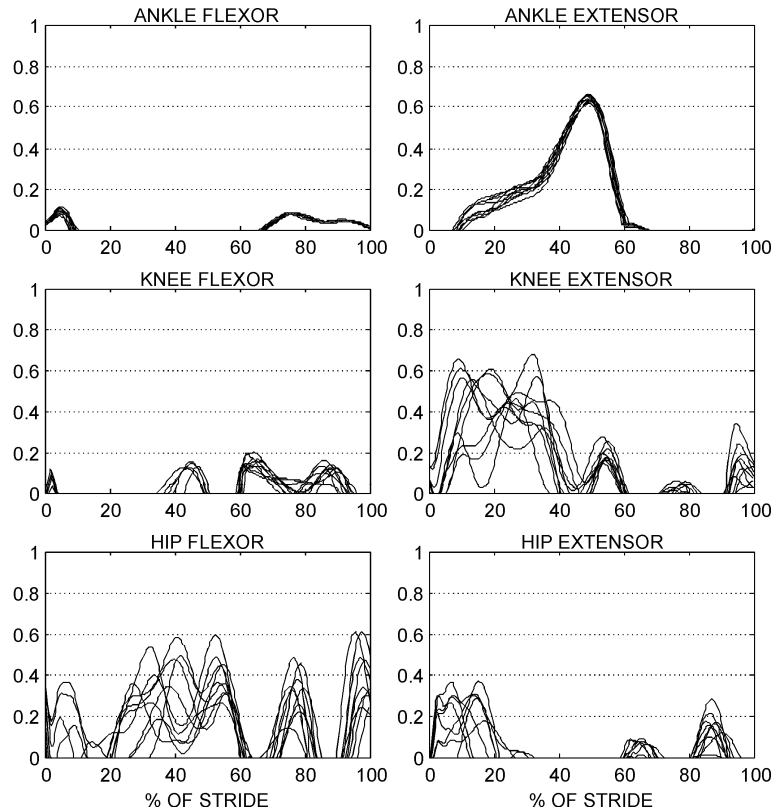
Fig. 4.7. Normalized muscle activations calculated as a result of simulating nine strides. Three consecutive strides were taken from three different trials made by subject 4 (Table I) at the gait speed of 1 m/s. The figure demonstrates intra- and intertrial reproducibility of the results generated by the optimal controller.

the average error made by the optimal controller, fits within the variability that is typical for normal gait. Therefore, on the basis of the values of $NRMSTE_T$ and $NMAXTE_T$, we could say that the generated gait patterns, which were classified as "good" tracking, varied from the target trajectories within the acceptable boundaries.

As demonstrated, the outputs of the optimal controller both intra and inter-trials were smooth and reproducible muscle activation profiles. Since the patterns are reproducible, they carry consistent information about the level and timing of muscle activity throughout the gait cycle. At the same time, the estimated gait patterns and the muscle activations demonstrate stride-to-stride variability. Recall, both of these features are essential for the design of a sensorimotor model that will lead to a robust rule-based controller. The generated joint torques were within the expected range for the model parameters and gait speeds used in the study (i.e., maximum torques normalized by the body weight were around 0.09, 0.11 and 0.19 Nm/N for the hip, knee and ankle joints, respectively [1]). In a hemiplegic individual, not only are the muscles weaker, but the reflexes, inertial parameters, and viscoelastic joint properties are altered as well. However, the optimal controller takes this into account automatically since the model is customized for the specific subject. Likely, the future use of this method for rehabilitation could cause the simulation to be confronted with cases when the muscles are not strong enough (activation level reaches maximum, and the tracking errors start accumulating) [4]. If this happens, the conclusion would be that another less demanding gait pattern has to be selected since the target gait pattern is not achievable [6].

The results for the estimator (Fig. 4.6 and Tables IV and V) show that standard feed-forward backpropagation ANNs can sufficiently estimate - from the outputs of a simple and practical sensory system - a range of signals describing the gait pattern when trained for the specific subjects. This is a general result implying that the estimator could also be used for the assessment of gait, which is of interest for many rehabilitation practitioners.

The ANNs, with relatively simple structure (i.e., one hidden layer, 10 neurons), trained on a few strides (~ 20) and in a short time (< 40 s), showed satisfactory performance over a range of gait speeds. The average NRMSE was below 6% and 7% for the estimation of joint angles and hip accelerations, respectively. The components of the GRF and the movement of the COP could be estimated with the

average NRMSE below 8% and 3%, respectively. By comparing our results to the benchmark data given in [1], we could conclude that the average estimation errors for joint angles and ground reaction forces were inside the range of normal variability of human gait. The estimator demonstrated interpolation capabilities, when tested at the gait speed that was not used for the training but was inside the range of speeds used in the training (i.e., 1 m/s), and extrapolation capabilities, when tested at the gait speeds that were outside the range of speeds used for the training (i.e., 0.6 m/s and 1.4 m/s). We attained similar average angle estimation errors (RMSE ~ 2°) to what Goulermas *et al.* [15] achieved by applying their best performing method (i.e., general regression networks). Moreover, in our study we designed and tested the estimator over a range of gait speeds and by using the data from real and not virtual sensors. The best angle estimation results (i.e., the lowest overall RMSE and standard deviation) were obtained for the estimation of knee angle. We achieved generally higher CCC values (average CCC ~ 0.977) in estimating the horizontal component of the ground reaction force compared to that of Savelberg *et al.* [16]. They obtained CCC values in the range of 0.85-0.96 for the gait speeds ranging from 1.2 to 2 m/s. Their estimation only included the horizontal component of the GRF while we estimated the complete GRF data. Moreover, they used pressure values from eight areas under the foot measured using Micro-EMED pressure insoles, while our method used only four FSRs (which are standard and non expensive components).

Our results were similar or even better when compared to the average measurement errors reported in the literature for the gait analysis systems based on MEMS sensors. By using accelerometers, Willemsen *et al.* [9] attained RMSE of 5.7° and 4.6° for the measurement of knee and hip angles, respectively. Tong *et al.* [22] reported CCC of 0.93 and RMSE of 6.42° for the knee angle measurement by using gyroscopes. We obtained the overall average CCC of about 0.99 and RMSE around 2° for the knee and hip joint angles. Schepers *et al.* [13] achieved better results (NRMSE ~ 1%) in the measurement of the GRF whereas reported precision of COP estimation was similar to ours (RMSE ~ 5 mm). It is important to say that the goal of this study was not to design a new measurement system that would be a general solution. The comparison was done for the assessment of the precision of our estimation method and in order to demonstrate that the estimated gait patterns are indeed suitable inputs for our gait simulations.

The methods presented in the paper will lead to an on-line sensory-driven rule-based controller for FES-assisted walking of hemiplegics. The end result of the steps depicted in Fig. 4.3 will be the rules in the form of a matrix [23], a decision tree [24], [25] or a set of propositional logic formulas [26]; the form depends on the specific machine learning technique used. Importantly, these representations are suitable for straightforward implementation within an FES stimulator based on a microcontroller. Moreover, as demonstrated in the paper, the controller will use sensors which are convenient for daily use (i.e., accelerometers and FSRs), this being essential for a clinical application. The method that we suggest will lead to a fully automated FES system with the stimulation intensity determined by the optimal control.

The plan is to apply the controller for FES used in walking therapy for hemiplegic individuals [27], [28]. The expectations are that due to changes in the sensory-motor systems after stroke, it would not be possible to achieve the "normal" gait characteristics of a healthy individual; however, the synthesized gait pattern will be "as-close-as-possible" to normal gait [4]–[6]. The expectations are founded on the facts that the sensorimotor model, which we create by simulation, uses subject-specific model parameters and target trajectories which are recorded in healthy individuals. In parallel, the sensory-driven control mimics natural control since it applies a central program (i.e., a sequence of events) which is constantly adjusted based on the sensory information.

REFERENCES

[1] D. A. Winter, *Biomechanics and Motor Control of Human Movement: Normal, Elderly and Pathological*, 2nd ed., Waterloo, Ontario, Canada: University of Waterloo Press, 1991.

[2] Anonymous. MEMS and Sensors (2008, June 4), Available: http://www.analog.com/en/ at/0,2878,764,00.html.

[3] M. J. Mathie, A. C. F. Coster, N. H. Lovell, and B. G. Celler, "Accelerometry: Providing an integrated, practical method for long-term, ambulatory monitoring of human movement," *Physiol. Meas.*, vol. 25, no. 2, 2004.

[4] S. Došen, D. B. Popović, and C. Azevedo-Coste, "Optiwalk: Un nouvel outil pour la conception et la simulation de lois de commande pour le controle de la marche de patients atteints de deficits moteurs," *Journal Europeen des Systemes Automatises*, vol. 41, no. 2, pp. 239-259, 2007.

[5] D. Popović, M. Radulović, L. Schwirtlich, and N. Jauković, "Automatic vs. hand-controlled walking of paraplegics," *Med. Eng. Phys.*, vol. 25, no. 1, pp. 63-73, 2003.

[6] D. Popović, R. B. Stein, M. N. Oguztoreli, M. Lebiedowska, and S. Jonić, "Optimal control of walking with functional electrical stimulation: A computer simulation study," *IEEE Trans. Rehabil. Eng.*, vol. 7, no. 1, pp. 69-79, 1999.

[7] Y. K. Thong, M. S. Woolfson, J. A. Crowe, B. R. Hayes-Gill, and D. A. Jones, "Numerical double integration of acceleration measurements in noise," *Measurement*, vol. 36, no. 1, pp. 73-92, 2004.

[8] T. S. Edwards, "Effects of aliasing on numerical integration," *Mech. Syst. Signal Proc.*, vol. 21, no. 1, pp. 165-176, 2007.

[9] A. T. M. Willemsen, C. Frigo, and H. B. K. Boom, "Lower extremity angle measurement with accelerometers-error and sensitivity analysis," *IEEE Trans. Biomed. Eng.*, vol. 38, no. 12, pp. 1186-1193, 1991.

[10] H. Dejnabadi, B. M. Jolles, E. Casanova, P. Fua, and K. Aminian, "Estimation and visualization of sagittal kinematics of lower limbs orientation using body-fixed sensors," *IEEE Trans. Biomed. Eng.*, vol. 53, no. 7, pp. 1385-1393, 2006.

[11] D. Roetenberg, P. J. Slycke, and P. H. Veltink, "Ambulatory position and orientation tracking fusing magnetic and inertial sensing," *IEEE Trans. Biomed. Eng.*, vol. 54, no. 5, pp. 883-890, 2007.

[12] H. J. Luinge and P. H. Veltink, "Measuring orientation of human body segments using miniature gyroscopes and accelerometers," *Med. Biol. Eng. Comput.*, vol. 43, no. 2, pp. 273-282, 2005.

[13] H. M. Schepers, H. F. J. M. Koopman, and P. H. Veltink, "Ambulatory assessment of ankle and foot dynamics," *IEEE Trans. Biomed. Eng.*, vol. 54, no. 5, pp. 895-902, 2007.

[14] F. Sepulveda, D. M. Wells, and C. L. Vaughan, "A neural network representation of electromyography and joint dynamics in human gait," *J. Biomech.*, vol. 26, no. 2, pp. 101-109, 1993.

[15] J. Y. Goulermas, D. Howard, C. J. Nester, R. K. Jones, and L. Ren, "Regression Techniques for the Prediction of Lower Limb Kinematics," *J. Biomech. Eng.*, vol. 127, no. 6, pp. 1020-1024, Nov. 2005.

[16] H. Savelberg and A. de Lange, "Assessment of the horizontal, fore-aft component of the ground reaction force from insole pressure patterns by using artificial neural networks," *Clin. Biomech.*, vol. 14, no. 8, pp. 561, 1999.

[17] C. Angeloni, P. O. Riley, and D. E. Krebs, "Frequency content of whole body gait kinematic data," *IEEE Trans. Rehabil. Eng.*, vol. 2, no. 1, pp. 40-46, 1994.

[18] E. K. Antonsson and R. W. Mann, "The frequency content of gait," *J. Biomech.*, vol. 18, no. 1, pp. 39-47, 1985.

[19] A. Kostov, B. J. Andrews, D. B. Popovic, R. B. Stein, and W. W. Armstrong, "Machine learning in control of functional electrical-stimulation systems for locomotion," *IEEE Trans. Biomed. Eng.*, vol. 42, no. 6, pp. 541-551, 1995.

[20] M. T. Hagan, and M. B. Menhaj, "Training feedforward networks with the Marquardt algorithm," *IEEE Trans. Neural Netw.*, vol. 5, no. 6, pp. 989-993, 1994.

[21] R. B. Stein, E. P. Zehr, M. K. Lebiedowska, D. B. Popović, A. Scheiner, and H. J. Chizeck, "Estimating mechanical parameters of leg segments in individuals with and without physical disabilities," *IEEE Trans. Rehabil. Eng.*, vol. 4, no. 3, pp. 201-211, 1996.

[22] K. Y. Tong and M. H. Granat, "A practical gait analysis system using gyroscopes," *Med. Eng. Phys.*, vol. 21, no. 2, pp. 87-94, 1999.

[23] S. Jonić, T. Janković, V. Gajić, and D. Popović, "Three machine learning techniques for automatic determination of rules to control locomotion," *IEEE Trans. Biomed. Eng.*, vol. 46, no. 3, pp. 300-310, 1999.

[24] B. W. Heller, P. H. Veltink, N. J. M. Rijkhoff, W. L. C. Rutten, and b. J. Andrews, "Reconstructing muscle activation during normal walking - a comparison of symbolic and connectionist machine learning techniques," *Biol. Cybern.*, vol. 69, no. 4, pp. 327-335, 1993.

[25] C. A. Kirkwood and B. J. Andrews, "Finite state control of FES systems: Application of AI inductive learning techniques," in *Proc. 11th Annu. Int. Conf. IEEE Eng. Med. Biol. Society*, Washington, DC, United States, pp. 1020-1021, 1989.

[26] Z. M. Nikolić and D. B. Popović, "Predicting quadriceps muscle activity during gait with an automatic rule determination method," *IEEE Trans. Biomed. Eng.*, vol. 45, no. 8, pp. 1081-1085, 1998.

[27] D. Popović and M. B. Popović, "Functional electrical therapy of walking," in *From Res. Pract. Proc. XVIth Congr. Int. Soc. Electrophysiol. Kinesiol. ISEK 2006*, Torino, Italy, pp. 170, 2006.

[28] D. Popović, "Functional Electrical Therapy of walking for neurorehabilitation in hemiplegic individuals", in *Motor Control (11 suppl.): Proc. Prog. Motor Control*, Santos, Brazil, pp. 1087-1640, 2007.

CHAPTER 5
Comparative Study:
Customized Modeling and Simulations
versus Electromyography[*]

   Summary– A sensorimotor model (SMM) is an essential component for the design of rule-based control of gait by means of functional electrical stimulation (FES). The SMM comprises sensory part (sensor data) and motor part (muscle activation profiles). We advocate the use of customized modeling and simulations (CMS) to generate the motor part of the SMM. This method uses biomechanical gait simulations customized to the subject to calculate muscle activation profiles. Alternative approach for determining the muscle activations for the SMM is to record electromyography (EMG) from muscles of able-bodied individuals. In this chapter, we confront these two methods (CMS-based and EMG-based approach) by generating the control signals for a four-channel surface FES system for restoration of hemiplegic gait. The system assists paretic leg in swing and stance phases by controlling knee and ankle joint torques. The input data for the simulations (gait kinetics and kinematics) and EMG from the muscles that are prime movers of the knee and ankle joints were recorded from an able-bodied individual walking at a self-paced gait speed. We confronted here: 1) recorded EMG patterns and muscle activities determined through simulation, and 2) trajectories achieved when EMG or simulated activities were used as controls driving the joints. The simulation minimized tracking errors from desired trajectories and levels of muscle activations. The optimal control was based on static optimization and moving-window dynamic optimization (MWDO). Additionally, we introduced optimization constraints that allowed imposing minimal level of coactivation of antagonistic muscles acting at the joint (i.e., cocontraction). We found that the simulation-generated profiles follow the same trend as EMG, yet they comprise substantial differences. Cross-correlation coefficient (CCC) used as a numerical measure of similarity was in the range of 0.58–0.94. The profiles were more similar (higher CCC) when the simulation used coactivation of antagonistic muscles. Furthermore, in the case of MWDO, introduction of coactivations actually improved the quality of tracking (i.e., decreased the tracking error). We showed that EMG can not be used as control input since this leads to unacceptable tracking errors; whereas, the simulation output leads to excellent tracking. The conclusion is that synthesis of controls should rely on muscle activation profiles determined through simulation, and that it is important to prescribe minimal level of cocontractions about the joint.

1 INTRODUCTION

A sensorimotor model (SMM) is required for determining the rules for rule-based control of gait by means of functional electrical stimulation (FES). The SMM comprises sensory component (sensor data) and motor component (muscle activation profiles) (see Chapter 1, Fig. 1.6). We advocate the use of customized modeling and simulations (CMS) to generate the motor component of the SMM [see Fig. 5.1(a)]. In the CMS approach, muscle activation profiles are calculated by using biomechanical gait simulations based on a reduced model that is customized for the user of FES. Therefore, the simulation considers inertial and muscle parameters that reflect the impairment caused by the injury of the central nervous system. Chapters 2-4 describe various methods for CMS that we have developed.

Alternatively, electromyography (EMG) recorded in able bodied individuals from the muscles that are prime movers of the joints could be used to determine muscle activations for the SMM [see Fig. 5.1(b)]. In several studies, rectified and smoothed EMG was used for determining the timing and intensity of stimulation for control of paralyzed muscles in an individual with disability. Normal EMG has been used as a template for determining the timing and intensity of stimulation by Kobetič and Marsolais [1]. The stimulation profiles for 48 leg and trunk muscles were estimated by handcrafting based on EMG recordings to assist walking of individuals with paraplegia. Matsushita *et al.* [2] created stimulation patterns for the control of wrist and hand of tetraplegic patients using the EMG recorded from 18 arm muscles in 15 healthy subjects. Mangold *et al.* [3] analyzed and compared averaged EMG signals reported in literature for the seven lower extremity muscles during gait of healthy persons with the aim to retrieve the stimulation profiles that can be used in FES for walking. O'Keeffe *et al.* [4], [5] developed a method for generating a stimulation profile which accurately reproduces normal EMG of *Tibialis Anterior m.* during gait of individuals with hemiplegia. Nikolić *et al.* [6], [7] used inductive learning to generate rules for predicting *Quadriceps m.* and *Gastrocnemius m.* activity determined from EMG recordings. Heller *et al.* [8] compared one symbolic (inductive learning) and one connectionist (multilayer perceptron type artificial neural network) machine learning technique for reconstruction of *Semitendinosus m.* and *Vastus Medialis m.* activity from kinematic data measured during normal human gait at several gait speeds.

However, there are several difficulties in cloning EMG profiles from healthy individuals for external activation of muscles in individuals with disability: 1) external electrical stimulation in paralyzed extremities results with muscle force outputs that are different from the one found in healthy individuals, 2) modified reflexes limit individual control of muscles that is typical for healthy individuals, and 3) sensory information reaching higher levels of central nervous system is greatly modified in individuals with disability compared to healthy individuals [9].
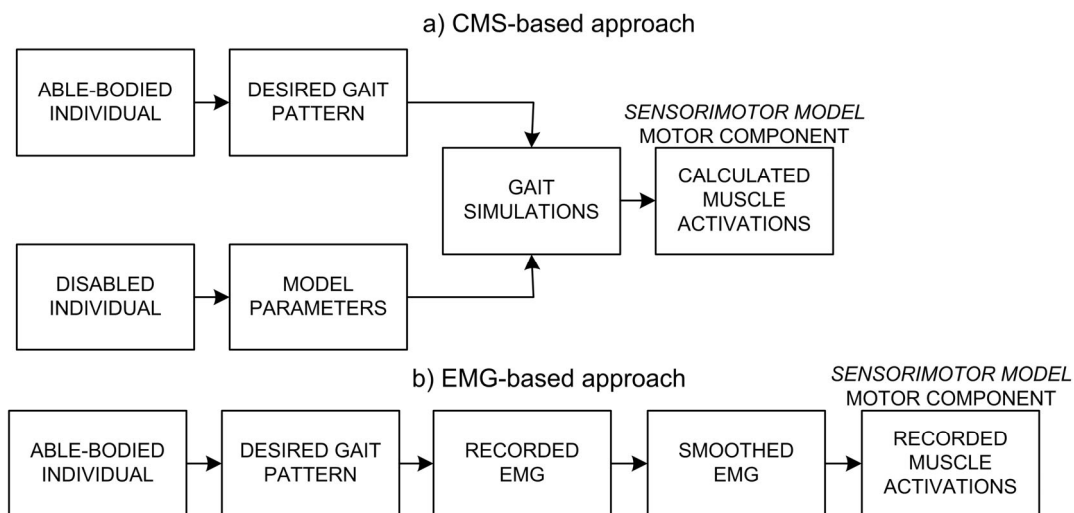

Fig. 5.1. Generation of the motor component of an SMM. Muscle activation profiles for the SMM can be determined by a) using customized modeling and simulations (CMS) or b) by recording and processing electromyography (EMG).

Here, we compare the activation profiles obtained from biomechanical simulations applying 1) Static Optimization (SO) and 2) Moving-Window Dynamic Optimization (MWDO) with the shapes of EMG profiles. Both simulations use the cost function that minimizes tracking errors and levels of muscle activations, and a constraint requiring minimum level of coactivation of agonist and antagonistic muscles. We also compare trajectories achieved if the activation profiles estimated through simulation were used as control signals with trajectories achieved when the EMG profiles were used as controls. The example presented analyzes the comparisons in a four-channel neuroprosthesis that could be used for restoration of walking in individuals with hemiplegia. The neuroprosthesis supports paretic leg in stance phase (knee extension, knee bounce at loading, push off) and swing phase (ankle dorsiflexion, knee flexion, controlled terminal extension) by controlling knee and ankle joint torques.

2 METHODS

2.1 Data collection and processing

Experimental data were collected from a healthy male individual (H=1.75 m; M=73 kg; 26 yr). The individual signed a consent form approved by the local ethical committee. The measurements were done in the Gait laboratory at the Center for Sensory Motor Interaction, Aalborg University, Denmark. The individual walked 20 times at a self-paced gait speed. The average gait speed, stride duration and stride length were 0.95 m/s, 1.51 s and 1.42 m, respectively.

Gait kinematics and kinetics were recorded by a laboratory fixed camera based motion capture system (8 ProReflex MCU240 cameras, Qualisys, SE) and a force plate (OR6-5, Advanced Mechanical Technology, USA) embedded in the floor at the middle of the walkway. Passive retro-reflective markers were placed on the individual's right leg according to recommendations for the human motion analysis software (Visual3D, C-Motion, USA) that was used for processing of the acquired motion capture data [10]. Simultaneously, surface bipolar EMG was recorded from the following muscles acting around the knee and ankle joints: *Hamstrings m.*, *Quadriceps m.*, *Tibialis Anterior m.*, and *Soleus m.* Wireless EMG monitor (TeleMyo 2400R, Noraxon, USA) was used for acquisition. High-pass (1st order, 10 Hz cutoff) and low-pass (8th order, 500 Hz cutoff) analog Butterworth filters were implemented at the amplifier inputs (input impedance > 100 MΩ, CMRR > 100 dB). First, the skin was prepared to lower down the impedance and then the pairs of electrodes (Ambu Neuroline 720, Ambu, UK) were placed over the muscles according to recommendations from the SENIAM committee [11]. Marker trajectories, force plate and EMG data were acquired using a desktop PC compatible computer equipped with the acquisition software (Qualisys Track Manager, Qualisys, SE) and data acquisition card (PCI-DAS1602/12, Measurement Computing Corporation, USA). Sampling frequencies were set to 100 Hz for the marker trajectories and 1.5 kHz for the force plate and EMG signals.

Data recorded by the cameras and the force plate were processed using the software for human motion analysis. Horizontal and vertical acceleration of the knee (a_{KX}, a_{KY}) and absolute angles of the thigh (φ_T), shank (φ_S), and foot (φ_F) from the horizontal axis were calculated from the marker data. Components (F_X, F_Y) of the ground reaction force (GRF) and trajectory of the center of pressure (*COP*) were determined from the force plate data. The gait pattern signals were low-pass filtered by a 2nd order dual-pass Butterworth filter at a cutoff frequency of 6 Hz [12]. The signals constituted desired trajectory (gait pattern) for the simulations.

The EMG signals were first high-pass filtered by a 2nd order dual-pass Butterwort filter at a cutoff frequency of 6 Hz. This was done in order to minimize movement artifacts. The EMG signals were then rectified and low-pass filtered using a 2nd order dual-pass Butterworth filter at a cutoff frequency of 15 Hz [13] to obtain linear envelopes. Finally, the EMG envelopes and GRF data were down-sampled to 100 Hz in order to synchronize them with the kinematic data.

2.2 Customized modeling and simulations

2.2.1 Model

We used a model that is suitable for control of walking in individuals with hemiplegia (see Fig. 5.2). The adopted reduced planar model of one leg was observable and controllable and the remaining parts of
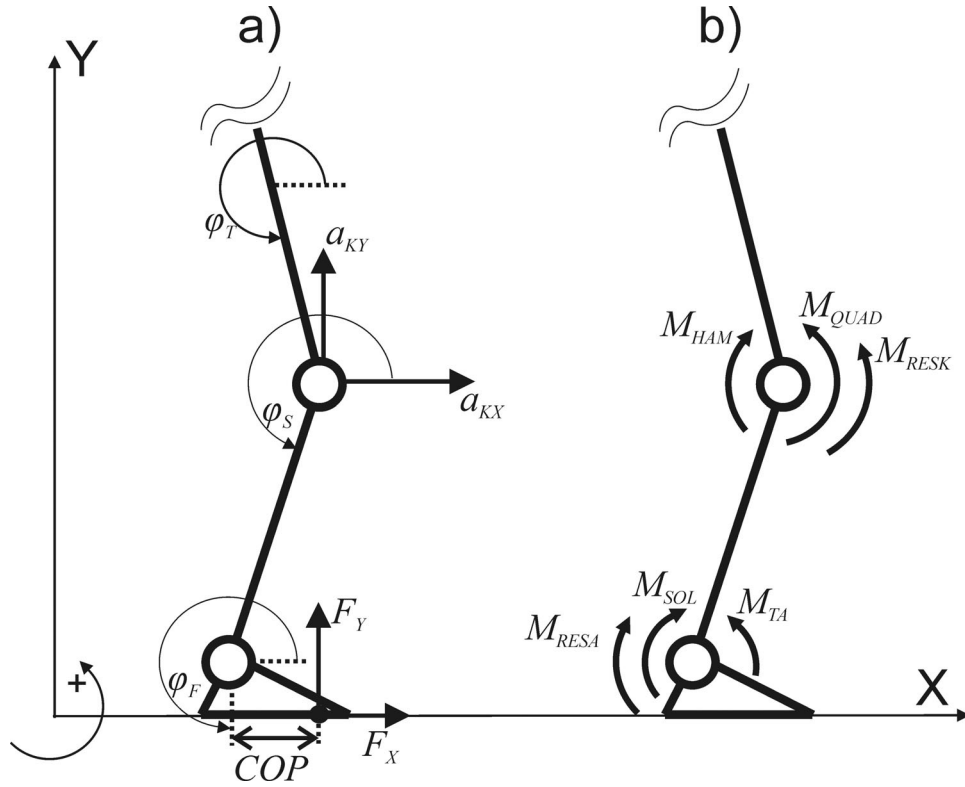
Fig. 5.2. Biomechanical model showing the a) angles, interface forces and b) torques. The notations are: φ_T, φ_S, φ_F – absolute angle of the thigh, shank and foot from horizontal axis; a_{KX}, a_{KY} – horizontal and vertical knee acceleration; F_X, F_Y – horizontal and vertical GRF; COP – trajectory of the center of pressure along the sole of the foot; M_{RESK}, M_{RESA} – resistive knee and ankle joint torques; M_{TA}. M_{SOL}, M_{HAM}, M_{QUAD} – active torques generated by *Tibialis Anterior*, *Soleus*, *Hamstrings* and *Quadriceps* muscles.

the body were replaced by an interface force and torque following D'Alembert's principle. The leg [see Fig. 5.2(a)] was modeled as a system of three rigid bodies (i.e., thigh, shank and foot) connected by pin joints (i.e., knee and ankle) allowing the rotations in the sagittal plane (i.e., knee flexion/extension, ankle plantar/dorsi flexion). Joint torques were assumed as the net results of resistive and active torques [see Fig. 5.2(b)]. The resistive torques at the knee and ankle (M_{RESK}, M_{RESA}) respectively are passive elastic joint properties. The active torques were assumed to be generated by *Quadriceps m.* (M_{QUAD}) and *Hamstrings m.* (M_{HAM}), acting at the knee and *Tibialis Anterior m.* (M_{TA}) and *Soleus m.* (M_{SOL}) acting at the ankle joint. Further details about the model are given in Chapters 2 and 3.

The model parameters used in the simulation were experimentally identified from the healthy individual by applying the techniques described in [14].

2.2.2 Simulations

The simulations were implemented by using two optimal control algorithms: 1) algorithm based on static optimization (SO) presented in Chapter 2 and 2) algorithm based on dynamic optimization (MWDO) described in Chapter 3. Recall that both simulations minimize tracking errors from desired gait pattern while penalizing the total muscle efforts. The cost function for optimization was:

$$F(u_1, u_2, u_3, u_4) = \int_0^T \left[\left(\frac{\varphi_S^*(t) - \varphi_S(t)}{\varphi_{S\,max}^*} \right)^2 + \left(\frac{\varphi_F^*(t) - \varphi_F(t)}{\varphi_{F\,max}^*} \right)^2 + \sum_{i=1}^4 u_i^2(t) \right] dt. \tag{5.1}$$

The variables φ_S^*, φ_F^* and φ_S, φ_F are desired and generated angles, respectively. The parameters φ_{Smax}^*, φ_{Fmax}^* are maximal values of the desired angles. The parameter T is simulation duration. The signals u_i ($i = 1, 2, 3, 4$) are normalized levels of activations for *Tibialis Anterior*, *Soleus*, *Hamstrings* and *Quadriceps* muscles, respectively. They are constrained to be between zero and one, zero meaning that the respective muscle is relaxed and one that the muscle is fully activated. The first two terms in (5.1) are sum of the squares of normalized tracking errors, while the third term is the total effort of muscles

expressed as the sum of the squares of their levels of activation.

In parallel, additional inequality constraints were defined:

$$u_1(t) + u_2(t) \geq \Omega_A, \quad u_3(t) + u_4(t) \geq \Omega_K, \quad u_i(t) \geq \Omega_i, i = 1, 2, 3, 4.$$ (5.2)

Desired level of coactivation of agonist and antagonist muscles (i.e., cocontraction) can be set by using parameters Ω_A, Ω_K and Ω_i ($i = 1, 2, 3, 4$). The parameters Ω_A and Ω_K prescribe minimum values of sums of activations for pairs of antagonistic muscles acting around the ankle and knee, respectively. The parameters Ω_i ($i = 1, 2, 3, 4$) set minimum levels of activations for the muscles individually. Higher values of these parameters result with stronger cocontraction.

We simulated in total twenty strides due to limitations imposed by the number of steps in which GRF was measured. Calculated muscle activations and linear envelopes of the recorded EMG were time normalized to the interval 0-100% of the gait stride. Amplitudes of the EMG envelopes were normalized to the maximum value of the envelope obtained from EMG recorded during maximum voluntary contractions. In order to quantify the similarity between the EMG envelops and calculated muscle activations cross-correlation coefficients (CCCs) were determined according to the following formula:

$$CCC(y_{SIM}, y_{EMG}) = \frac{\sum_{n=1}^{N} y_{SIM}(n) y_{EMG}(n)}{\sqrt{\sum_{n=1}^{N} y_{SIM}^2(n)} \sqrt{\sum_{n=1}^{N} y_{EMG}^2(n)}}$$ (5.3)

where y_{SIM} and y_{EMG} are the profiles of calculated activations and recorded EMG, respectively. The parameters n and N are sample index and total number of samples, respectively.

In order to assess the quality of tracking we calculated the tracking error, that is, the difference between the desired joint angles and joint angles generated by the simulation. The knee (φ_K) and ankle (φ_A) joint angles were calculated from the segment angles (i.e., $\varphi_K = \varphi_T - \varphi_S$ and $\varphi_A = \varphi_F - \varphi_S$).

3 RESULTS

We illustrate the findings with a representative example that shows results of simulations for one selected gait stride. The results for other strides over the complete set of data were similar.

Fig. 5.3 shows the results of simulation implementing SO without prescribing minimal level of cocontractions. The parameters Ω_A, Ω_K and Ω_i ($i = 1, 2, 3, 4$) were all set to zero. Notice that the periods of major muscle activity predicted by the simulation coincide with the EMG activity. *Tibialis Anterior m.* is active at the beginning of stance and throughout the swing. The activation of *Soleus m.* gradually increases during the stance phase and reaches maximum at the push off. Similarly, the overall agreement between the simulation-determined activity and EMG is evident for the *Quadriceps m.* and *Hamstrings m.* as well. However, there are also noticeable differences between the two profiles both in timing and normalized levels of activations. EMG shows variable level of cocontraction of antagonistic muscles during the gait stride. The simulated muscle activations for antagonistic muscles show no coactivation at all, due to the optimization that minimizes the muscle efforts.

Fig. 5.4 shows the results of simulation by using SO but now with a minimum level of cocontractions prescribed by setting the parameters heuristically to the following values: $\Omega_A = \Omega_K = 0.2$ and $\Omega_i = 0.05$ ($i = 1, 2, 3, 4$). Notice that simulation-determined activations for antagonistic muscles, in this case, exhibit coactivation. The calculated activations and recorded EMG became more similar. This is confirmed by the values of CCCs. Namely, the CCCs in Fig. 5.4 are higher from the CCCs in Fig. 5.3 consistently for all analyzed muscles. However, the quality of tracking is very similar in both cases (compare lower plots in Figs. 5.3 and 5.4). Maximal tracking errors in both simulations are less then 2.5°.

The results of simulations by using MWDO are given in Figs. 5.5 and 5.6. Fig. 5.5 shows the simulation in which cocontractions were not imposed (i.e., $\Omega_A = \Omega_K = 0$, $\Omega_i = 0$, $i = 1, 2, 3, 4$). Although the optimization minimizes cocontractions, the calculated activations still exhibit short periods of low-level coactivations, particularly during the phases in which activity was transferred from a muscle to its

Fig. 5.3. Results of simulation implementing SO without prescribing minimal level of cocontractions. Vertical axes in upper plots are normalized muscle activations (SIM) superimposed to normalized recorded EMG. Lower plots show desired joint angles (DES) and simulation-generated joint angles (GEN). The plots show one gait stride starting with the heel strike. The toe off is at 58% of the gait stride. The periods of major muscle activity as predicted by the simulation coincide with the EMG activity. However, the EMG shows cocontraction of antagonistic muscles while there is no coactivation of antagonistic muscles in the simulation-determined activations.
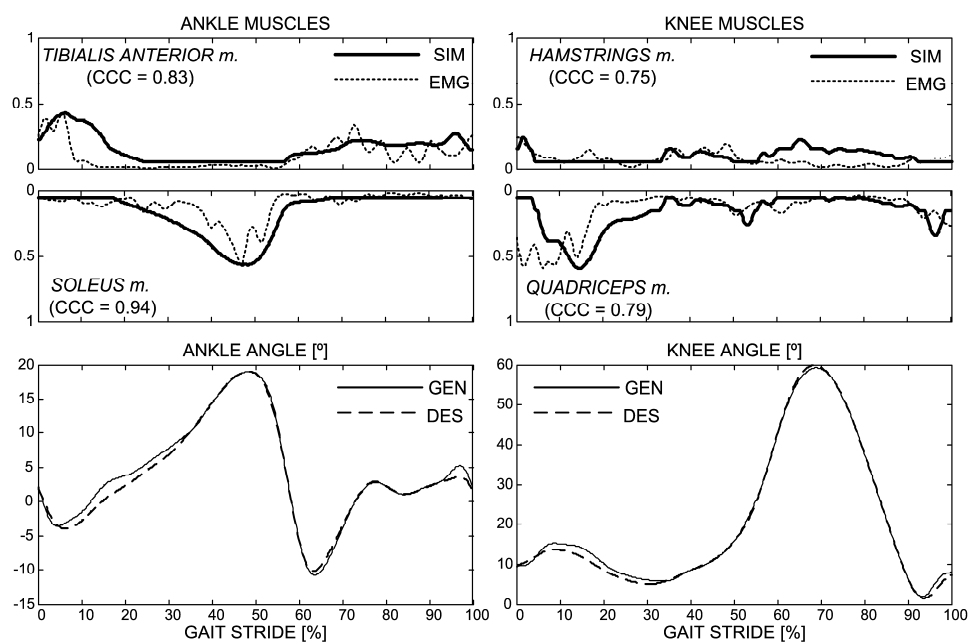
Fig. 5.4. Results of simulation implementing SO with minimal level of cocontractions prescribed. Vertical axes in upper plots are normalized muscle activations (SIM) superimposed to normalized recorded EMG. Lower plots depict desired (DES) and simulation-generated (GEN) joint angles. The figure demonstrates that the muscle activations are more similar (i.e., higher CCC values) to the recorded EMG if cocontractions of antagonistic muscles are imposed in the simulation.
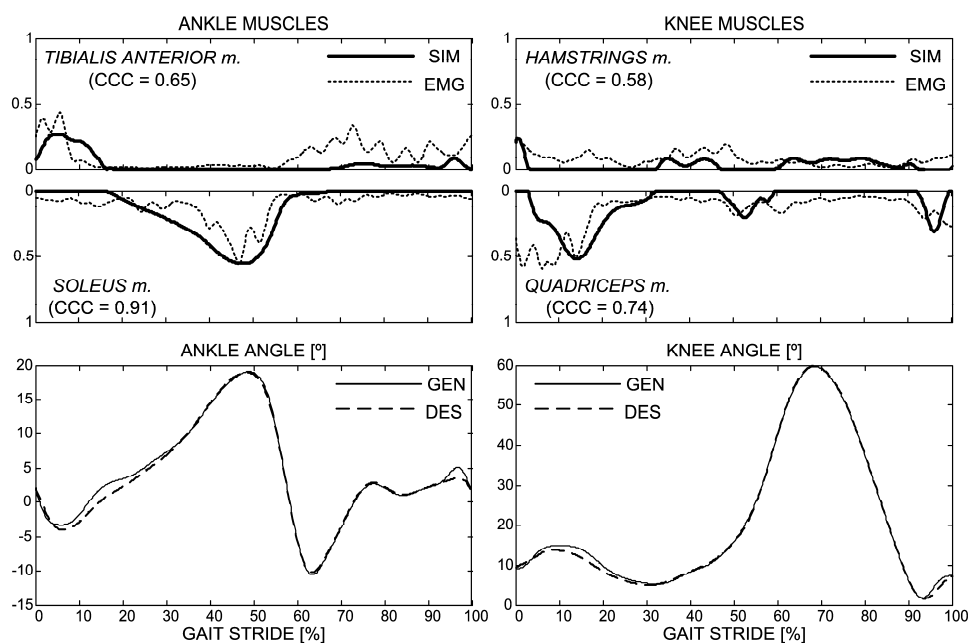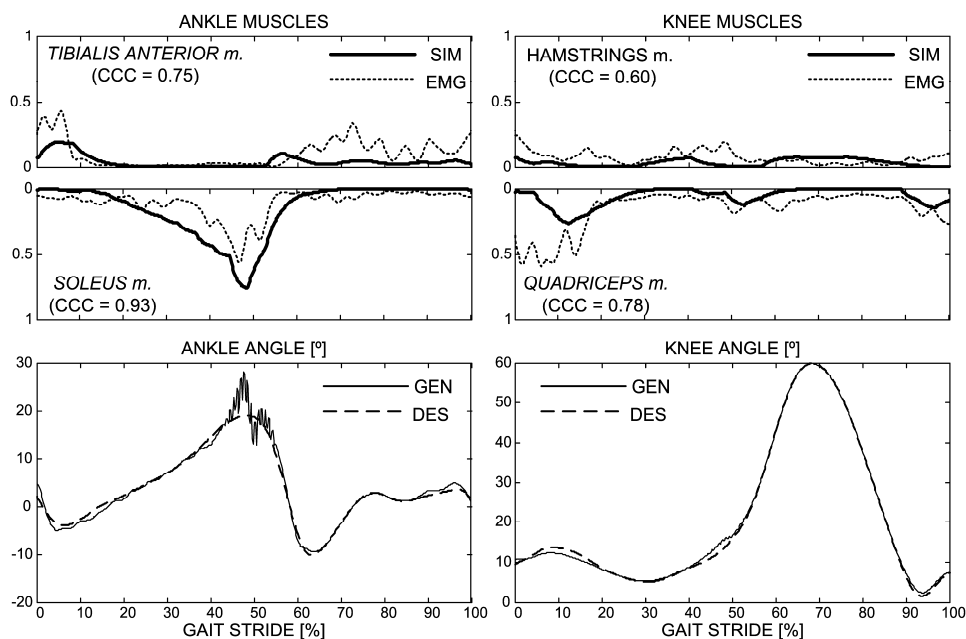
Fig. 5.5. Results of simulation implementing MWDO without prescribing minimal level of cocontractions. Vertical axes in upper plots are normalized muscle activations (SIM) superimposed to normalized recorded EMG. Lower plots depict desired (DES) and simulation-generated (GEN) joint angles. Notice the tracking error and oscillations in the generated trajectory for the ankle joint angle between 45 % and 55 % of the gait stride.
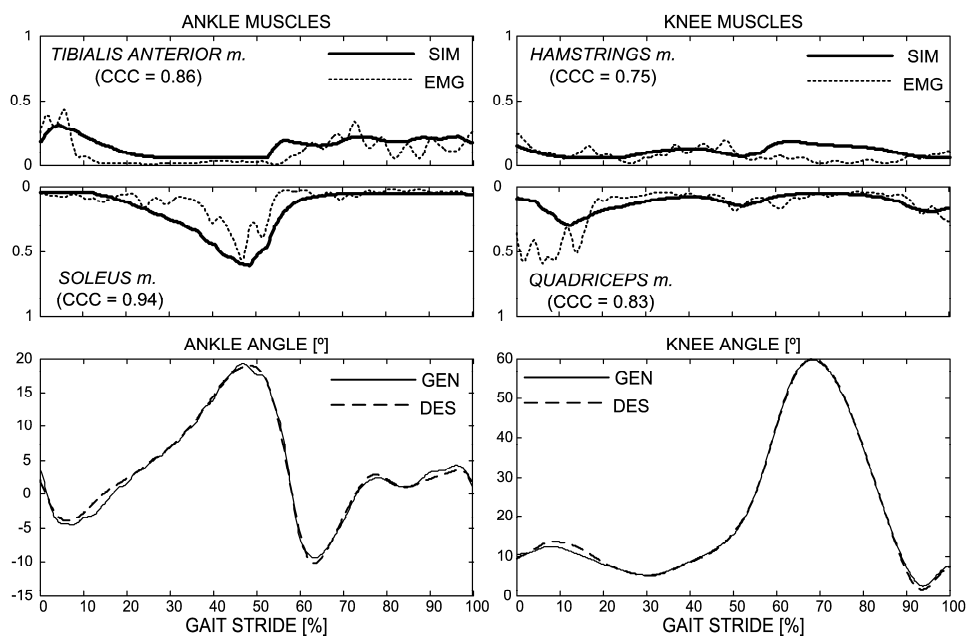
Fig. 5.6. Results of simulation implementing MWDO with minimal level of cocontractions prescribed. Vertical axes in upper plots are normalized muscle activations (SIM) superimposed to normalized recorded EMG. Lower plots depict desired (DES) and simulation-generated (GEN) joint angles. Notice that the tracking error for the ankle joint angle is lower compared to Fig. 5.5. Furthermore, there are no oscillations in the generated ankle angle.
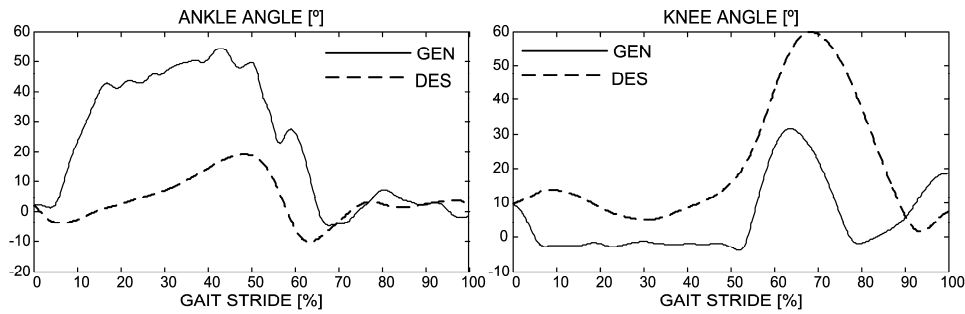
Fig. 5.7. Results of simulating the model by using the normalized recorded EMG as input (muscle activations). The plots depict desired (DES) and generated (GEN) joint angles.

antagonist. Consequently, the CCCs in Fig. 5.5 are somewhat higher than the respective CCCs for SO without cocontractions (see Fig. 5.3). Regarding the quality of tracking, generated trajectory for the ankle joint (see Fig. 5.5, lower plot) noticeably deviates from the desired one over the section of the gait stride between 45% and 55%. Moreover, the generated angle exhibits marked oscillations. Maximal and mean tracking errors are 11.58° and 0.95°, respectively.

Fig. 5.6 shows the results for MWDO with minimal level of cocontractions prescribed (i.e., $\Omega_A=\Omega_K=0.2$ and $\Omega_i = 0.05$, $i = 1, 2, 3, 4$). As indicated by CCCs this type of simulation results with the best matching between the calculated activations and EMG. More importantly, introduction of coactivations generates better tracking (lower tracking error) and completely eliminates oscillations in the ankle joint. Maximal and mean tracking errors for the ankle angle are 1.87° and 0.51°, respectively.

The second goal of the study was to compare the trajectories generated when the controls are from simulation and from EMG profiles. Fig. 5.7 shows the trajectories when the EMG profiles are used as controls. The normalized linear envelops of the EMG shown in Figs. 5.3 to 5.6 were used as inputs: $u_1 = u_{TA}$, $u_2 = u_{SOL}$, $u_3 = u_{HAM}$, and $u_4 = u_{QUAD}$. Deviations of generated trajectories from the desired ones are substantial. In several other examples tested the simulation was diverging, that is, it was not possible to estimate the trajectory.

4 DISCUSSION

In the result sections we showed the following: 1) simulated profiles superimposed over EMG profiles when SO and MWDO algorithms were implemented (see Figs. 5.3 to 5.6, top panels), and 2) achieved (generated) trajectories when the simulated and EMG profiles were used as controls (see Figs. 5.3 to 5.6, bottom panels and Fig. 5.7).

When the controls (inputs to the model) had the form of the EMG profiles, major discrepancy between the desired and achieved trajectories is obvious. In many other steps that were analyzed, the simulation even diverged (not shown here). These results show that mimicking EMG as the input to activation of the electronic stimulator would not lead to the desired walking pattern when considering the muscle properties that are appropriate for the user.

When the activation of muscles determined through SO was applied as input to the model, the tracking errors (see Fig. 5.3 and Fig. 5.4, bottom panels) were very small (only few degrees). However, when the activation obtained through MWDO was applied as input to the model, and no constraint of minimal level of coactivation of agonist and antagonistic muscles was used, oscillatory tracking errors can be observed (see Fig 5.5, bottom panel). The oscillatory tracking errors disappeared when the constraint about the minimal level of coactivations was implemented (see Fig. 5.6).

The second goal of the study was to analyze differences between EMG profiles recorded during walking with the muscle activation profiles determined by using customized biomechanical model and simulation and a desired trajectory recorded in parallel with the EMG. The overall conclusion is that profiles follow the same trends.

When analyzing the profiles of EMG and simulation results, the obvious difference can be seen at the beginning of the gait cycle (loading phase after heel contact). The EMG recorded from the knee extensor
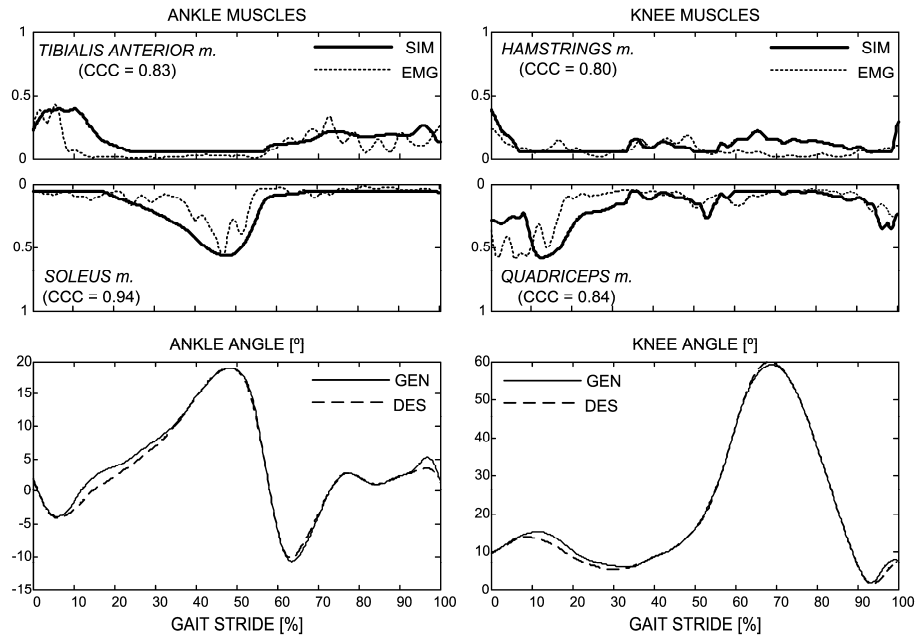
Fig. 5.8. Results of simulation implementing SO ($\Omega_A=\Omega_K=0.2$, $\Omega_i = 0.05$, $i = 1,2,3,4$) in which the level of coactivation of the knee muscles was increased further during the intervals 0%–10% and 95%–100% of the gait stride. Vertical axes in upper plots are normalized muscle activations (SIM) superimposed to normalized recorded EMG. Lower plots depict desired (DES) and simulation-generated (GEN) joint angles. Note that the calculated activity for the knee extensor in the loading phase has increased compared to Figs. 5.3 to 5.6.

was high compared with the muscle activation level obtained through simulation. We carefully analyzed this behavior, and the finding is that the actual projection of the GRF is operating as the knee extensor in the model; hence, no muscle activity is required to guarantee almost perfect tracking and the condition is the minimization of muscle efforts. The likely reason that the EMG is high is the readiness of the biological control to respond to potential perturbations. The loading is critical phase, since the gravity is major force acting on the body, and it is concentrated in the GRF during the loading phase. In the case that the knee does not provide support during the loading, a catastrophic effect will follow (i.e., falling down). Importantly, the optimizations that we developed are actually flexible enough to consider this fact. This is illustrated in Fig. 5.8. It shows the results of SO in which the minimal level of cocontraction was prescribed, by using the same parameters as in the simulation shown in Fig. 5.4 (i.e., $\Omega_A=\Omega_K=0.2$, $\Omega_i = 0.05$, $i = 1,2,3,4$). However, the level of coactivation for the knee muscles was increased further, but only over the selected subsection of the gait stride (loading phase). This selective boost in coactivation makes the calculated profiles for the knee muscles even more similar to the recorded EMG (i.e., highest CCCs overall).Coactivation of agonist and antagonistic muscles is an important component of motor control in able-bodied individuals. It is used to regulate joint stiffness and postural stability [15]. Lamontagne *et al.* [16] suggested that cocontraction is an important mechanism in individuals with disabilities. Reduced coactivation on the paretic side may contribute to poor postural stability and poor locomotor performance of the post-stroke individuals with hemiplegia. Therefore, designing the stimulation profiles that include coactivation of antagonistic muscles is of direct relevance for gait rehabilitation. Importantly, both SO and MWDO algorithms allow prescribing the desired level of coactivation and thereby fine tuning the tradeoff between a certain level of joint stiffness (stability) and minimization of muscle fatigue.

Simulation based on SO is relatively fast; in each step, only one activation value is calculated by applying static optimization. Simulation of a gait stride by using SO lasted less then 2 minutes. In the examples shown in Figs. 5.3 and 5.4, the muscles were strong enough (healthy individual) to generate the selected gait pattern. Due to this fact and because the control was implemented off-line, we obtained an excellent tracking of the desired trajectories. Moreover, the introduction of cocontractions did not affect the tracking. The activations of antagonistic muscles did increase. However, the change was proportional and the net joint torques (driving the model) stayed essentially unchanged.

MWDO uses dynamic optimization that computes several control inputs at once. Simulation of a gait stride by using MWDO lasted between 8 and 15 minutes. Importantly, MWDO includes additional constraints that make the simulation more realistic and closer to the real-life application. MWDO calculates piecewise constant muscle excitations which are similar to stair-like stimulation profiles typically used in FES. Muscle activation dynamics are modeled. Therefore, the muscles are not ideal torque generators; instead, they are activated gradually. Making the model more similar to the real system has several consequences. The activity can not be transferred abruptly between the antagonistic muscles. As a result, the simulation generates certain level of coactivations even in the case when the coactivations were not prescribed (see Fig. 5.5). The tracking error and oscillations can emerge (see Fig. 5.5). However, introduction of cocontractions stabilizes the ankle (see Fig. 5.6). Due to spring-like properties of the muscles, coactivation increases the joint stiffness, and thereby reduces the oscillations. Therefore, an important conclusion is that the introduction of cocontractions not only generates the profiles which are more similar to EMG, but significantly increases the quality of tracking as well.

Another important reason for applying the simulation is the use of customized model. The importance comes from the fact that the simulation considers a model characterized by parameters of an individual with disability. The characteristics of motor systems in individuals with disability are very different from the ones typical for healthy individual (e.g., weaker muscles, spasticity, altered viscoelastic joint properties, etc.). This is to say, that the method could be used to test the feasibility of various walking patterns (trajectories); thus, in the case that one trajectory shows to be unfeasible, a different set of trajectories could be tested and the feasible one selected for implementation [17]–[19].

REFERENCES

[1] R. Kobetič and E. B. Marsolais, "Synthesis of paraplegic gait with multichannel functional neuromuscular stimulation," *IEEE Trans. Rehabil. Eng.*, vol. 2, no. 2, pp. 66-79, 1994.

[2] N. Matsushita, Y. Handa, M. Ichie, and N. Hoshimiya, "Electromyogram analysis and electrical stimulation control of paralyzed wrist and hand," *J. Electromyogr. Kinesiol.*, vol. 5, no. 2, pp. 117-128, 1995.

[3] S. Mangold, M. R. Popović, and T. Keller, "Muscle activity during normal walking and its relevance for the functional electrical stimulation applications," in *Proc. 7th Vienna Int. Workshop FES*, Vienna, Austria. 2001.

[4] D. T. O'Keeffe, A. E. Donnelly, and G. M. Lyons, "The development of a potential optimized stimulation intensity envelope for drop foot applications," *IEEE Trans. Neural Syst. Rehabil. Eng.*, vol. 11, no. 3, pp. 249-256, 2003.

[5] C. A. Byrne, D. T. O'Keeffe, A. E. Donnelly, and G. M. Lyons, "Effect of walking speed changes on tibialis anterior EMG during healthy gait for FES envelope design in drop foot correction," *J. Electromyogr. Kinesiol.*, vol. 17, no. 5, pp. 605-616, 2007.

[6] Z. M. Nikolić and D. B. Popović, "Predicting quadriceps muscle activity during gait with an automatic rule determination method," *IEEE Trans. Biomed. Eng.*, vol. 45, no. 8, pp. 1081-1085, 1998.

[7] Z. M. Nikolić and D. B. Popović, "Automatic rule determination for finite state model of locomotion," in *Proc. IEEE Annu. Int. Conf. EMBS*, pp. 1382-1383 1994.

[8] B. W. Heller, P. H. Veltink, N. J. M. Rijkhoff, W. L. C. Rutten, and B. J. Andrews, "Reconstructing muscle activation during normal walking - a comparison of symbolic and connectionist machine learning techniques," *Biol. Cybern.*, vol. 69, no. 4, pp. 327-335, 1993.

[9] D, Popović, and T. Sinkjaer, *Control of Movement for the Physically Disabled*. 1 ed., London: Springer, 2000.

[10] Anonymous (accessed on June 4th 2008). Visual3D on-line documentation. Available online at: http://c-motion.com/help/.

[11] Anonymous (accessed on June 4th 2008). SENIAM committee official web site. Available online: www.seniam.org.

[12] D. A. Winter, *Biomechanics and Motor Control of Human Movement: Normal, Elderly and Pathological*, 2nd ed., Waterloo, Ontario, Canada: University of Waterloo Press, 1991.

[13] R. Shiavi, C. Frigo, and A. Pedotti, "Electromyographic signals during gait: Criteria for envelope filtering and number of strides," *Med. Biol. Eng. Comput.*, vol. 36, no. 2, pp. 171-178, 1998.

[14] R. B. Stein, E. P. Zehr, M. K. Lebiedowska, D. B. Popovic, A. Scheiner, and H. J. Chizeck, "Estimating mechanical parameters of leg segments in individuals with and without physical disabilities," *IEEE Trans. Rehabil. Eng.*, vol. 4, no. 3, pp. 201-211, 1996.

[15] R. Baratta, M. Solomonow, B. H. Zhou, D. Letson, R. Chuinard, and R. D'Ambrosia, "Muscular coactivation. The role of the antagonist musculature in maintaining knee stability," *Am. J. Sports Med.*, vol. 16, no. 2, pp. 113-122, 1988.

[16] A. Lamontagne, C. L. Richards, and F. Malouin, "Coactivation during gait as an adaptive behavior after stroke," *J. Electromyogr. Kinesiol.*, vol. 10, no. 6, pp. 407-415, Dec.2000.

[17] S. Došen, D. B. Popović, and C. Azevedo-Coste, "Optiwalk: Un nouvel outil pour la conception et la simulation de lois de commande pour le controle de la marche de patients atteints de deficits moteurs," *Journal Europeen des Systemes Automatises*, vol. 41, no. 2, pp. 239-259, 2007.

[18] S. Došen and D. B. Popović, "Accelerometers and Force Sensing Resistors for Optimal Control of Walking of a Hemiplegic," *IEEE Trans. Biomed. Eng.*, vol. 55, no. 8, pp. 1973-1984, 2008.

[19] D. Popović, M. Radulović, L. Schwirtlich, and N. Jauković, "Automatic vs. hand-controlled walking of paraplegics," *Med. Eng. Phys.*, vol. 25, no. 1, pp. 63-73, 2003.

CHAPTER 6
Conclusions

Functional Electrical Stimulation (FES) is the basic instrument for operation of a motor neuroprosthesis (MNP). The goal of FES is to produce movement and restore motor function. Today, most components of MNPs reached maturity: effective interfaces (electrodes and connectors) have been designed and tested, there are commercially available programmable electronic stimulators, micromachining technology provides effective sensors, and computing power of microcomputers is substantial. Yet, the MNPs are still not widely accepted for restoring gait. We suggest that design of an effective controller which guaranties that an FES system operates at the level where individuals with paralysis are satisfied would ensure much wider usage of MNP in daily life. We also suggest that MNP should use life-like control. The artificial controller should mimic the operation of sensory-motor systems characteristic for healthy individuals. However, our understanding of the biological mechanisms for the control of movement is not yet at the level that would allow these mechanisms to be expressed explicitly and formally. Therefore, there is a lack of expert knowledge that could be used to create an algorithm for life-like control of walking.

The goal of this thesis was therefore to develop a set of methods and tools that can be used to generate the knowledge necessary for designing the life-like control of multichannel MNPs for assisting of the walking. The knowledge is provided in the form of sensorimotor models (SMMs). An SMM comprises sensory component (sensor data) and motor component (muscle activations). In effect, the SMM represents an input-output model of the desired controller, from which the controller itself can be generated by using machine learning.

Specifically, the goal was to develop novel, efficient and flexible simulation methods that can be used to generate the SMMs. Importantly, the simulations should provide the sensorimotor data in the form that leads to a rule-based control that is effective, practical and robust. Therefore, we defined a set of requirements that the components of such an SMM must fulfill. We started from the facts that the sensory component of the SMM is incorporated into the feedback while the motor component becomes feedforward command of the generated rule-based controller. Therefore, the sensory component must be generated by using a set of gait sensors convenient for daily application. The motor component should be custom-made for each disabled individual (user of FES) by considering the muscle and inertial properties that reflect his/her specific impairment. Additionally, the motor component should be generated by taking into account the fact that the muscles are activated artificially (by using FES). The form of the muscle activation profiles have to be suitable for implementation by an electronic stimulator. Finally, the profiles should incorporate the control of joint stiffness. In this thesis, we developed a set of simulation methods and tools that provide the means for efficient generation of SMMs that have these characteristics. The methods were developed to answer the research questions RQ1-6 defined in Chapter 1.

We developed novel simulation methods (see RQ1) based on static and dynamic optimization. Nonlinear programming (NLP) was used to implement both optimizations. NLP was selected as a method that is flexible with respect to the form of cost functions and constraints. Namely, the cost functions and the constraints in NLP could be arbitrary (nonlinear, multimodal, discontinuous, and/or multivariable) functions. By using the method, we implemented a number of improvements in the simulations. The improvements are discussed below in detail.

The simulations based on static and dynamic optimizations used a biomechanical model that was reduced to a controllable and observable form. Model parameters could be experimentally identified and thereby the model could be customized for the given subject. The inputs for the simulations were model parameters and a desired gait pattern. Optimal control minimized tracking errors from desired trajectories while penalizing total muscle efforts. The outputs were: 1) control signals for the leg muscles and 2) gait pattern generated when the calculated controls were applied to the model.

Optimal control based on static optimization (see Došen and Popović, 2006 [1], and Došen *et al.*, 2007 [2]) was validated within a user-customized planar model of paretic leg. The flexibility of static optimization based on NLP was used to define new cost functions and optimization constraints. Physiological constraints (e.g., joint range of motion) and constraints on the level of muscle activations were included in the simulations in the form of optimization constraints (see RQ1). In order to implement the tracking of desired trajectories in different phase spaces (see RQ4), the cost functions were formulated that used tracking errors defined in terms of segment angles, angular velocities or angular

accelerations. Therefore, the simulation inputs could be provided by using practical gait sensors, such as, gyroscopes or accelerometers. An example of using the simulation based on static optimization with new cost functions and constraints is given in Došen and Popović, 2007 [3].

We implemented our novel customized modeling and simulation approach as a user-friendly Windows compatible software tool named OptiWalk. First, the prototype was realized and tested in MATLAB 7.4 (see Došen and Popović, 2006 [1]) and then a standalone application was developed (see Došen *et al.*, 2007 [2]). OptiWalk offers a complete environment for biomechanical gait simulations: it integrates data management (database of subjects, database of desired gait patterns), simulation engine and visualization. Thereby, the tool offers considerable flexibility that can be used for efficient generation of SMMs leading to optimal performance (control). A number of simulations with different gait patterns and optimization parameters can be executed easily for the selected subject. The simulation with the best results (quality of tracking, level of muscle efforts) can be chosen and used as an SMM for the design of a real-time rule-based control for the subject. OptiWalk was critical for testing of the simulations. We created a number of records (models, gait patterns) in both databases and then successfully tested the simulation on a numerous examples.

We selected the profiles in the form of piecewise constant signals as convenient for implementation of rule-based control of electrical stimulation (see RQ2). We developed a simulation method based on dynamic optimization and termed moving-window dynamic optimization (MWDO) to generate the profiles in such form (see Došen and Popović, 2008 [4]). The MWDO simulation takes into account the constraints of muscle activation dynamics (see RQ1). MWDO is a flexible method. The length of the optimization window and the length of the constant-amplitude segments in the generated signals are the parameters of the algorithm. The parameters allowed controlling the tracking errors and setting the desired level of coarseness of the generated profiles, respectively. We tested the MWDO method by using experimental data recorded from an able-bodied individual walking at a range of gait speeds. The goal was to test if the method would give satisfactory tracking of desired trajectories despite the fact that the control signals were constrained to have simple piecewise constant shape. The method showed to be very robust and the tracking errors were within the prescribed limits.

We developed methods for designing the stimulation profiles that include control of stiffness at the joint level (see RQ3). We implemented this feature, both in static and dynamic optimizations, by formulating optimization constraints that allowed prescribing minimal level of coactivation of antagonistic muscles (see Došen *et al.*, 2008 [5]). The implementation is flexible. Different levels of coactivations can be set for different muscle pairs. Furthermore, the prescribed level of coactivations can be varied during the gait stride. In case of simulations based on static optimization, the introduction of cocontractions did not affect the quality of tracking. However, in MWDO, oscillatory tracking errors can emerge if the cocontractions are not prescribed (i.e., low stiffness in the joint). An increase in the stiffness stabilizes the joint; thereby, the cocontractions improved the quality of tracking (eliminated oscillations, decreased tracking errors). The ability to design the profiles that integrate stiffness control has a direct relevance for rehabilitation [6].

The tracking of desired trajectories directly in the phase spaces of angular velocities and accelerations by using static optimization showed to be infeasible. The simulation-generated trajectories were drifting in the joint angle domain. Therefore, the simulations were divergent (see RQ4). In response to these results, we decided to develop methods that transform the data from practical gait sensors to the form that leads to a simulation that converges (see RQ5). The methods were based on machine learning. Artificial neural networks were trained to estimate gait kinematics and kinetics from the data recorded by the sensors. By conducting preliminary experiments to test the quality of estimation, we reduced an initial (larger) set of sensors and finally selected sensory system comprising four dual-axes accelerometers and four force sensing resistors. The adopted system was practical and simple but still sufficiently redundant for robust estimation. We integrated the estimation method with the simulation that we developed earlier. The end result was an optimal controller (see Došen and Popović, 2008 [7]) that receives the inputs from the sensors and generates activation profiles for the leg muscles. First stage of the controller was the estimator. The second stage of the controller implemented optimal tracking of the estimated trajectories based on the static optimization. We tested the controller by using experimental data recorded from

several able-bodied subjects walking at a range of gait speeds. The tests confirmed that both the estimation and the tracking errors were within the acceptable error margins. Therefore, the optimal controller can be used to track desired gait patterns recorded by using the selected practical sensors.

Finally, optimal control simulations that we developed were compared to biological control (see RQ6). Muscle activations calculated by using static optimization and MWDO were superimposed to linear envelopes of the recorded EMG (see Došen *et al.*, 2008 [5]). General time and amplitude similarities were found in the profiles, but also noticeable differences. Introduction of coactivations in the simulation made the profiles more similar. We also compared the trajectories (gait patterns) that were generated when the calculated muscle activation profiles or EMG were used as control inputs driving the model. We showed that using EMG led to unacceptable tracking errors; whereas, the simulation output resulted in excellent tracking. The conclusion is that synthesis of controls should rely on muscle activation profiles determined through simulations.

Fig. 6.1 depicts the overall methodology that we suggest for designing rule-based controllers for gait restoration. The figure shows in bold the methods developed in this thesis with relevant references in which they were described. Fig. 6.1 demonstrates how the novel methods complement the previous developments resulting in a comprehensive framework for the design of rule-based control. Database of functional gait patterns can be created by using the methods from Došen and Popović, 2008 [7]. Model parameters for the database of subjects can be determined by using the techniques explained in Stein *et al.*, 1996 [8]. For the selected subject and a desired gait pattern, several optimization methods, such as, dynamic programming (see Popović *et al.*, 1998 [9]), static optimization (see Došen and Popović, 2007 [2], Došen and Popović, 2008 [7]), and MWDO (see Došen and Popović, 2008 [4]) can be used to generate muscle activation profiles that have optimal characteristics: 1) desired shape ("continuous" or piecewise constant), 2) prescribed level of joint stiffness and 3) prescribed level of coarseness. Software tool OptiWalk provides a user friendly environment for testing and comparing the results of these different simulations. The simulation outcome is an SMM comprising sensor data and activation profiles in the form convenient for implementation of an effective and practical rule-based control. Different connectionist (Jonić *et al.*, 1999 [10]) and symbolic (Nikolić and Popović, 1994 [11], Nikolić and Popović, 1998 [12]) machine learning techniques can be used to map the sensory and motor components of the SMM in order to derive the rules for real-time control. One example in which adaptive-neuro-fuzzy-inference systems were used to map accelerometer data to muscle activations is shown in Došen and Popović, 2008 [13]. Finally, the generated rules can be implemented within a programmable electronic stimulator and the system could be used for gait training by means of FES.

The methods developed in this thesis are not limited to FES or rule-based control. They can be used for model-based control in general. The simulation algorithms based on static and dynamic optimizations are flexible enough to generate optimal control for any system described by a mathematical model in the state-space form. Application of the methods for the control of an above knee prosthesis is described in Caltenco *et al.*, 2007 [14] and Melendez *et al.* [15]. In Heliot *et al.* [16], optimal control simulations were integrated with an oscillator-based model of gait and used to control ankle joint by means of FES.

Throughout the thesis, the developed simulation methods were validated by using planar leg models. The models are adequate to design the control for an MNP that could be used to assist walking of individuals with hemiplegia. Contemporary FES systems for hemiplegic gait are mostly considering the drop-foot syndrome. However, the drop-foot is only the most prominent deficiency that limits the walking. Hemiplegia also affects hip and knee flexion and extension of the paretic leg, and often leads to crouched walking with major asymmetry. The impaired leg affects and changes the movement of the non-paretic leg. Therefore, it is of interest to provide better assistance of walking in individuals with hemiplegia in order to increase the walking speed and symmetry.

Importantly, the presented simulation methods are general enough to integrate different musculoskeletal models. The models used for the simulations could be reduced even further (one-joint model) or made more complex (3D model of the leg, Popović *et al.*, 2003 [17]). By selecting a proper model, one can use the methods developed in the thesis to design rule-based controllers for treating drop-foot (one-joint model), assisting hemiplegic gait (planar model) or restoring paraplegic gait (3D model).
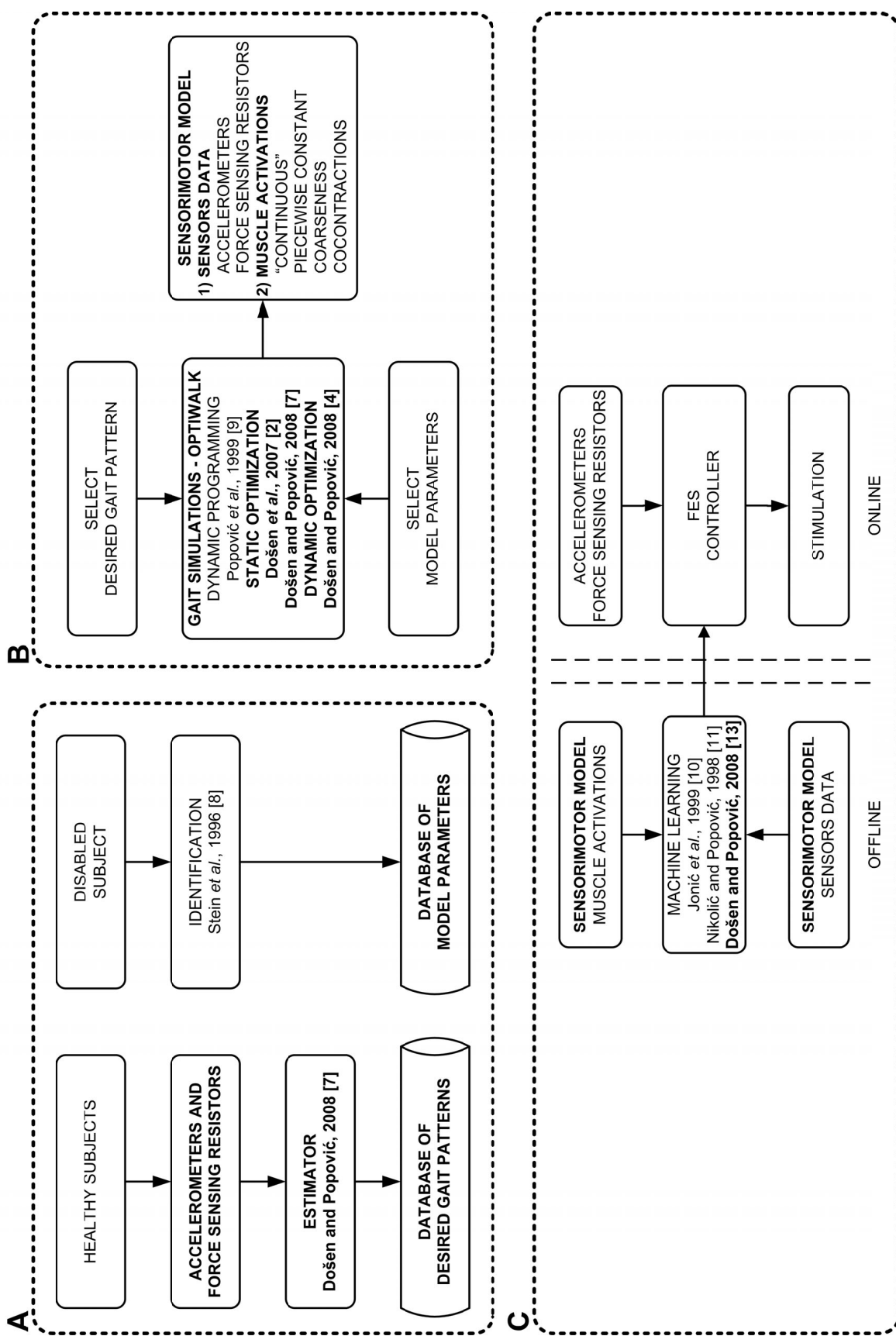
Fig. 6.1. Designing controllers for gait restoration by using customized modeling and simulations and artificial reflex control: A) creating a database of functional gait patterns and a database of subjects, B) using biomechanical gait simulations to generate sensorimotor models (SMM) of gait in the proper form, C) generating the rules by implementation of machine learning using the SMM as a knowledge base. The methods developed in the thesis and the respective references in which they were published are given in bold.

REFERENCES

[1]   **S. Došen** and D. B. Popović, "Functional electrical stimulation: a Matlab based tool for designing stimulation patterns," in *Proc. 28th Annu. Int. Conf. IEEE EMBS*, EMBS'06, New York, USA, pp. 5404-5407, 2006.

[2]   **S. Došen**, D. B. Popović, and C. Azevedo-Coste, "Optiwalk: un nouvel outil pour la conception et la simulation de lois de commande pour le contrôle de la marche de patients atteints de déficits moteurs," *Journal Européen des Systèmes Automatises*, vol. 41, no. 2, pp. 239-259, 2007.

[3]   **S. Došen** and D. B. Popović, "Optimal Control of walking with functional electrical stimulation: inclusion of physiological constraints," in *Proc. 11th Med. Conf. Med. Biol. Eng. and Comput.*, MEDICON 2007, Ljubljana, Slovenia, 2007.

[4]   **S. Došen** and D. B. Popović, "Control of multi-channel electrical stimulation of paretic leg in individuals with hemiplegia: Moving-window dynamic optimization," *IEEE Trans. Biomed. Eng.*, (submitted).

[5]   **S. Došen**, D. B. Popović, and M. B. Popović, ""Design of optimal profiles of electrical stimulation for restoring of the walking," *Med. Eng. Phys.*, (submitted).

[6]   A. Lamontagne, C. L. Richards, and F. Malouin, "Coactivation during gait as an adaptive behavior after stroke," *J. Electromyogr. Kinesiol.*, vol. 10, no. 6, pp. 407-415, Dec.2000.

[7]   **S. Došen** and D. B. Popović, "Accelerometers and force sensing resistors for optimal control of walking of a hemiplegic," *IEEE Trans. Biomed. Eng.*, vol. 55, no. 8, pp. 1973-1984, 2008.

[8]   R. B. Stein, E. P. Zehr, M. K. Lebiedowska, D. B. Popović, A. Scheiner, and H. J. Chizeck, "Estimating mechanical parameters of leg segments in individuals with and without physical disabilities," *IEEE Rehabil. Eng.*, vol. 4, no. 3, pp. 201-211, 1996.

[9]   D. Popović, R. B. Stein, M. N. Oguztoreli, M. Lebiedowska, and S. Jonić, "Optimal control of walking with functional electrical stimulation: A computer simulation study," *IEEE Trans. Rehabil. Eng.*, vol. 7, no. 1, pp. 69-79, 1999.

[10] S. Jonić, T. Janković, V. Gajić, and D. Popović, "Three machine learning techniques for automatic determination of rules to control locomotion," *IEEE Trans. Biomed. Eng.*, vol. 46, no. 3, pp. 300-310, 1999.

[11] Z. M. Nikolić and D. B. Popović. Automatic rule determination for finite state model of locomotion. D. B. Popovic. 1382-1383. 1994.

[12] Z. M. Nikolić and D. B. Popović, "Predicting quadriceps muscle activity during gait with an automatic rule determination method," *IEEE Trans. Biomed. Eng.*, vol. 45, no. 8, pp. 1081-1085, 1998.

[13] **S. Došen** and D. Popović, "Functional electrical stimulation for walking: rule based controller using accelerometers", in *Proc. Annu. IEEE Student Paper Conf. AISPC'08*, Aalborg, Denmark, 2008.

[14] H. A. Caltenco-Arciniega, **S. Došen**, A. Melendez-Calderon, and J. E. Chong-Quero, "Comparison of Different Fuzzy Controllers for Powered Prosthetic Gait," in *Proc. Electron. Robo. Autom. Mech. Conf.*, CERMA, Cuernavaca, Mexico, pp. 651-656. 2007.

[15] A. Melendez-Calderon, H. A. Caltenco-Arciniega, **S. Došen**, and J. E. Chong-Quero, "On-line Simulation Tool for the Design and Analysis of Lower-limb Prosthetic Devices," in *Proc. 4th Int. Conf. Elect. Electron. Eng.,* ICEEE, 2007, pp. 98-101. 2007.

[16] R. Heliot, **S. Došen**, C. Azevedo, B. Espiau, and D. B. Popović, "Online adaptation of optimal control of externally controlled walking of a hemiplegic individual," in *Proc. 3rd Int. IEEE EMBS Conf. Neural Eng.*, Kohala Coast, HI, pp. 36-39, 2007.

[17] D. Popović, M. Radulović, L. Schwirtlich, and N. Jauković, "Automatic vs. hand-controlled walking of paraplegics," *Med. Eng. Phys.*, vol. 25, no. 1, pp. 63-73, 2003.

Summary

Motor neuroprosthesis (MNP) based on electrical stimulation is a system for restoring or augmenting motor functions (e.g., standing, walking, reaching, grasping) that are lost or diminished due to injury or disease of the nervous system. Until today, many MNPs have been developed and tested. New technologies emerged (e.g., microcomputers, micromachining, biocompatible materials) and they have been used to design the components of an MNP (e.g., programmable stimulators, sensors, and electrodes). However, the MNPs are still not widely used for restoration of the walking. The likely reason is the lack of an efficient control that would make an MNP operate at the level that would actually improve the quality of life of disabled individuals. We suggest that MNP should use life-like control. If the artificial controller mimics the operation of sensory-motor systems, it could be seamlessly integrated into those components of biological (volitional) control that are still preserved and functional after the injury or disease of the central nervous system. However, the biological mechanisms for the control of walking are still not fully known and understood. Therefore, an expert knowledge that could be used to design the life-like control is still lacking.

This was direct motivation for our research. The overall aim was to provide the knowledge necessary for designing the life-like control of multichannel MNP for assisting of the walking. Specifically, the goal was to develop a set of methods and tools for biomechanical gait simulations that can be used to generate sensorimotor models. In effect, a sensorimotor model represents an input-output model of the desired controller, from which the controller itself can be computer-generated by using machine learning. An important objective was to make the simulations flexible so that the sensorimotor data can be provided in the form that leads to a control that is effective, robust and convenient for practical implementation.

We developed novel, efficient and flexible simulation methods based on static (Chapter 2) and dynamic optimizations (Chapter 3). The simulations used a reduced biomechanical model that can be customized for the specific subject. The inputs for the simulation were experimentally identified model parameters and a desired gait pattern. Optimal control minimized tracking errors from the desired trajectories while penalizing the total muscle efforts. The outputs were: 1) control signals for the leg muscles, and 2) gait pattern generated when the calculated controls were applied to the model.

The simulation is implemented as a user friendly software tool named OptiWalk. The tool integrates a database of subjects, a database of gait patterns, simulation and visualization engines. OptiWalk can be used to test the feasibility of tracking of the selected gait pattern by using (impaired) neuromusculoskeletal system of the selected subject. Additionally, the tool can be used to find the minimal plant responses needed for the desired activity. OptiWalk outputs a sensorimotor model (senor data and controls for the muscles) that can be used, as described above, to design a controller for an MNP.

The simulation based on static optimization is time-efficient. The control values are calculated on a sample-by-sample basis without taking into account previous or future values. Constraints of musculoskeletal physiology (e.g., range of motion in the joints) as well as prescribed minimal and maximal values of muscle activations are enforced during the simulation. The simulation was tested and showed to be robust across different subjects, gait patterns and gait speeds.

The simulation based on dynamic optimization, termed moving window dynamic optimization (MWDO), calculates the controls by applying optimal tracking over a section of the gait pattern, thereby calculating several control values at once. We developed MWDO in order to generate the control that is convenient for implementation. Namely, the method calculates the muscle excitations in the form of piecewise constant signals. Furthermore, the MWDO takes into account muscle activation dynamics. We tested the method by using experimental data collected from an able-bodied subject walking at a range of gait speeds. The tests demonstrated that, although the controls were constrained to be piecewise constant, the desired trajectories could be tracked within the prescribed error margins.

In order to design the control that is robust and resistant to disturbances, we incorporated the control of joint stiffness in the simulations (Chapter 4). The stiffness control was implemented in both static and dynamic optimizations by introducing optimization constraints that allowed prescribing minimal level of coactivation of antagonistic muscles around the joint. The implementation was flexible; different

coactivation levels could be prescribed for different joints, and the levels could be varied during the gait stride. It was shown that in the case of MWDO, the introduction of coactivations actually improved the quality of tracking (decreased the tracking errors). Furthermore, the coactivations made the simulation-generated control more similar to biological control [i.e., electromyography (EMG)].

We developed methods that allow the simulation inputs (desired gait patterns) to be provided by using practical set of gait sensors (Chapter 5). An optimal controller was developed that uses data from four dual-axes accelerometers and four force sensing resistors and outputs muscle activations for the six equivalent muscles acting around the hip, knee and ankle joints. The controller included two stages. The first stage was a set of artificial neural networks that estimated gait kinetics and kinematics from the data recorded by the sensors. The second stage used optimal control simulation for the tracking of the estimated trajectories. The controller was tested by using data collected from several subjects walking at a range of gait speeds. The tests showed that the controller could track the recorded trajectories with satisfactory precision. Namely, both the estimation and the tracking errors were within the prescribed limits.

Finally, we compared the control generated by the simulations to the biological control (Chapter 6). Muscle activations calculated by using static optimization and MWDO were superimposed to linear envelopes of the recorded EMG. General time and amplitude similarities were found in the profiles. We showed that using EMG profiles as the control input for the model led to unacceptable tracking errors; whereas, the simulation-generated controls resulted in excellent tracking. The conclusion is that the synthesis of controls for an MNP should rely on muscle activation profiles determined through simulations.

The set of methods and tools developed in this thesis can be used to generate sensorimotor models of gait that are necessary for designing the control of multichannel MNP for assisting of the walking. Importantly, the methods are flexible and allow the simulations to be run easily with different inputs and parameters. Since a sensorimotor model is actually a model of the controller, the components of the controller (inputs, outputs) can be shaped offline through interactive experiments. Finally, when the results are satisfactory, the controller could be implemented in one step (by using machine learning) and used to control an MNP.

Sammenfatning

Neurale protester (NP) baseret på elektrisk stimulation er systemer, der har til formål at hjælpe og støtte med genindlæring af motoriske funktioner, som er tabt som følge af skader eller sygdomme i nervesystemet. Dette kan f.eks. være genindlæring af evnen til at stå oprejst med fuld vægtbæring på begge ben og evnen til at gå, og for overekstremiteterne at række og gribe med hænderne. Gennem tiden er der udviklet mange neurale protester, og når nye teknologier er opstået er mange af disse også forsøgt anvendt i udviklingen af neurale proteser, som f.eks. mikrocomputere, mikromaskiner og biokompatible materialer. Disse teknologier har været anvendt til udviklingen af delkomponenter som f.eks. programmerbare stimulatorer, sensorer og elektroder. Stadigvæk er neurale proteser endnu ikke blevet en fundamental del af genindlæringen af gangfunktionen. En sandsynlig årsag til dette kan være manglen på et effektivt kontrolværktøj, der sikrer at den neurale protese arbejder med intensiteter der har potentiale for at hjælpe den enkelte patient. Et sådant værktøj vil kunne forbedre livskvaliteten dramatiske for patienter med funktionsnedsættelse. Vi foreslår derfor at anvende "life-like" kontrol i udviklingen af neurale proteser. Ideen er, at kontrolleren efterligner det sanse- motoriske system, hvorved det sandsynligvis mere problemfrit kan integreres sammen med de motoriske funktioner, der efter en skade stadige er funktionelle og under frivillig kontrol. Dog er den fulde forståelse af de biologiske mekanismer, der styrer og kontrollerer gangfunktionen stadig begrænset, og den ekspertviden der skal til for at designe en "life-like" kontroller er desværre mangelfuld. Dette var den direkte motivation for dette forskningsprojekt.

Det overordnede mål for projektet var at udforske og fremskaffe den viden, der er vital for at kunne designe et system til "life-like" kontrol af en flerkanals neural protese til rehabilitering af gang. Dette affødte målet om at udvikle et sæt metoder og værktøjer til biomekanisk simulation af gang, der kan bruges til at generere en sansemotorisk model, der repræsenterer input-output forholdet for den ønskede kontroller. Når denne model er designet, kan den egentlige kontroller efterfølgende computergenereres via "machine learning" teknikker. Et andet af projektets vigtige mål var at gøre simulationen fleksibel således, at sansemotorisk data kan udnyttes på en måde, der sikrer at den endelige neurale protese bliver både effektivt, robust og praktisk anvendelig i et klinisk miljø.

Vi har udviklet nye, effektive og fleksible metoder baseret på statisk (Kapitel 2) og dynamisk optimering (Kapitel 3). Simulationsværktøjet anvender en reduceret biomekanisk model, der kan tilpasses til den enkelte patient. Input til simulationerne var eksperimentelt identificerede modelparametre samt et ønsket gangmønster. Optimal kontrolteori er anvendt til at minimere fejlen ("tracking error") til det ønskede trajektorie og samtidig straffe ("penalizing") den totale mængde muskel arbejde. Output fra simuleringerne var 1) benmusklernes aktiveringsmønstre og 2) gangmønsteret genereret under forudsætning af disse aktiveringsmønster.

Simulationsværktøjet er implementeret som en brugervenlig softwarepakke, der kaldes OptiWalk og indeholder to databaser med forsøgspersoner og gangmønstre samt redskaber til simulation og grafisk visning af resultaterne. OptiWalk kan anvendes til at teste anvendeligheden af et ønsket gangmønster ved at simulere et svækket eller skadet neuro-motorisk system på en given forsøgsperson. Ligeledes kan værktøjet anvendes til at finde det aktiveringsmønster, hvormed en ønsket aktivitet kan gennemføres med minimal muskelarbejde. OptiWalk genererer en sansemotorisk model bestående af sensoriske data og aktiverings signaler til benmusklerne, der kan anvendes til efterfølgende at designe selve kontrolenheden til en tilpasset neural protese.

Simulationen, baseret på statisk optimering, er særdeles tidseffektiv, da kontrolværdierne beregnes sample for sample uden at inddrage tidligere og fremtidige simuleringsværdier. Begrænsninger i det neuro-motoriske system, som f.eks. nedsat bevægelsesområde af et bestemt led, nedsat eller forøget muskelaktivitet af specifikke muskler mv., kan integreres i simuleringerne. Simulationen er testet og viste sig at være robust og uafhængigt at forskellige forsøgspersoner, gangmønstre og ganghastigheder.

Stimulationerne baseret på dynamisk optimering benævnt "moving-window dynamic optimization" (MWDO) beregner muskelaktiveringssignalerne ved at anvende "optimal tracking" over en brugervalgt tidsperiode af gangmønsteret og derved beregne flere muskelaktiveringsværdier på en gang. Årsagen til at vi udviklede et MWDO var for at kunne genere de aktiveringsmønstre, der er anvendelige ved praktisk

implementation, det vil sige, at metoden udregner direkte muskelaktiveringsprofiler i form af stykvise konstante aktiveringssignaler, ligesom der i MWDO tages højde for muskelaktiveringsdynamik. Vi testede metoden ved brug af eksperimentelle data målt fra raske forsøgspersoner gående ved forskellige hastigheder. Testen viste, at selvom aktiveringsmønsteret var begrænset til at være stykvise konstante kunne det ønskede gangmønster opnås indenfor de fastsatte fejlmarginer.

For at sikre at kontrolenheden var robust og ufølsom over for forstyrrelser, har vi indarbejdet kontrol af led-stivheden i simulationerne (Kapitel 4). Dette er implementeret i både den statiske og den dynamiske optimering ved at introducere optimeringsbegrænsninger, der tillader, at man kan indstille det minimale niveau af co-aktivering af antagonistiske muskler for et bestemt led. Denne implementation er så fleksibel, at der for hvert led kan defineres forskellige grader af co-aktivering i forskellige underfaser af et skridt. Testen viste, at bruges co-aktiverings paramenterne i MWDO-delen blev fejlen ("tracking error") væsentligt mindre, desuden havde det muskelaktiveringssignal genereret med aktive co-aktiverings-paramenter større, lighed med biologisk kontrolsignaler som f.eks. electromyography (EMG).

Der er udviklet et sæt metoder, der tillader at give det ønskede gangmønster som inputsignaler via nogle praktiske målemetoder i form af 4 stk. 2-kannals accelerometer samt 4 stk. kraftfølsomme modstande (Kapitel 5). Output fra simuleringen er muskelaktiveringsprofiler for 6 muskel ækvivalenter virkende rundt om hhv. hofte, knæ og ankel ledet. Kontroller delen består af to dele. I første del anvendes en række kunstige neurale netværk til at estimere kinetik og kinematik baseret på de målte inputsignaler fra accelometerene og kraftsensorene. I anden del anvendes optimal kontrolteori til at simulere, hvor godt de estimerede kurver tilnærmer sig til det ønskede gangmønster. Kontrolleren blev testet ved at bruge data optaget fra en række forskellige forsøgspersoner ved en række varierende ganghastigheder og viste både estimeringfejlen og tracking error var inden for de fastsatte fejlmarginer, hvorved det konkluderes, at kontrolleren kunne generere de målte data med en tilfredsstillende fejlmargin.

I den sidste test sammenlignede vi simulationen af muskelaktiveringsmønsteret med det målte biologiske aktiveringsmønster (Kapitel 6). Her blev muskelaktiveringsprofilerne fra hhv. statisk optimering og MWDO sammenlignet med målte EMG signaler ("linear envelopes"). Testen viste, at der generelt var god overensstemmelse i både tids og amplitude profilerne for målte og simulerede data. Desuden viste et forsøg med at bruge EMG profiler som input, at dette resulterede i uacceptable store tracking error hvorimod de aktiveringsmønstre der var genereret af simulatoren resulterede i en meget lille tracking error. Dermed konkluderes det, at kontrolsignaler til en neural protese bør baseres på muskel aktiveringsprofiler, der er bestemt via simulation.

Det sæt metoder og værktøjer der er udviklet i denne afhandling kan anvendes til at generere en sansemotorisk model af gang. Denne model er vital for efterfølgende at kunne designe det kontrolsignal, der skal anvendes i en egentlig neural protese, der kan støtte patienter i deres gangfunktion. Det udviklede værktøj er fleksibelt og tillader at det er let at anvende forskellige inputsignaler til at drive simulationen med, ligesom vitale parametre let kan ændres, og en ny simulation kan startes. Da den udviklede sansemotoriske model simulerer det egentlige system bestående af både biologisk system og kontroller, kan de enkelte delkomponenter justeres offline gennem interaktive eksperimenter. Når et tilfredsstillende resultat er opnået kan den virkelige kontroller implementeres i et skridt ved hjælp af f.eks. "machine learning" teknikker.